DRA

CHARACTERIZATION OF IMPULSE NOISE AND ANALYSIS OF ITS EFFECTS UPON CORRELATION RECEIVERS

CR-123611

by

RONALD C. HOUTS
Project Director

and

JERRY D. MOORE
Research Associate

October, 1971

TECHNICAL REPORT NUMBER 135-102

COMMUNICATION SYSTEMS GROUP

BUREAU OF ENGINEERING RESEARCH

UNIVERSITY OF ALABAMA UNIVERSITY, ALABAMA

CHARACTERIZATION OF IMPULSE NOISE AND ANALYSIS OF ITS EFFECTS UPON CORRELATION RECEIVERS

by

RONALD C. HOUTS
Project Director

and

JERRY D. MOORE
Research Associate

October, 1971

TECHNICAL REPORT NUMBER 135-102

Prepared for

National Aeronautics and Space Administration
George C. Marshall Space Flight Center
Huntsville, Alabama

Under Contract Number

NAS8-20172

Communication Systems Group
Bureau of Engineering Research
University of Alabama

ABSTRACT

A noise model is formulated to describe the impulse noise in many digital systems. A simplified model, which assumes that each noise burst contains a randomly weighted version of the same basic waveform, is used to derive the performance equations for a correlation receiver. The expected number of bit errors per noise burst is expressed as a function of the average signal energy, signal-set correlation coefficient, bit time, noise-weighting-factor variance and probability density function, and a time range function which depends on the cross-correlation of the signal-set basis functions and the noise waveform. A procedure is established for extending the results for the simplified noise model to the general model. Unlike the performance results for Gaussian noise, it is shown that for impulse noise the error performance is affected by the choice of signal-set basis functions and that Orthogonal signaling is not equivalent to On-Off signaling with the same average energy. The error performance equations are upper bounded by a procedure which removes the dependence on the noise waveform and the signal-set basis functions. A looser upper bound which is also independent of the noise-weighting-factor probability density function is obtained by applying Chebyshev's inequality to the previous bound result. It is shown that the correlation receiver is not optimum for impulse noise because the signal and noise are correlated and the error performance can be improved by inserting a properly specified nonlinear device prior to the receiver input.

ACKNOWLEDGEMENT

The authors would like to express their appreciation to the personnel of the Telemetry and Data Technology Branch, Marshall Space Flight Center, for their useful technical consulations. In particular, Messrs. Frost, Emens, and Coffey have rendered valuable assistance and direction. Also, the technical discussions with Messrs. Perry and Stansberry of SCI Electronics Inc. were very helpful. A significant portion of the computer programming for this investigation was performed by Mr. R. H. Curl.

TABLE OF CONTENTS

LIST OF FIGURES

LIST OF TABLES

CHAPTER 1

INTRODUCTION

1.1 STATEMENT OF PROBLEM

Traditionally, the performance analyses of digital systems have incorporated additive white Gaussian (AWG) noise to model the interference introduced by the communication channel. With this assumption it has been shown that the optimum receiver consists of a bank of correlators, each of which compares the incoming noisy waveform with one of the possible received noise-free signals. Although the AWG noise assumption gives satisfactory error rate predictions for many situations, it has failed to predict the much higher error rates observed on some classes of digital systems. Another type of additive noise, commonly referred to as impulse noise, is currently being modeled and used to explain this discrepancy on atmospheric radio channels and both switched and dedicated baseband channels. The impulse noise models proposed in the literature differ in several respects, but all impulse noise is characterized by brief periods of large amplitude excursions, separated by intervals of quiescent conditions.

The relatively new area of impulse noise analysis suffers from the problems of nonstandardization and incompleteness. It is difficult to compare the results of two authors and impossible to obtain comparison of the major binary signaling techniques, because of the multitude of noise models, signal sets, analytical methods and

simplifying assumptions. In this work the primary objective is to establish a mathematical model that can be used to approximate additive impulse noise and then apply this model in the error performance analysis for a correlation receiver. The secondary goal is to present a collection of specific performance results from which it will be possible to draw some general conclusions regarding impulse noise and its effect on digital systems.

1.2 IMPULSE NOISE LITERATURE REVIEW

Almost all papers concerning impulse noise have been published since 1960. A wide variety of mathematical models have been proposed to describe different aspects of impulse noise. Only a few authors [1,2]* have discussed the noise waveforms obtained from actual systems, while much emphasis has been placed on empirically obtained amplitude and/or time distributions for the noise [1,3-8]. Proposed impulse noise models have assumed such waveforms as the ideal impulse function, with either constant weight [9] or probabilistic weighting [10,11], and the unit-impulse response of the channel being studied [12,13]. Another approach has been to assume various probabilistic descriptions for the noise at the receiver output [14]. The majority of performance studies have been limited to the analysis of a specific binary signaling technique [2,6,12,13,15-20] although several authors [9,11,21-24] have obtained performance curves and compared more than one signal set based

---

*Enclosed numbers refer to corresponding entries found in List of References.

on their assumed noise models. Zeimer [10] and Millard & Kurz [25] have extended their analyses to the consideration of M-ary signaling.

The basic approach to error analysis for the practical case of a general noise waveform which can change from one noise burst to another has been developed by Houts & Moore [11] and forms the foundation of the work documented here. Although specific performance results were not obtained for the general model, upper and lower bounds on signal set error performances were derived.

Signals corrupted by impulse noise are often detected by receivers that were designed for use in AWG noise. It is reasonable to expect that the error performance of these receivers can be improved. Several receiver-improvement modifications have been proposed [26-30] based upon intuition or experimental results. The subject of optimum receiver design for binary signals in the presence of impulse noise has received limited treatment in the literature. Snyder [31] has investigated the design of an optimum receiver for VLF atmospheric noise. The noise model has a combination of AWG noise and impulse noise generated by exciting a filter with idealized delta functions. Specific results are not obtained and remain a topic for further investigation. A different approach has been used by Rappaport & Kurz [32] who assume that the noise waveform duration is short compared to the bit time and that independent samples can be obtained by uniformly sampling the received signal.

1.3 APPROACH OUTLINE

The first step in any error performance analysis should be the development of a realistic noise model. Simplifying assumptions are sometimes included in the model for the purpose of making the analysis mathematically tractable, which in turn aids in understanding the role played by the various noise parameters. However, the results from such a model often fail to predict actual system performance. In Chapter 2 a generalized impulse noise (GIN) model is presented which can be used to approximate the impulse noise structure in a broad class of digital systems. In particular, the model is applicable to a baseband channel with near dc response of the type found in telephone circuits and sophisticated avionics systems such as the proposed data bus for NASA's Space Shuttle vehicle. The performance analysis for a band-limited channel using a correlation receiver in the presence of impulse noise described by the GIN model is presented in Chapter 3. In addition, new and more definitive performance bounds are obtained for typical binary signal sets. The effects of selecting various noise weighting factor descriptions, signal sets, and noise waveforms are documented in Chapter 4. Several performance improvement methods are surveyed in Chapter 5 and specific results are presented for the case where a nonlinear device is inserted prior to the correlation receiver. The results show that the performance can be improved; consequently, the correlation receiver is not optimum for impulse noise corrupted signals.

CHAPTER 2

IMPULSE NOISE MODEL

A mathematical model is developed which is sufficiently flexible to approximate the additive impulse noise in a broad class of digital systems. Also, the power-density spectrum and probability density function (p.d.f.) are established for certain special cases of the noise model.

2.1 HEURISTIC CONSIDERATIONS

The waveform description of impulse noise depends on the noise source, the coupling media, and the characteristics of the channel under observation. Capacitive and inductive coupling along with switching transients comprise the major methods by which impulse noise is introduced into a system. For instance, impulse noise in a channel might be caused by a lightning discharge or engine ignition noise. Telephone and telemetry systems experience noise from electromechanical relay switching. Other sources include environmental conditions such as shock, vibration, and maintenance disruptions, i.e., a temporary short circuit. These sources have the common characteristic that the noise produced occurs in bursts of large amplitude variations separated by relatively long intervals of negligible amplitude variations. This observation is the foundation for the mathematical model presented in Section 2.2.

The determination of the noise waveforms can be a time consuming and expensive process. The number of different waveforms encountered can be very large, and normally the measuring equipment must have large bandwidth and a capability for handling aperiodic waveforms. Kurland & Molony [2] experimentally determined and ranked the error performance for 15 different noise waveforms at various signal-to-noise ratios (SNR). No pattern appeared to exist in the relative standing of the various waveforms as the SNR was changed. Fennick [1] has reported on specific switched telephone lines where 2000 distinct waveforms have been analyzed. The result was widely varying amplitude and phase spectra characteristics. However, when a subset of approximately 200 of the waveforms were added together, the composite noise spectrum appeared to approximate the channel transfer characteristic. This would suggest that a weighted unit-impulse response of the channel could be used as a typical noise waveform. For dedicated lines such as private telephone lines or a Space Shuttle data bus, the channel characteristics will remain constant in contrast with the switched telephone system. Furthermore, the number of possible noise sources are greatly reduced. Measurements of noise which is induced by relay switching have been made on a Space Shuttle data bus [33,34] and reveal noise bursts composed of a random number of aperiodic waveforms. It is difficult to describe the shape of the waveforms from data presented. A reasonable conjecture is that the waveforms can be modeled as exponentially-decaying sinusoids.

2.2 MATHEMATICAL MODEL

A typical noise process based on the discussion of Section 2.1 is modeled as the sum of NB bursts and is shown in Fig. 2-1a. The k^{th} burst, $b_k(t-T_k)$, occurs at time T_k and is composed of a random number, NG, of aperiodic waveforms as shown in Fig. 2-1b. In a restricted special case, a burst consists of only one waveform as shown in Fig. 2-1c.

The generalized impulse noise (GIN) model is formulated as

$$n(t) = \sum_{k=1}^{NB} b_k(t-T_k), \quad 0 \leq t \leq T_n, \quad NB = 1,2,\ldots \tag{2.1}$$

It is assumed that each burst, $b_k(t-T_k)$, k = 1,..., NB, has a finite duration TF_k, viz.,

$$b_k(t-T_k) \neq 0 \quad T_k < t < T_k+TF_k \cdot \tag{2.2}$$

Furthermore, each burst is represented as

$$b_k(t) = \sum_{j=1}^{NG} I_{kj} g_{kj}(t-T_{kj}) , \tag{2.3}$$

where NG is the number of sample functions that occur, $g_{kj}(t)$ is a waveform that is chosen at random from the k^{th} ensemble of sample functions $\{G_1(t), G_2(t),\ldots, G_N(t)\}^k$, I_{kj} is a random variable weighting function and T_{kj} is the occurrence time of the j^{th} sample function. As an example, let the k^{th} noise burst contain three sample functions, i.e.,

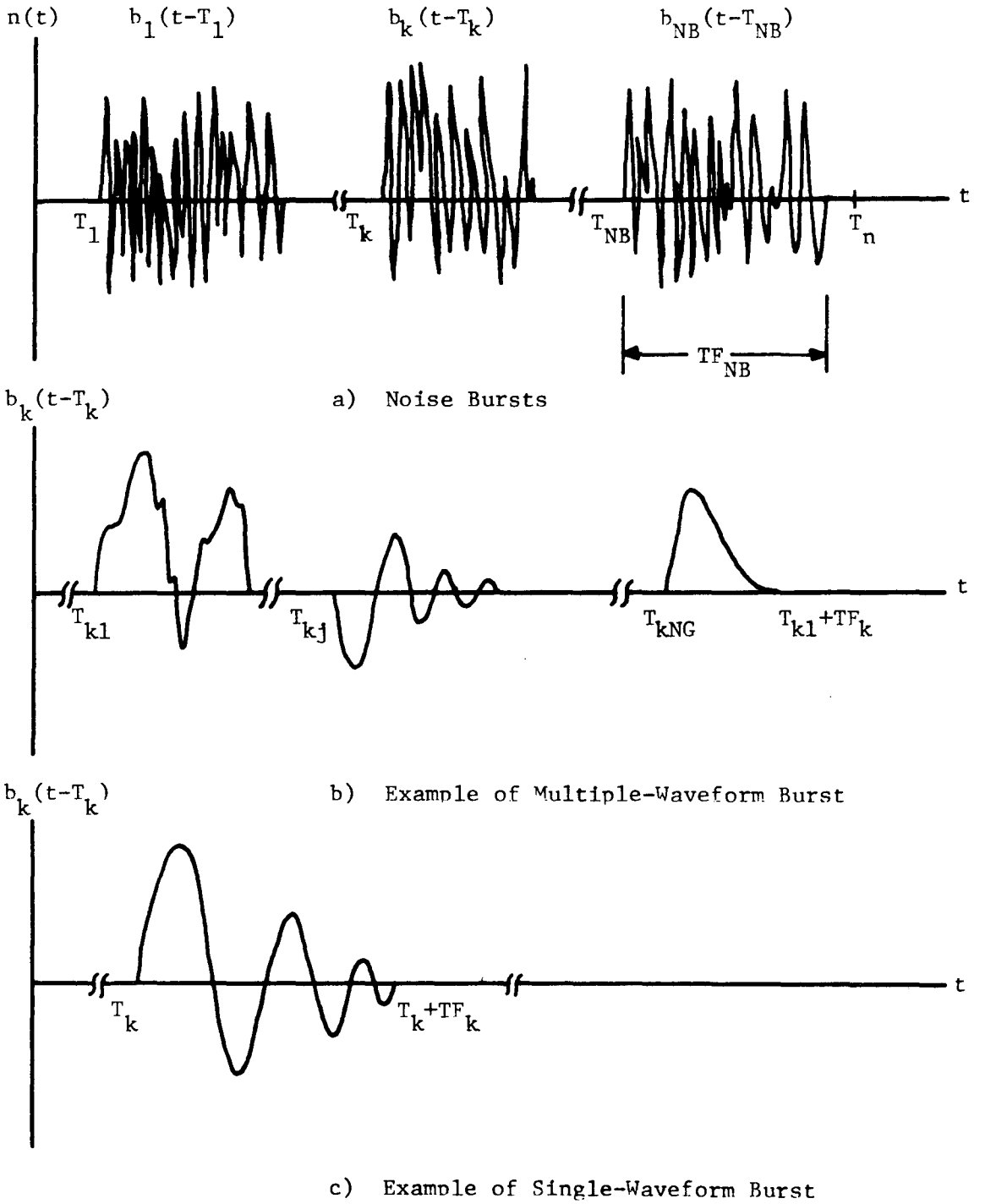

Fig. 2-1. Impulse Noise Model Waveshapes

NG = 3, with each chosen from the k^{th} ensemble $\{G_1(t), G_2(t), G_3(t), G_4(t), G_5(t)\}$ which consists of five sample functions. One possible description for the burst is

$$b_k(t) = I_{k1}\, G_5(t-T_{k1}) + I_{k2}\, G_3(t-T_{k2}) + I_{k3}\, G_5(t-T_{k3}) \ . \qquad (2.4)$$

Note that the sample functions $G_1(t)$, $G_2(t)$, $G_4(t)$ did not appear while $G_5(t)$ was present twice.

Three specialized versions of the GIN model are now presented. Each of these models is formed by restricting the previous model. The first specialized version restricts each burst to be composed of sample functions selected from the same ensemble $\{G_1(t), G_2(t),..., G_N(t)\}$, and will be identified as the GIN (Single Ensemble) model. This allows a noise burst to be represented by

$$b_k(t) = \sum_{j=1}^{NG} I_{kj} g_j(t-T_{kj}) \ , \qquad (2.5)$$

where the k subscript for $g_j(t)$ used in (2.3) can be omitted since each burst is formed from the same ensemble. The second specialized model is obtained by adding the additional restriction that each burst contains exactly one sample function. Thus,

$$n(t) = \sum_{k=1}^{NB} I_k g_1(t-T_k) \ . \qquad (2.6)$$

Note that $g_1(t-T_k)$ is randomly selected from the same ensemble of sample functions for each value that k assumes. This model will be called the

GIN (Single Function) model. The third specialized version restricts the sample function of (2.6) to be the same waveform f(t) for each occurence, i.e.,

$$n(t) = \sum_{k=1}^{NB} I_k f(t-T_k) \ . \qquad (2.7)$$

This is identified as the GIN (Unique Waveform) model. If f(t) is chosen to represent the channel unit-impulse response then (2.7) is similar to the model used by Bellow & Esposito [12] and to the model suggested by Fennick [1,20]. The idealized impulse used by Ziemer [10] and Houts & Moore [11] can be obtained by setting $f(t)=\delta(t)$.

Some of the important properties of these noise models are presented in Section 2.3. It is shown in Chapter 3 that the performance analysis for the GIN (Unique Waveform) model can be extended to include the other models as well.

2.3 NOISE CHARACTERISTICS

Several plausible assumptions will be made concerning the random variables involved in the GIN model. Also, the power-density spectrum and the p.d.f. for the GIN (Unique Waveform) model will be determined as functions of the various noise parameters.

The reasonable hypothesis that each sample functions, $g_{kj}(t-T_{kj})$, is equally likely to occur at any time in the burst time range, 0 to TF_k, leads to a uniform distribution for T_{kj}, i.e.,

$$p_T(\alpha) = \frac{1}{TF_k} , \quad 0 \leq \alpha \leq TF_k . \tag{2.8}$$

Consequently, for statistically independent occurrence times a Poisson distribution with the average occurrence rate ν can be assumed for the number of waveforms, NG, in a burst time TF_k, i.e.,

$$P[NG=m] = \frac{(\nu\ TF_k)^m}{m!}\ e^{-\nu TF_k} . \tag{2.9}$$

A similar result applies to the number of noise bursts in time T_n if the bursts are equally likely to occur at any time.

The p.d.f. descriptions for the random variables associated with burst type, sample function selection, and the weighting factor are established by the particular system being analyzed. However, it will be assumed that the weighting factor p.d.f., $p_{I_{kj}}(i)$, is symmetrical about a zero mean. This allows both positive and negative versions of the noise waveforms $g_{kj}(t)$. It is assumed that the statistical descriptions of the noise parameters are not time dependent. For some systems this will be a valid assumption, while for others it is an approximation that must be limited to short time periods.

It is shown in Appendix A that the GIN (Unique Waveform) model yields a one-sided power-density spectrum given by

$$S_n(f) = 2\ \nu_B \sigma^2 |F(f)|^2 , \tag{2.10}$$

where ν_B is the average occurrence rate of the bursts, σ^2 is the variance of each weighting factor I_{kj}, and F(f) is the Fourier transform

of the noise waveform f(t). The result of (2.10) can be extended to the GIN (Single Function) model by taking the expected value with respect to the waveform type, cf., (A.11). Note that the power-density spectrum of (2.10) depends on the sample function and is a function of frequency, i.e., the spectrum is not necessarily white. For the special case where $f(t)=\delta(t)$, then $F(f)=1$ and white noise results since $S_n(f)=2\nu_b\sigma^2$. Similar results have been given for the idealized impulse noise model by Ziemer [10] and Houts & Moore [11].

The performance results obtained for impulse noise can be compared with those for AWG noise, by relating the dependent variables. The convention established for AWG noise is to plot the error probability as a function of signal-to-noise ratio, defined as the ratio of the average signal energy, E_{AVG}, to the one-sided noise power-density spectrum, N_o, i.e.,

$$SNR = \frac{E_{AVG}}{N_o} . \tag{2.11}$$

Previous results [11] have shown that the error performance for additive idealized impulse noise depends on an energy-to-noise parameter (ENP), viz.,

$$ENP = \frac{E_{AVG}T_b}{\sigma^2} , \tag{2.12}$$

where T_b is the bit time. Thus for the idealized impulse noise,

$$ENP = 2\ \nu_B T_b\ SNR . \tag{2.13}$$

For colored Gaussian noise the performance is expressed as a ratio of signal power to noise power contained in some specified bandwidth. The comparison of SNR and ENP for generalized impulse noise would be more complicated than the simple relation shown by (2.13) and will not be determined in this work.

An interesting characteristic which can be obtained for the GIN (Unique Waveform) model is the first-order p.d.f. for the noise $n(t)$, i.e., $p_n(\alpha)$. Following the lead of Rice [35], Middleton [36], and Ziemer [10], it is shown in Appendix A that when the number of noise bursts in time T_n is modeled by a Poisson process with average rate ν_B, then

$$p_n(\alpha) = \lambda_2^{-1/2}\,\psi^{(0)}(x) + \frac{\lambda_3\lambda_2^{-2}}{3!}\,\psi^{(3)}(x) + \left[\frac{\lambda_4\lambda_2^{-5/2}}{4!}\,\psi^{(4)}(x) + \frac{\lambda_3^2\lambda_2^{-7/2}}{72}\,\psi^{(6)}(x)\right] + \ldots, \tag{2.14}$$

where
$$\lambda_m = \nu_B E\{I^m\} \int_0^{T_n} f^m(t-\tau)\, d\tau, \tag{2.15}$$

and
$$\psi^{(k)}(x) = \frac{1}{\sqrt{2\pi}} \frac{d^k}{dx^k}\left[e^{-x^2/2}\right]; \quad x = \alpha/\sqrt{\lambda_2}. \tag{2.16}$$

The first term in $p_n(\alpha)$ is of order $\nu_B^{-1/2}$, the second term of order ν_B^{-1}, and the third term enclosed by the brackets is of order $\nu_B^{-3/2}$. Also, the first term assumes the form of a Gaussian distribution, thus the remaining terms show how $p_n(\alpha)$ approaches Gaussian as ν_B increases.

If the Poisson process assumption used to establish (2.14) is replaced with the assumption that at most one noise burst can occur in time T_n, the p.d.f. becomes

$$p_n(\alpha) = P[NB=0]\ \delta(\alpha) + \frac{P[NB=1]}{T_n} \int_{-\infty}^{\infty} \int_{0}^{T_n} p_I(i)\ \delta(\alpha - if(t-\tau))\ d\tau di\ . \qquad (2.17)$$

In receivers where the bit decision is based on sampling the received signal and comparing to a voltage threshold, the p.d.f.'s of (2.14) and (2.17) could be used to determine the probability of error. Using (2.17), the probability that the noise exceeds a positive threshold V_{th} is

$$\int_{V_{th}}^{\infty} p_n(\alpha)\ d\alpha = \frac{P[NB=1]}{T_n} \iint_{R_{th}} p_I(i)\ d\tau di, \qquad (2.18)$$

where the region R_{th} is defined such that $i \cdot f(t-T_1) > V_{th}$. The performance of a correlation receiver is determined in Chapter 3.

CHAPTER 3

CORRELATION RECEIVER PERFORMANCE ANALYSIS

The expression for the error performance is derived for a digital system that uses a correlation receiver. Although the derivation is limited to the GIN (Unique Waveform) model, a procedure is presented for extending the results to the unrestricted GIN model. The error performance is bounded by a function of the average signal energy, the signal set correlation coefficient, and the variance and p.d.f. description of the noise weighting factor. The bound dependence on the p.d.f. is removed by applying Chebyshev's inequality.

3.1 GENERAL OBSERVATIONS

A method for judging the error performance of a digital system is presented in the section. Subsequently, the analysis for the GIN model is obtained in terms of the GIN (Unique Waveform) model. The effect of the communication channel on the analysis of the correlation receiver is discussed. Several assumptions regarding the GIN (Unique Waveform) model parameters are summarized for use in the derivation of Section 3.2.

3.1.1 Performance Criterion

Two performance criteria were considered for use in this work: namely, the probability of bit error and the expected number of bits in error given a burst has occurred. The probability of bit error is used extensively for AWG noise analysis. There is some precedent [6,9-12] for using this criterion in impulse noise analysis; however, the more definitive criterion of the expected number of bits in error per noise burst has been employed [20,24] and will be used in this work. Each method allows an easy comparison of theoretical and experimental results, since the difference between the experimental numerical average and the theoretical statistical probability can be made arbitrarily small as the number of observations is increased. The expected number of bits in error per noise burst can be converted to the probability of bit error by multiplying by the probability of a noise burst and dividing by the expected number of bits transmitted during the burst. The relative performance of various signaling methods will be based on equal average signal energy.

3.1.2 Rational for Unique Waveform Restriction

The performance analysis for the GIN model is reduced to the analysis for the GIN (Unique Waveform) model through a series of conditional probability steps. The expected number of bit errors per noise burst, $E\{N\}$, can be represented as a summation of terms that are conditioned on the type of noise burst,

$$E\{N\} = \sum_{j} E\{N \mid \text{Burst Type } j\} \; P\{\text{Burst Type } j\} \; . \tag{3.1}$$

The evaluation procedure for each conditional term, $E\{N \mid \text{Burst Type } j\}$, would be identical to that used for the GIN (Single Ensemble) model where only one burst type is allowed. The analysis procedure can be further simplified by assuming that the waveforms within a noise burst do not overlap. Consequently, the total number of bits in error per noise burst, N, is equal to the sum of N_m, the number of bits in error due to each waveform, viz,

$$N = N_1 + N_2 + \ldots + N_m + \ldots + N_{NG}. \tag{3.2}$$

Furthermore, the expected value of N can be written in terms of the number of waveforms per burst, NG, as

$$E\{N\} = \sum_{i=1}^{\infty} E\{N \mid NG=i\} \; P[NG=i]. \tag{3.3}$$

Using (3.2) to express $E\{N \mid NG=i\}$ gives

$$E\{N\} = \sum_{i=1}^{\infty} P[NG=i] \sum_{m=1}^{i} E\{N_m\} \; . \tag{3.4}$$

The evaluation of $E\{N_m\}$ is conditioned on the type of sample function, $G_k(t)$, that occurs and the probability of the occurrence, i.e.,

$$E\{N_m\} = \sum_{k=1}^{NE} E\{N_m \mid G_k(t)\} \; P[G_k(t)], \tag{3.5}$$

where NE is the number of sample functions in the ensemble. Assuming that the probability $P[G_k(t)]$ is the same for each waveform in the burst, it follows that $E\{N_1\} = E\{N_j\}$, $j = 2,3,\ldots$. Consequently, it follows from (3.4) that the expected number of bit errors per noise burst is

$$E\{N\} = \sum_{i=1}^{\infty} i\ P[NG=i] \sum_{k=1}^{NE} E\{N_1|G_k(t)\}\ P[G_k(t)]. \tag{3.6}$$

This can be written as

$$E\{N\} = E\{NG\} \sum_{k=1}^{NE} E\{N_1|G_k(t)\}\ P[G_k(t)]. \tag{3.7}$$

The evaluation of the terms within the summation would be the same as for the GIN (Single Function) model, while the evaluation of each $E\{N_1|G_k(t)\}$ would use the same procedure as for the GIN (Unique Waveform) model. Consequently, a procedure for determining the error performance of a signal set in the presence of noise described by the GIN (Unique Waveform) model can be extended to noise described by the GIN model.

The expected number of bits in error per noise burst which contains one unique waveform, i.e., the GIN (Unique Waveform) model, will be determined by considering each bit that the noise waveform could possibly effect. The data bit which is present at the time of occurrence of the noise waveform will be identified as B_1. The bits are numbered consecutively through the K^{th}-bit, B_K, which is the last bit that the noise burst can overlap. An expression for the number of bits in error due to the waveform can be written as

$$N_1 = \sum_{m=1}^{K} x_m, \tag{3.8}$$

where x_m=1 if the m^{th} bit is in error and x_m=0 otherwise. The expected number of bits in error per noise burst, $E\{N_1\}$, is obtained from (3.8) by recognizing that the expected value of a sum of random variables is equal to the sum of the expected values. Using the notation $E\{x_m\}=P[\varepsilon_m]$, i.e., the expected value of x_m is the probability of error for the m^{th} bit, gives

$$E\{N\} = E\{N_1\} = \sum_{m=1}^{K} P[\varepsilon_m] \ . \tag{3.9}$$

3.1.3 Channel and Receiver Considerations

The digital communication system shown in Fig. 3-1 has been selected for analysis. The effect of the linear time-invariant channel response, h(t), is resolved prior to the error performance derivation in Section 3.2. The channel output, $r^o(t)$ can be written as the convolution of the input signal, r(t) and the channel unit-impulse response, h(t), i.e.,

$$r^o(t) = r(t)*h(t) = s_j(t)*h(t) + n(t)*h(t) = s_j^o(t) + n^o(t) \ . \tag{3.10}$$

If the noise is AWG, the minimum probability of bit error is obtained by using the filtered-reference correlation receiver [37]. No claim of optimality is made when impulse noise is added to the channel. The effect of the channel on impulse noise is to change the waveforms in

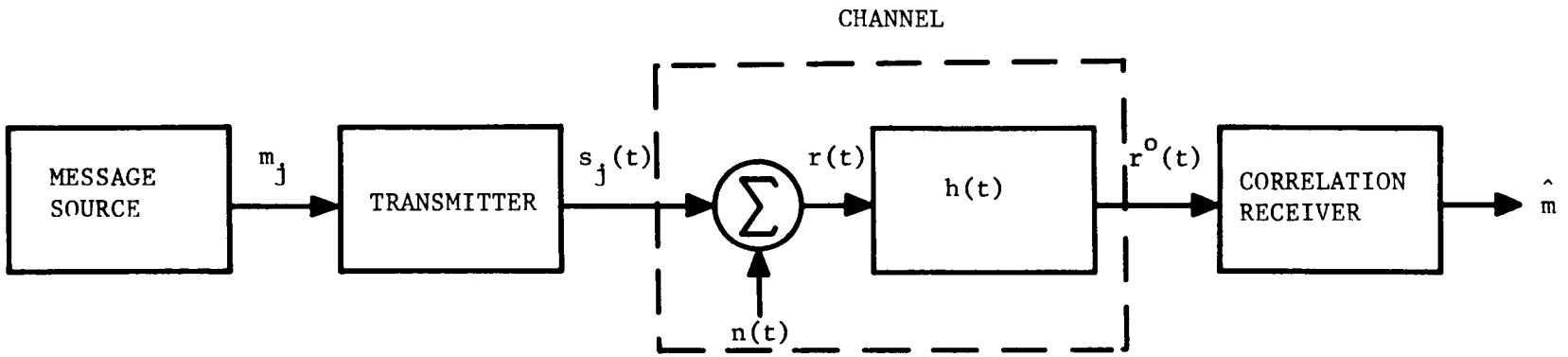

Fig. 3-1. Digital Communication System

the set $\{G_1(t), G_2(t),..., G_{NE}(t)\}$ from which n(t) is composed. Although the channel changes the signal and noise waveforms, the performance analysis procedure for the receiver remains the same. Consequently, the channel response, h(t), will be ignored.

3.1.4 Assumptions Regarding Noise Parameters

The GIN (Unique Waveform) model involves four parameters, i.e., the number of noise bursts NB, the unique waveshape f(t), the occurrence time of the burst T, and the weighting factor I. The following assumptions regarding these parameters are used in Sections 3.2 and 3.3: (1) the weighting factor I is symmetrically distributed and has zero mean, (2) the occurrence time of a burst is uniformly distributed over the bit time in which it occurs, (3) the waveform f(t) has unit energy and the p.d.f. for I is determined from a histogram of the square root of the energy in the weighted waveforms, and (4) no more than one noise burst can occur in a bit interval.

3.2 DERIVATION OF GENERALIZED ERROR PERFORMANCE EQUATION

The digital system shown in Fig. 3-1 and the optimum Gaussian correlation receiver of Fig. 3-2 are used in the evaluation of $P[\varepsilon_m]$. The first step is to find an expression for error probability in terms of the receiver conditional decision statistic, D^j, j=0, 1, which represents the decision statistic, D, given that message symbol m_j was selected at the source. The second step uses a sequence of conditional

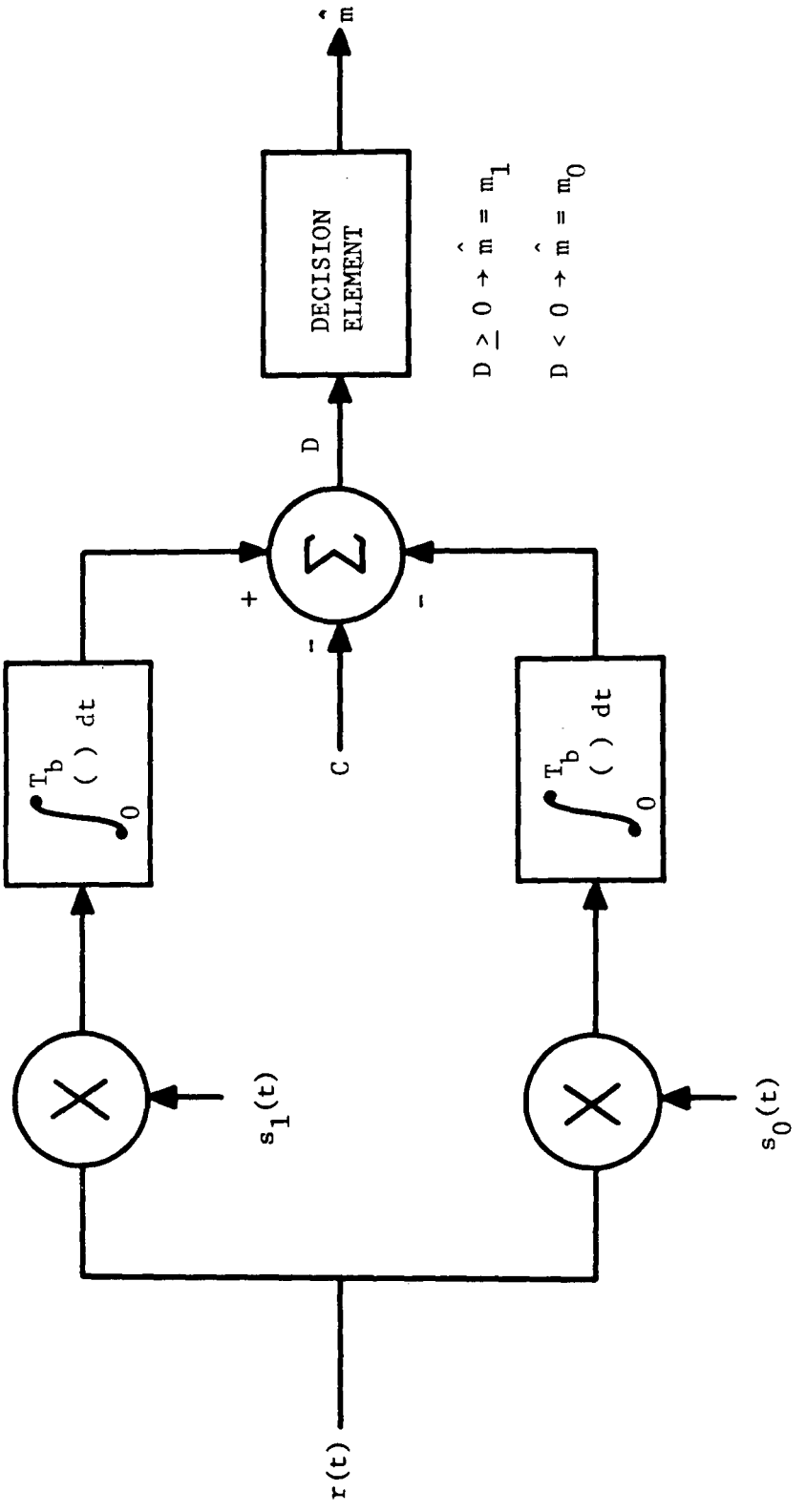

Fig. 3-2. Correlation Receiver

probability operations to establish a form for the conditional error probability. The third step is to normalize the error performance equation and simplify the results by introducing the time range function $T_R(i)$.

3.2.1 Error Performance in Terms of Receiver Decision Statistic

The receiver decision statistics for the m^{th} bit which the noise waveform affects can be written as

$$D = \int_{(m-1)T_b}^{mT_b} r(t)[s_1(t) - s_0(t)]\, dt - C \,. \tag{3.11}$$

For the Gaussian noise the bias term C is given by

$$C = \frac{E_1 - E_0}{2} - \frac{N_o}{2} \ln\left[\frac{P[m_0]}{P[m_1]}\right] , \tag{3.12}$$

where E_j, j=0,1, represents the energy of $s_j(t)$ and N_o is the one-sided noise power-density spectrum. For equal message probabilities the bias term reduces to

$$C = \frac{E_1 - E_0}{2} \,. \tag{3.13}$$

The assumption that $P[m_0] = P[m_1]$ will be used throughout the remaining analysis. Restating (3.11) with the substitution

$$r(t) = s_j(t) + n(t), \tag{3.14}$$

and using a correlation coefficient ρ defined by

$$\rho = \frac{1}{E_1}\int_0^{T_b} s_0(t)s_1(t)\ dt\ , \tag{3.15}$$

yields after straightforward manipulation the receiver conditional decision statistic D^j, viz.,

$$D^j = \int n(t)[s_1(t) - s_0(t)]\ dt - C_j\ . \tag{3.16}$$

The limits of integration have been dropped and are understood to be over the bit interval, and

$$C_j = C - (-1)^j(\rho E_1 - E_j)\ . \tag{3.17}$$

Substituting (3.13) for C it can be shown that

$$C_0 = -C_1 = \frac{(1-2\rho)E_1 + E_0}{2}\ . \tag{3.18}$$

Replacing n(t) in (3.16) with the GIN (Unique Waveform) model of (2.7), i.e.,

$$n(t) = \sum_{k=1}^{NB} I_k f(t-T_k)\ , \tag{3.19}$$

gives

$$D^j = \sum_{k=1}^{NB} I_k \int f(t-T_k)[s_1(t) - s_0(t)]\ dt - C_j\ . \tag{3.20}$$

Considerable simplification results when it is assumed that at most one burst can occur during a bit interval. Conditioning D^j on this assumption gives

$$D^j|(NB=1) = I_1 \int f(t-T_1)[s_1(t) - s_0(t)]\, dt - C_j \ ,$$
$$D^j|(NB=0) = -C_j \ . \tag{3.21}$$

It has been shown [11] that (3.21) can be used to form a lower bound to error performance when the number of bursts, NB, is described by the Poisson distribution. Furthermore, it was shown that the lower bound becomes a good approximation as the product of the average occurrence rate ν_B and the bit time T_b becomes small, i.e., $\nu_B T_b << 1$.

Considering the receiver decision rule from Fig. 3-2, i.e.,

$$D \geq 0 \text{ assign output to } m_1$$
$$D < 0 \text{ assign output to } m_0 \ , \tag{3.22}$$

it follows that the probability of error conditioned on message symbol m_j can be expressed as

$$P[\varepsilon_m|m_j] = P[(-1)^j D^j > 0], \quad j = 0,1 \tag{3.23}$$

and the total probability of bit error is given by

$$P[\varepsilon_m] = \sum_{j=0}^{1} P[\varepsilon_m|m_j]\, P[m_j] \ . \tag{3.24}$$

3.2.2 Conditional Bit Error Probability Formulation

Two conditional probability operations are performed on (3.23) in order to obtain results which depend on the p.d.f. descriptions for the weighting factor and occurrence time.* First the expression involving D^j is conditioned on whether or not a burst occurs, i.e.,

$$P[(-1)^j D^j > 0] = \sum_{k=0}^{1} P[(-1)^j D^j > 0 \,|\, NB=k]\; P[NB=k] \; . \tag{3.25}$$

For k=0, it is obvious that no error can occur since from (3.21)

$$D^j \,|\, (NB=0) = -C_j \; . \tag{3.26}$$

Thus,

$$P[(-1)^j D^j > 0] = P[(-1)^j D^j > 0 \,|\, NB=1]\; P[NB=1] \; . \tag{3.27}$$

A normalized probability of error is defined to help simplify the notation, i.e.,

$$P_1[\varepsilon_m | m_j] = \frac{P[\varepsilon_m | m_j]}{P[NB=1]} = P[(-1)^j D^j > 0 \,|\, NB=1]. \tag{3.28}$$

The expression for the decision statistic given that one burst has occurred is obtained from (3.21), namely

$$D^j \,|\, (NB=1) = I \int f(t-T)[s_1(t) - s_0(t)]\, dt - C_j, \tag{3.29}$$

---

*An alternative method is presented in Appendix B.

where the 1 subscripts for I and T have been dropped. The integral over the bit interval is represented as

$$V\ F(T) = \int f(t-T)[s_1(t) - s_0(t)]\ dt\ , \tag{3.30}$$

where V is the magnitude of the peak voltage of $s_1(t)$ and/or $s_0(t)$. It follows that

$$D^j\,|\,(NB=1) = I\ V\ F(T) - C_j \tag{3.31}$$

and

$$P_1[\varepsilon_m|m_j] = P[(-1)^j\ I\ V\ F(T) > (-1)^j\ C_j]\ . \tag{3.32}$$

Since $C_0=-C_1$, it follows that the term $(-1)^j\ C_j$ can be replaced by C_0, hence

$$P_1[\varepsilon_m|m_j] = P[(-1)^j\ I\ F(T) > C_0/V]\ . \tag{3.33}$$

The right side of (3.33) can be expressed as the marginal probability form of a mixed mode probability density function, viz.,

$$P[(-1)\ I\ F(T) > C_0/V] =$$

$$\int_i \int_\tau P[(-1)^j\ i\ F(\tau) > C_0/V\,|\,I=i,T=\tau]p_I(i)p_T(\tau)\ d\tau di\ . \tag{3.34}$$

Given values for I and T, the conditional probability term within the integrals of (3.34) will equal unity if $(-1)^j\ i\ F(\tau) > C_0/V$ and zero

otherwise. Thus the integrals over i and τ can be restricted to the region R_j where this inequality is true, yielding

$$P_1[\varepsilon_m|m_j] = \iint_{R_j} p_I(i)p_T(\tau)\, d\tau di \ . \tag{3.35}$$

3.2.3 Normalized Bit Error Probability Formulation

The bit error probability, $P[\varepsilon_m]$, is obtained by invoking the assumption that I is symmetrically distributed, i.e., $p_I(i)=p_I(-i)$. It follows from (3.34) that

$$P[I\ F(T) > C_0/V] = P[I\ F(T) < -C_0/V] \ . \tag{3.36}$$

Consequently, substituting (3.33) and (3.36) into (3.24) yields

$$\begin{aligned} P_1[\varepsilon_m] &= \Big[P[m_0] + P[m_1]\Big]\, P_1[\varepsilon_m|m_0] \\ &= \iint_{R_0} p_I(i)p_T(\tau)\, d\tau di \ . \end{aligned} \tag{3.37}$$

Assuming that T is uniformly idstributed over a bit interval T_b, then integrating over τ where $i\ F(\tau) > C_0/V$ gives time ranges $T_{RN}(i)$ and $T_{RP}(i)$ which depend respectively on the negative and positive values of i. Hence,

$$P_1[\varepsilon_m] = \frac{1}{T_b}\int_{-\infty}^{0} T_{RN}(i)p_I(i)\ di + \frac{1}{T_b}\int_{0}^{\infty} T_{RP}(i)p_I(i)\ di$$

$$= \frac{1}{T_b}\int_{0}^{\infty} [T_{RN}(-i) + T_{RP}(i)]p_I(i)\ di\ , \qquad (3.38)$$

where the last equality follows by changing variables and using $p_I(i)$ $= p_I(-i)$. Let F_{max} represent the maximum value of $|F(\tau)|$, and set

$$I_{min} = \frac{C_0}{V\ F_{max}}\ . \qquad (3.39)$$

For values of $i < I_{min}$ both $T_{RN}(-i)$ and $T_{RP}(i)$ are equal to zero. Let $T_R(i)$ represent the sum of the time range functions. Thus,

$$P_1[\varepsilon_m] = \frac{1}{T_b}\int_{I_{min}}^{\infty} T_R(i)p_I(i)\ di\ . \qquad (3.40)$$

It is possible to determine $T_R(i)$ without first determining $T_{RN}(-i)$ and $T_{RP}(i)$. This requires that the integration over τ in (3.37) be performed such that $i|F(\tau)|>C_0/V$.

It is convenient to transform I into a normalized (unit variance) random variable N. Using the change in variables $N = I/\sigma$ yields a density function $p_N(n)$ which is equal to $\sigma p_I(\sigma n)$. Consequently, (3.40) can be expressed as

$$P_1[\varepsilon_m] = \frac{1}{T_b}\int_{I_{min}/\sigma}^{\infty} T_R(\sigma n)p_N(n)\ dn. \qquad (3.41)$$

The dependence of the time range $T_R(\sigma n)$ on the variance, can be removed if a new function $T_{R1}(n)$ is determined by integrating over τ such that $n|F(\tau)|>C_0/(\sigma V)$. This gives the desired form for the results as

$$P_1[\varepsilon_m] = \frac{1}{T_b} \int_{I_{min}/\sigma}^{\infty} T_{R1}(n) p_N(n)\, dn \ . \tag{3.42}$$

The analytical evaluation of $T_{R1}(n)$ can be extremely difficult; often, numerical methods are necessary. An illustration of a particular method is shown in Fig. 3-3, where the function $|F(\tau)|$ is plotted versus τ for $0 \leq \tau \leq T_b$. First, a set of K values for n, $\{n_1, n_2, \ldots, n_K\}$, are chosen and the corresponding set of slice levels $\{SL_1, SL_2, \ldots, SL_K\}$ are calculated from the expression

$$SL_k = \frac{C_0}{\sigma V n_k} , \quad k = 1,2,\ldots, K \ . \tag{3.43}$$

Next, as shown in Fig. 3-3, the plot of $|F(\tau)|$ is compared to each slice level and a set of time range values $\{T_{R1}(n_1), T_{R1}(n_2), \ldots, T_{R1}(n_K)\}$ are calculated. The value obtained in Fig. 3-3 for the time range corresponding to SL_k is

$$T_{R1}(n_k) = (\tau_{k2}-\tau_{k1}) + (\tau_{k4}-\tau_{k3}) \ . \tag{3.44}$$

This data can be used to evaluate (3.42) numerically.

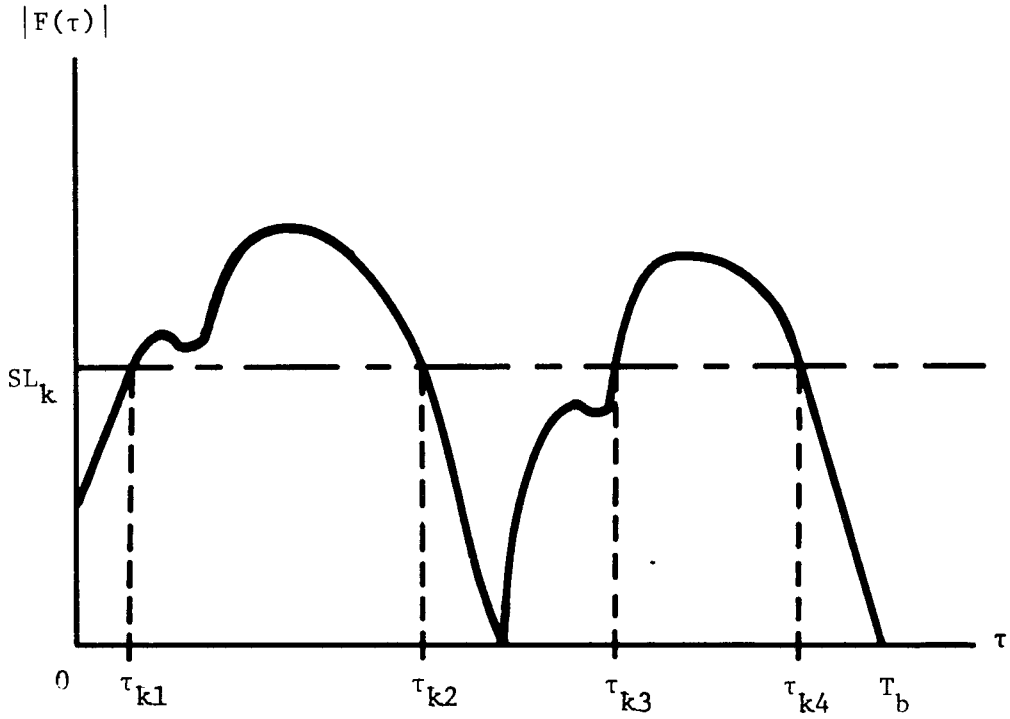

Fig. 3-3. Interpretation of Time Range $T_{R1}(n)$

3.3 PERFORMANCE EQUATIONS FOR SPECIFIC SIGNAL SETS

The performance analysis which culminated in (3.42) used a general form for the signal set $\{s_0(t), s_1(t)\}$. Although many signal sets have been used for binary communications, it is possible to classify them into a few basic catagories. Unfortunately, a standard identification procedure does not exist. For binary signal sets having a correlation coefficient, $\rho=0$ or $\rho=-1$, three clasifications are proposed as follows:

On-Off: $$s_j(t) = jV\psi(t) \quad j = 0,1 \tag{3.45}$$

Antipodal: $$s_j(t) = (-1)^{j+1}V\psi(t) \quad j = 0,1 \tag{3.46}$$

Orthogonal: $$s_j(t) = V\psi_j(t) \quad j = 0,1 \tag{3.47}$$

where $\psi_j(t)$, $j = 0,1$, are orthogonal basis functions. The expression for $F(T)$ as given by (3.30) is simplified for the On-Off ($\rho=0$) and Antipodal ($\rho=-1$) cases, viz.,

$$VF(T) = (1-\rho)V \int f(t-T)\ \psi(t)\ dt$$

$$= (1-\rho)V\ F_1(T)\ . \tag{3.48}$$

Equation 3.48 can be used for Orthogonal signaling ($\rho=0$) by replacing $\psi(t)$ with $\psi_1(t)-\psi_0(t)$. It follows that the time range $T_{R1}(n)$ can be determined from the condition $|F_1(T)| > C_0/[(1-\rho)V\sigma n]$ and that $I_{min}/\sigma = C_0/[(1-\rho)V\sigma F_{1max}]$, where F_{1max} is the maximum value of $|F_1(T)|$.

It is possible to express $C_0/[(1-\rho)V\sigma]$ in terms of the energy-to-noise parameter, ENP, defined by (2.12). First, the average signal energy, E_{AVG}, for equally likely message symbols is defined as

$$E_{AVG} = \frac{E_1 + E_0}{2} . \tag{3.49}$$

For the three classifications under study, C_0, as defined by (3.18), can be expressed in terms of E_{AVG}, viz.,

$$C_0 = (1-\rho)E_{AVG} . \tag{3.50}$$

The voltage V can be written as a function of ENP once the basis functions, $\psi(t)$ and $\psi_j(t)$, are defined. Two functions are considered: namely, $\psi_p(t)$ for a pulse and $\psi_s(t)$ for a sinusoid. They are defined as

$$|\psi_p(t)| = 1 \qquad 0 \leq t < T_b \tag{3.51}$$

and

$$\psi_s(t) = \sin(2\pi f_c t) \qquad 0 \leq t < T_b . \tag{3.52}$$

The corresponding peak voltages, V_p and V_s, for On-Off and Antipodal signaling can be expressed as functions of E_{AVG}, i.e.,

$$V_p = \sqrt{\frac{2\ E_{AVG}}{(1-\rho)T_b}} \tag{3.53}$$

and

$$V_s = \sqrt{\frac{4\ E_{AVG}}{(1-\rho)T_b}} \ . \tag{3.54}$$

Hence, for these two classes of signal sets

$$\frac{C_0}{(1-\rho)\sigma\ V_p} = \sqrt{\frac{(1-\rho)E_{AVG}T_b}{2\sigma^2}} = \sqrt{\frac{(1-\rho)ENP}{2}} \tag{3.55}$$

and

$$\frac{C_0}{(1-\rho)\sigma\ V_s} = \sqrt{\frac{(1-\rho)ENP}{4}} \ . \tag{3.56}$$

It follows from (3.42) that the error performance for the m^{th} bit is given for On-Off or Antipodal pulse signaling as

$$P_1[\varepsilon_m] = \frac{1}{T_b} \int_{\frac{\sqrt{(1-\rho)ENP/2}}{F_{1max}}}^{\infty} T_{R1}(n)\ p_N(n)\ dn \ , \tag{3.57}$$

where $T_{R1}(n)$ is determined such that $n|F_1(\tau)| > \sqrt{(1-\rho)ENP/2}$. For sinusoidal basis functions and the same two signal sets the error performance is given by

$$P_1[\varepsilon_m] = \frac{1}{T_b} \int_{\frac{\sqrt{(1-\rho)ENP/4}}{F_{1max}}}^{\infty} T_{R1}(n)\ p_N(n)\ dn \ , \tag{3.58}$$

where $T_{R1}(n)$ is determined such that $n|F_1(\tau)| > \sqrt{(1-\rho)ENP/4}$. In a similar fashion the result for Orthogonal pulse signaling is

$$P_1[\varepsilon_m] = \frac{1}{T_b} \int_{\frac{\sqrt{ENP}}{F_{1max}}}^{\infty} T_{R1}(n)\ p_N(n)\ dn \ , \tag{3.59}$$

where $T_{R1}(n)$ is determined such that $n|F_1(\tau)| > \sqrt{ENP}$. For Orthogonal sinusoidal signaling the performance is given by

$$P_1[\varepsilon_m] = \frac{1}{T_b} \int_{\frac{\sqrt{ENP/2}}{F_{1max}}}^{\infty} T_{R1}(n)\, p_N(n)\, dn \quad , \tag{3.60}$$

where $T_{R1}(n)$ is determined such that $n|F_1(\tau)| > \sqrt{ENP/2}$.

Two significant distinctions are found in comparison of the impulse noise error probabilities with their equivalent AWG noise expressions. Comparing (3.60) to (3.59) or (3.58) to (3.57) it is seen that the lower limits of integration differ by a factor of $\sqrt{2}$, i.e., the choice of basis function to represent the On-Off, Antipodal, or Orthogonal waveform has an effect on the error performance. This is in contrast to AWG noise results where the performance does not depend on the basis function. Likewise, comparing Orthogonal to On-Off signaling for the same basis function and equal average signal energy, e.g., (3.60) to (3.58), reveals a similar difference in the lower limit. Again this performance discrepancy is in contrast to AWG results. Conversely, from (3.57) or (3.58) a comparison of the performance expressions for Antipodal and On-Off signaling indicates the same 3 dB improvement in ENP for Antipodal as was realized in AWG noise theory. Performance curves for selected noise waveforms and signal sets are presented in Chapter 4.

3.4 DERIVATION OF PERFORMANCE BOUNDS

There is motivation for bounding the error performance results since determining the noise waveshapes can be extremely difficult,

and the results must be specialized for each communication system considered. In this section, an error performance bounding procedure is developed using an upper bound, B^j, on the receiver decision statistic, D^j. In particular V·F(T), cf., (3.30), is bounded by applying the Schwarz inequality, i.e.,

$$V \cdot F(T) = \int f(t-T)[s_1(t)-s_0(t)]\, dt$$

$$\leq \sqrt{\int f^2(x-T)\, dx \int [s_1(y)-s_0(y)]^2\, dy}. \qquad (3.61)$$

Assuming that the p.d.f. for the weighting factor is determined from the square root of the energy contained in the weighted waveforms yields

$$\int_{(m-1)T_b}^{mT_b} f^2(t-T)\, dt \leq \int_{-\infty}^{\infty} f^2(t)\, dt = 1 \; . \qquad (3.62)$$

It follows from substitution of (3.62) into (3.61) that

$$V \cdot F(T) \leq \sqrt{(1-2\rho)E_1 + E_0} \; . \qquad (3.63)$$

Consequently, using (3.63) in (3.31) it follows that an upper bound B^j can be defined as

$$B^j = I\sqrt{(1-2\rho)E_1 + E_0} - C_j \geq D^j \,|\, (NB=1) \; . \qquad (3.64)$$

The probability that $(-1)^j B^j > 0$ is greater than or equal to the probability that $(-1)^j D^j | (NB=1) > 0$. Hence, the error performance, as given by (3.28), can be bounded by

$$P_1[\varepsilon_m | m_j] \leq P[(-1)^j B^j > 0] = P[I > \sqrt{[(1-2\rho)E_1 + E_0]/4}] \ . \quad (3.65)$$

For On-Off, Antipodal, and Orthogonal signal sets it follows from (3.50), after changing to the normalized random variable $N=I/\sigma$, that

$$P_1[\varepsilon_m | m_j] \leq P[N > \sqrt{(1-\rho)E_{AVG}/(2\sigma^2)}] \ . \quad (3.66)$$

This result is independent of m_j, thus

$$P_1[\varepsilon_m] \leq \int_{\sqrt{\frac{(1-\rho)E_{AVG}}{2\sigma^2}}}^{\infty} p_N(n)\, dn \ . \quad (3.67)$$

This bound does not depend on the noise waveform, but the p.d.f. for the weighting factor must be known. A bound that is independent of $p_N(n)$ can be obtained for (3.67) by applying Chebyshev's inequality, which for a zero mean, unit variance, symmetrically distributed random variable states

$$P[|N| \geq L] = \frac{1}{2} P[N \geq L] \leq \frac{1}{2L^2} \ . \quad (3.68)$$

Applying (3.68) to (3.67) yields

$$P_1[\varepsilon_m] \leq \int_{\sqrt{\frac{(1-\rho)E_{AVG}}{2\sigma^2}}}^{\infty} p_N(n)\, dn \leq \frac{\sigma^2}{(1-\rho)E_{AVG}} . \qquad (3.69)$$

These results are presented in Fig. 3-4 for the five two-sided p.d.f.s of Table 3.1. A comparison of the bounds to performance results for specific signal sets is presented in Chapter 4.

TABLE 3.1

NORMALIZED PROBABILITY DENSITY FUNCTIONS

Distribution	Density Function $p_N(n)$	Restrictions
Gaussian	$\frac{1}{\sqrt{2\pi}} \exp[-n^2/2]$	
Rayleigh (Two-Sided)	$\lvert n \rvert \exp[-n^2]$	
Lognormal (Two-Sided)	$\frac{1}{2\sqrt{2\pi}\,\alpha\,\lvert n \rvert} \exp\left[-\frac{[\ln\lvert n \rvert + \alpha^2]^2}{2\alpha^2}\right]$	$\alpha > 0$
Uniform	$\frac{1}{\sqrt{12}}$	$\lvert n \rvert < \sqrt{3}$
Hyperbolic (Two-Sided)	$\frac{1}{\sqrt{2}} \frac{(m-1)[(m-2)(m-3)]^{(m-1)/2}}{[\sqrt{(m-2)(m-3)} + \sqrt{2}\,\lvert n \rvert]^m}$	$3 < m \leq 6$

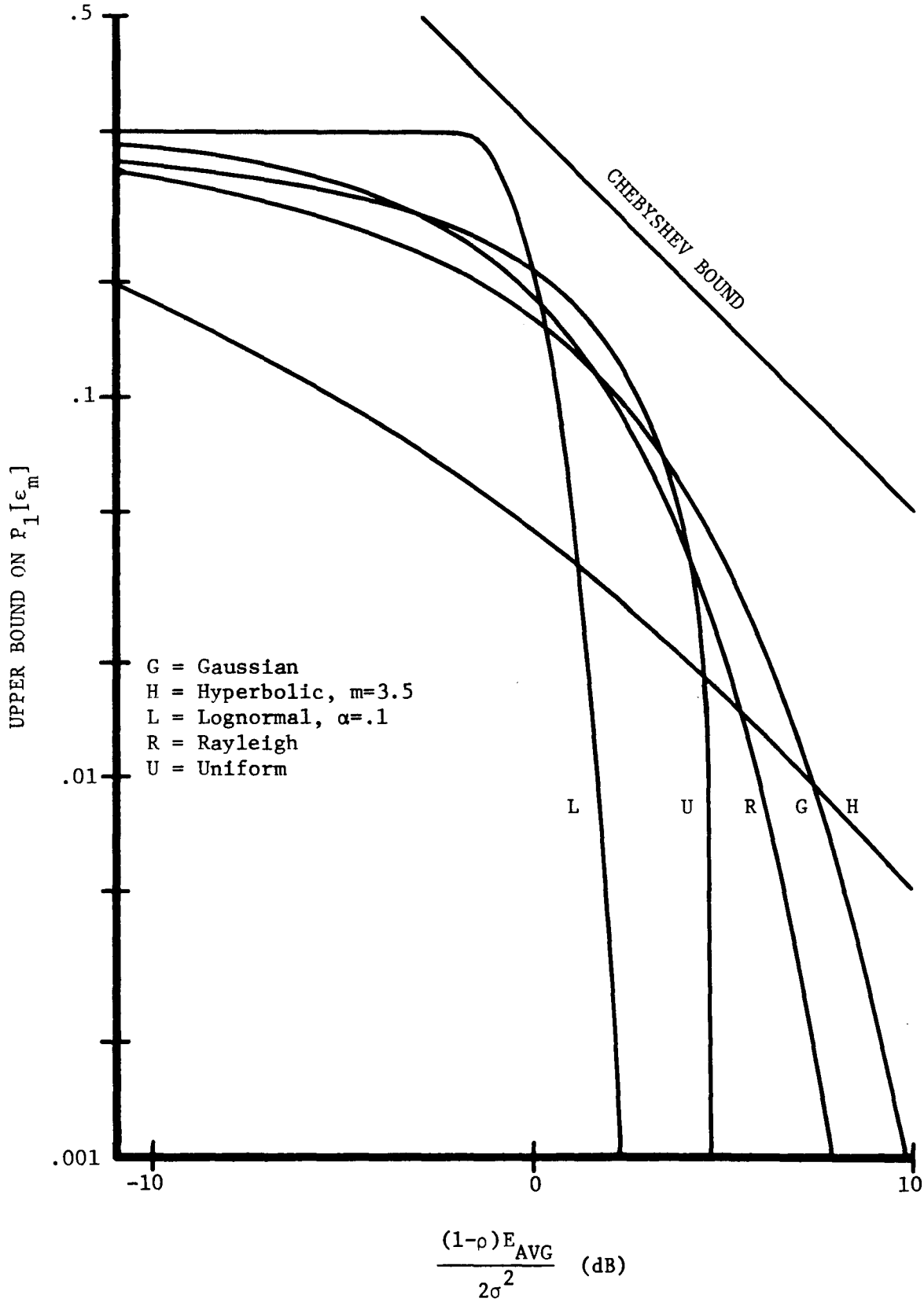

Fig. 3-4. Performance Bounds

CHAPTER 4

SPECIFIC PERFORMANCE RESULTS

Waveforms are chosen for the GIN (Unique Waveform) model and used to calculate numerical performance results, illustrate the effect of the weighting factor p.d.f., compare performances of various signal sets, and study the tightness of the bound curves derived in Chapter 3.

4.1 GENERALIZED IMPULSE NOISE WAVEFORMS

The determination of the impulse noise waveforms present in a communication system requires extensive measurements and the use of special test equipment. Two specific waveforms, a decaying exponential and an exponentially-decaying sinusoid, are selected for closer examination, based upon the measurements on the simulated Space Shuttle data bus [33] and the unit-impulse-response conjecture proposed in Section 2.1.

4.1.1 Decaying Exponential

The decaying exponential is the unit-impulse response of a channel modeled by a first-order Butterworth transfer function. In order to conserve computer time, the waveform is truncated at TF seconds. The expression for the truncated, unit-energy waveform is

$$f(t) = A \exp(-bt), \qquad 0 \leq t \leq TF \tag{4.1}$$

where the decay rate depends on the time constant (1/b) and for the assumption of unit energy

$$A = \sqrt{\frac{2b}{1 - \exp(-2bTF)}} \, . \tag{4.2}$$

Usually the waveform duration (TF) is chosen to equal several time constants. Waveforms are presented in Fig. 4-1 for time constant and duration values that are used in obtaining the performance results of Section 4.2. A unit-energy pulse is shown for comparison. It follows from (4.2) that the noise waveforms have larger peak values as the time constant and duration are decreased.

4.1.2 Exponentially-Decaying Sinusoid

The second unit-energy waveform selected is the truncated, exponentially-decaying sinusoid, i.e.,

$$f(t) = C \sin(2\pi f_o t) \exp(-dt). \qquad 0 \leq t \leq TF \tag{4.3}$$

It is assumed that the waveform duration is a multiple of the sinusoid period, i.e.,

$$TF = \frac{n}{f_o} \, , \qquad n = 1,2,\ldots \tag{4.4}$$

Hence, to preserve the unit-energy assumption it follows that

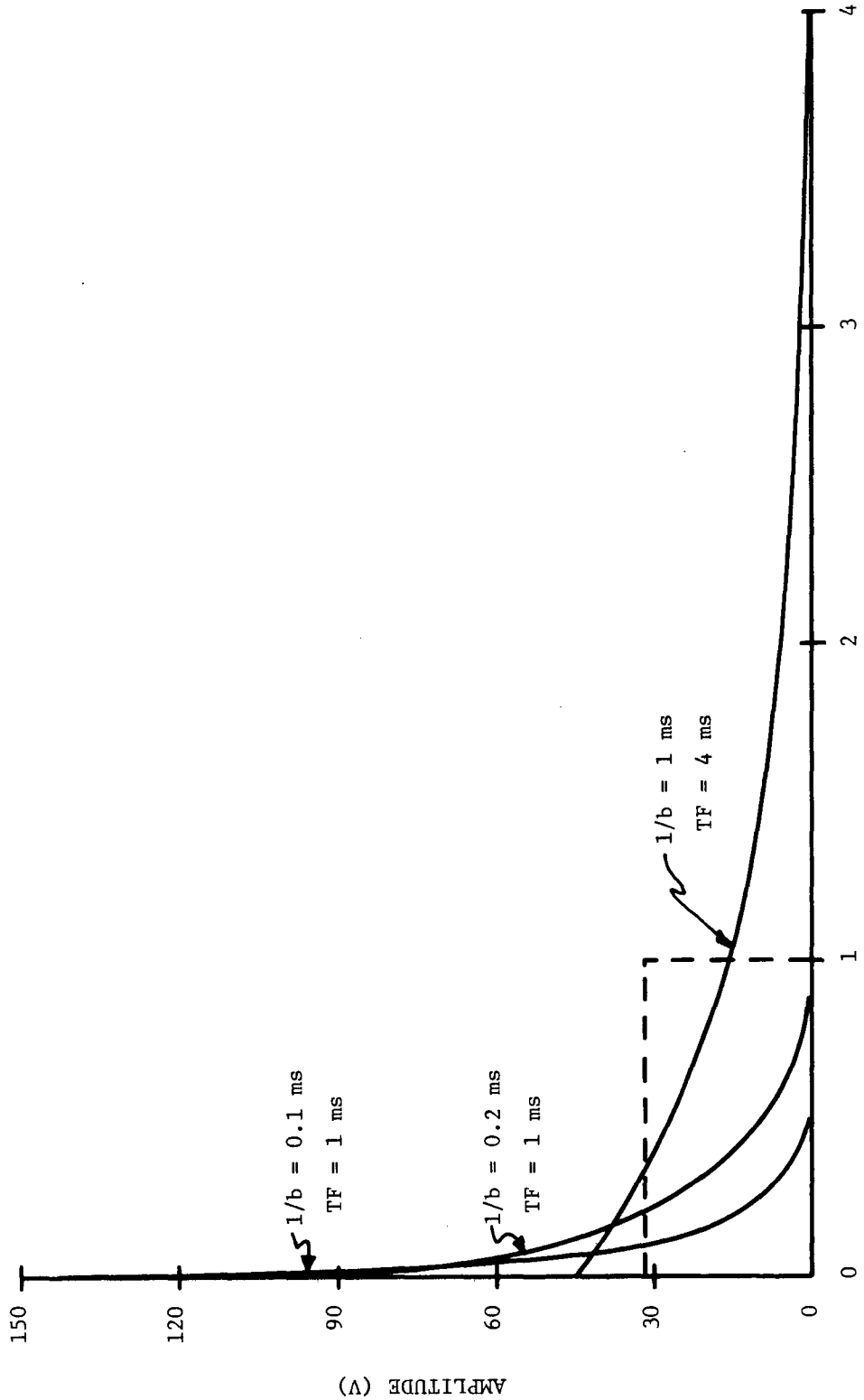

Fig. 4-1. Decaying-Exponential Waveforms

$$C = \frac{1}{\pi f_o}\sqrt{\frac{d[d^2 + 4(\pi f_o)^2]}{[1 - \exp(-2dTF)]}} \qquad (4.5)$$

The values for d, f_o, and TF can be chosen to model both baseband channels without dc response and band-pass channels.

4.2 PERFORMANCE RESULTS FOR DECAYING EXPONENTIAL

Several sets of performance results are presented and comparisons made to illustrate the effect of the weighting factor p.d.f., signal set, and noise waveform. Results for the five signal sets shown in Fig. 4-2 with a 1 ms bit time are obtained using the Fortran-IV computer program GINIMP which is described in Appendix C. A frequency of 1 kHz is used for the ASK and PSK signal sets. For FSK, a frequency of 1 kHz is used for $s_1(t)$ while 2 kHz is used for $s_0(t)$. The program requires approximately 2.5 minutes of IBM System/360 computer time for each overlapped data bit and ENP value analyzed; consequently, only three or four points are computed for each case and a smooth curve drawn through the points to obtain the performance curve. Bound curves are displayed for comparison with the performance results. These bounds are obtained after multiplying the $P_1[\varepsilon_m]$ value obtained from Fig. 3-4 by the number of data bits that the noise waveform can possibly overlap. Although the bounds are not tight, they do have the general shape of the actual performance curves and can be obtained without knowledge of the noise waveform.

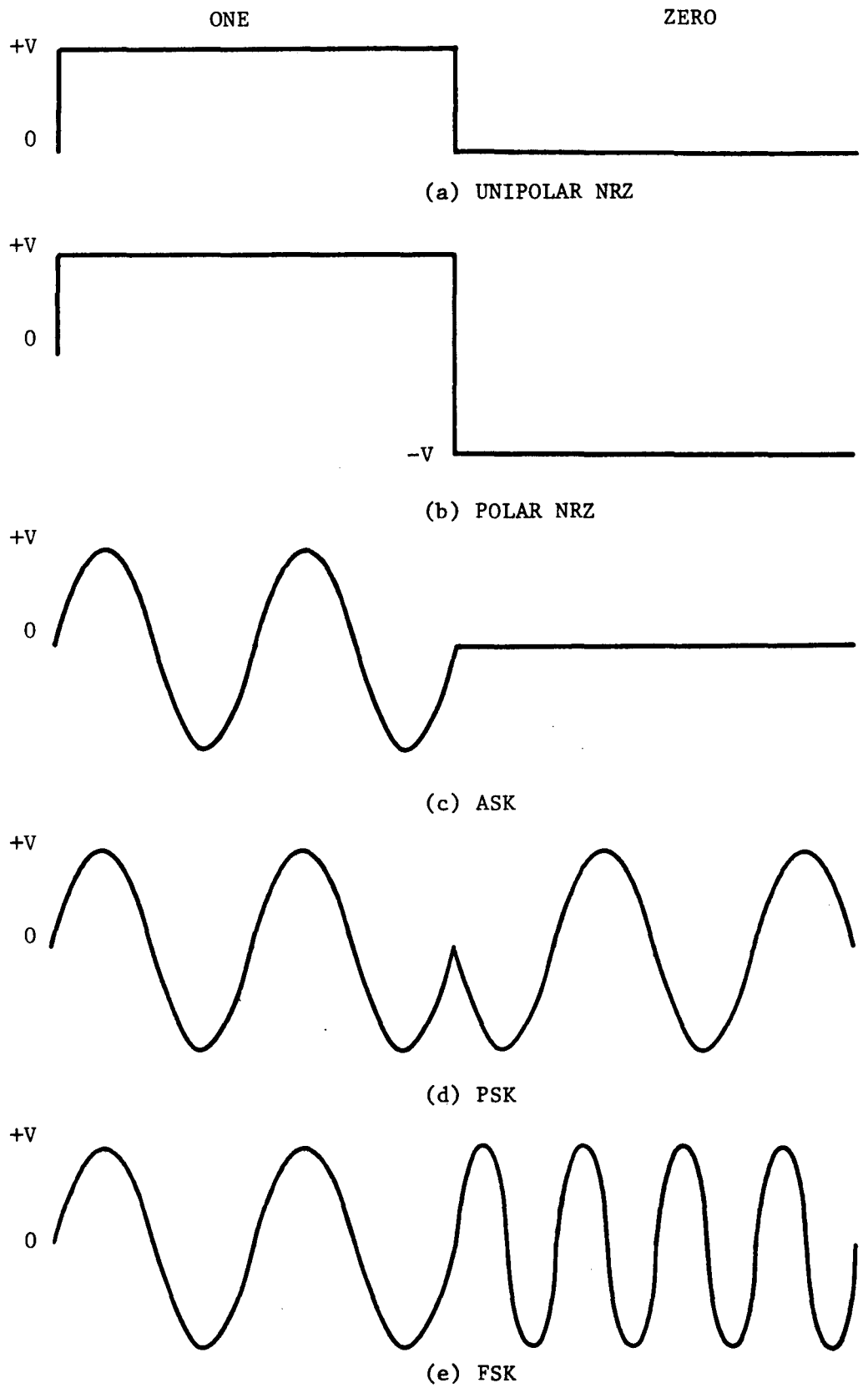

Fig. 4-2. Five Typical Signal Sets

4.2.1 Weighting Factor Distribution

The effect of changing the weighting factor (I) p.d.f. is demonstrated in Fig. 4-3. Unipolar signaling and the decaying-exponential noise waveform with a 0.2 ms time constant are used to obtain performance results for the five weighting factor p.d.f.s of Table 3.1. The Gaussian, Rayleigh, and uniform distributions yield results which are approximately equal. The results for the lognormal and hyperbolic distributions were obtained for parameter values α=0.1 and m=3.5, respectively. The parameter value controls the shape of these p.d.f.s and should have a corresponding control in the shape of the error performance curves. Results for typical parameter values in these distributions and an idealized impulse waveform have been presented by Houts & Moore [11]. The Gaussian p.d.f is selected as being typical and is used exclusively in determining the remaining performance results.

4.2.2 Waveform Time Constant

The effect of changing the decaying-exponential time constant is studied in Fig. 4-4 for Unipolar signaling and a Gaussian p.d.f. It was necessary to increase the waveform duration (TF) for the 1 ms time constant in order to calculate its true impact on the data. The expected number of bit errors increases with the time constant, which is intuitively satisfying since for large time constants the noise waveform more closely approximates the Unipolar

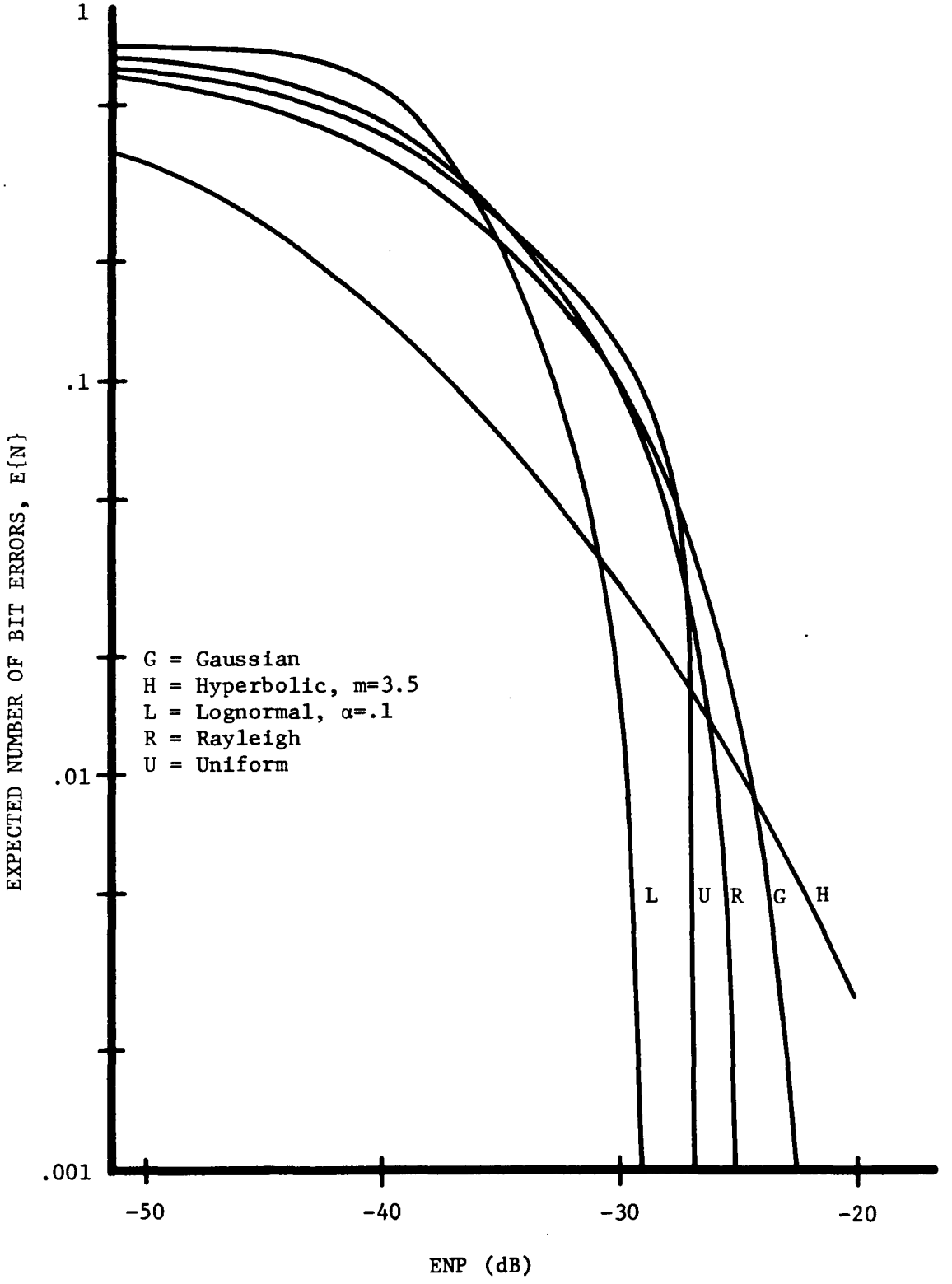

Fig. 4-3. Effect of Weighting Factor P.D.F. on Unipolar Signaling in the Presence of Decaying-Exponential Noise with 0.2 ms Time Constant

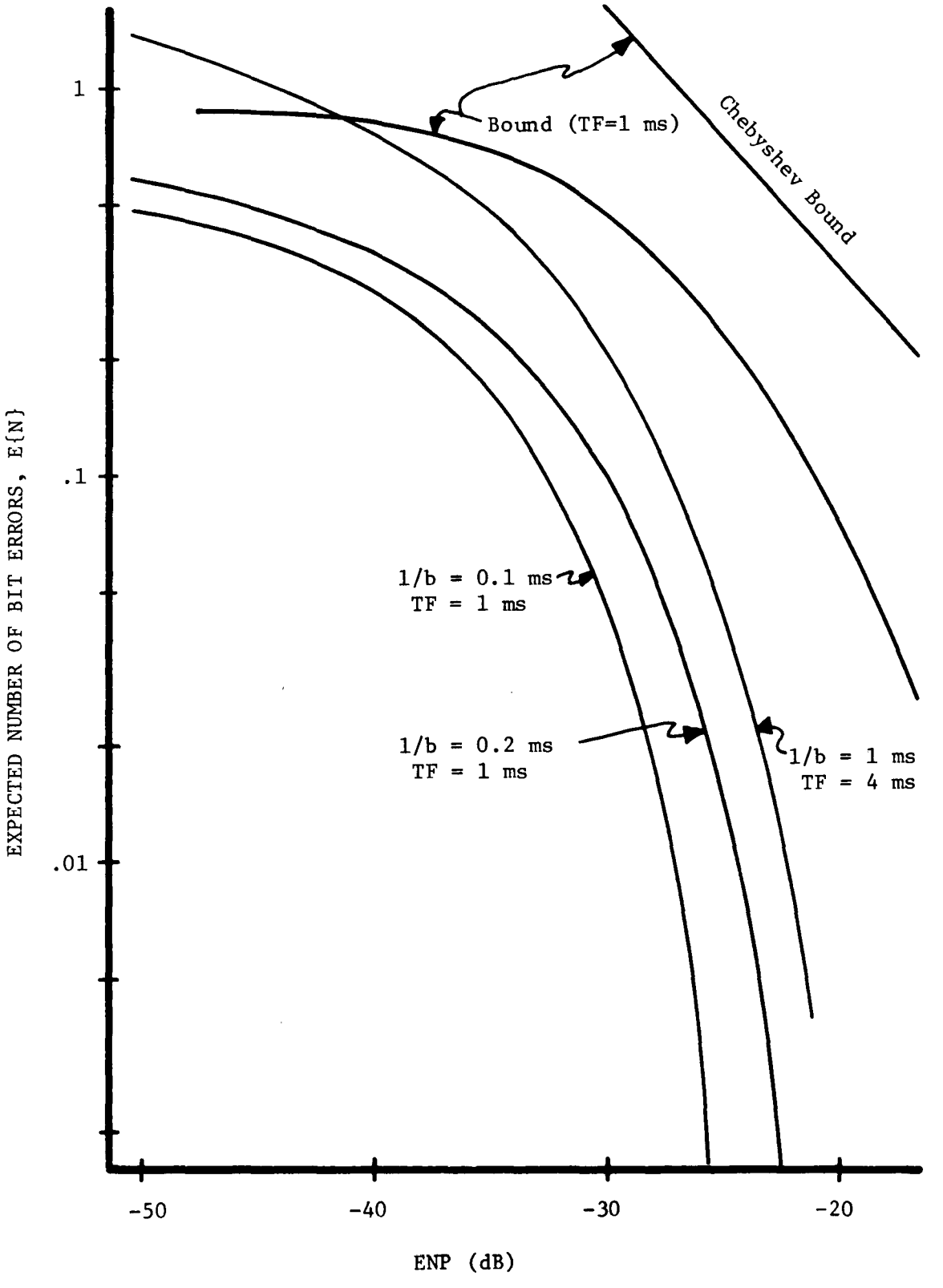

Fig. 4-4. Effect of Decaying-Exponential Waveform Time Constant on Performance of Unipolar Signaling

waveform. Hence, the correlation receiver would be more likely to mistake the noise for a signal bit.

A similar presentation is made in Fig. 4-5 for ASK signaling. Note that for ENP values greater than -43 dB, the curve for the 1 ms time constant indicates a lower error rate than the curves for the shorter time constants. A plausible explanation for this apparent contradiction to the trend is the lower peak cross-correlation which results from the unit-energy noise waveforms. The peak value of the noise must decrease as the time constant and/or duration are increased. As the peak value decreases, the minimum weighting factor, I_{min}, must increase before an error occurs; however, the probability of I assuming values greater than the new I_{min} is smaller, thus the error rate decreases. The effect of the peak values in the correlation function becomes evident as the ENP value increases. The bound curves presented in Figs. 4-4 and 4-5 are obtained by doubling (3.69); hence, they only apply to the noise waveforms of 1 ms duration. The bound for the 4 ms waveform appears in Fig. 4-10.

The relative performance of the Unipolar and ASK signal sets is dependent on the time constant of the decaying-exponential noise waveform, as illustrated in Fig. 4-6. The ASK performance shows a 5 to 10 dB improvement for the larger time constant. This reflects the generally lower ASK-noise crosscorrelation values (including peak values). For the 0.1 ms time constant, the Unipolar-noise crosscorrelation function (including peaks) is slightly larger than for ASK signaling, which explains the better performance of ASK at

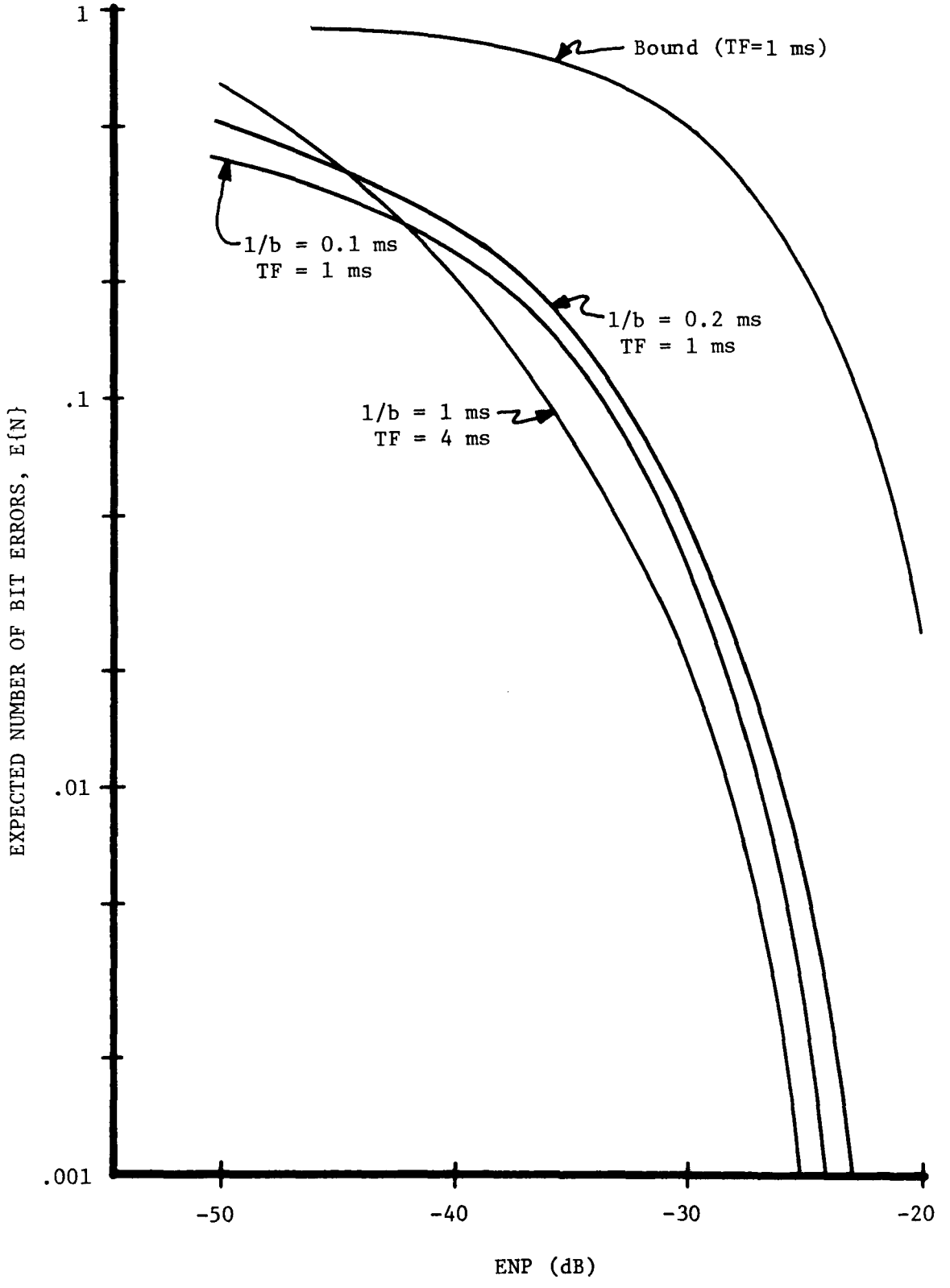

Fig. 4-5. Performance of ASK Signaling for Various Decaying-Exponential Time Constants

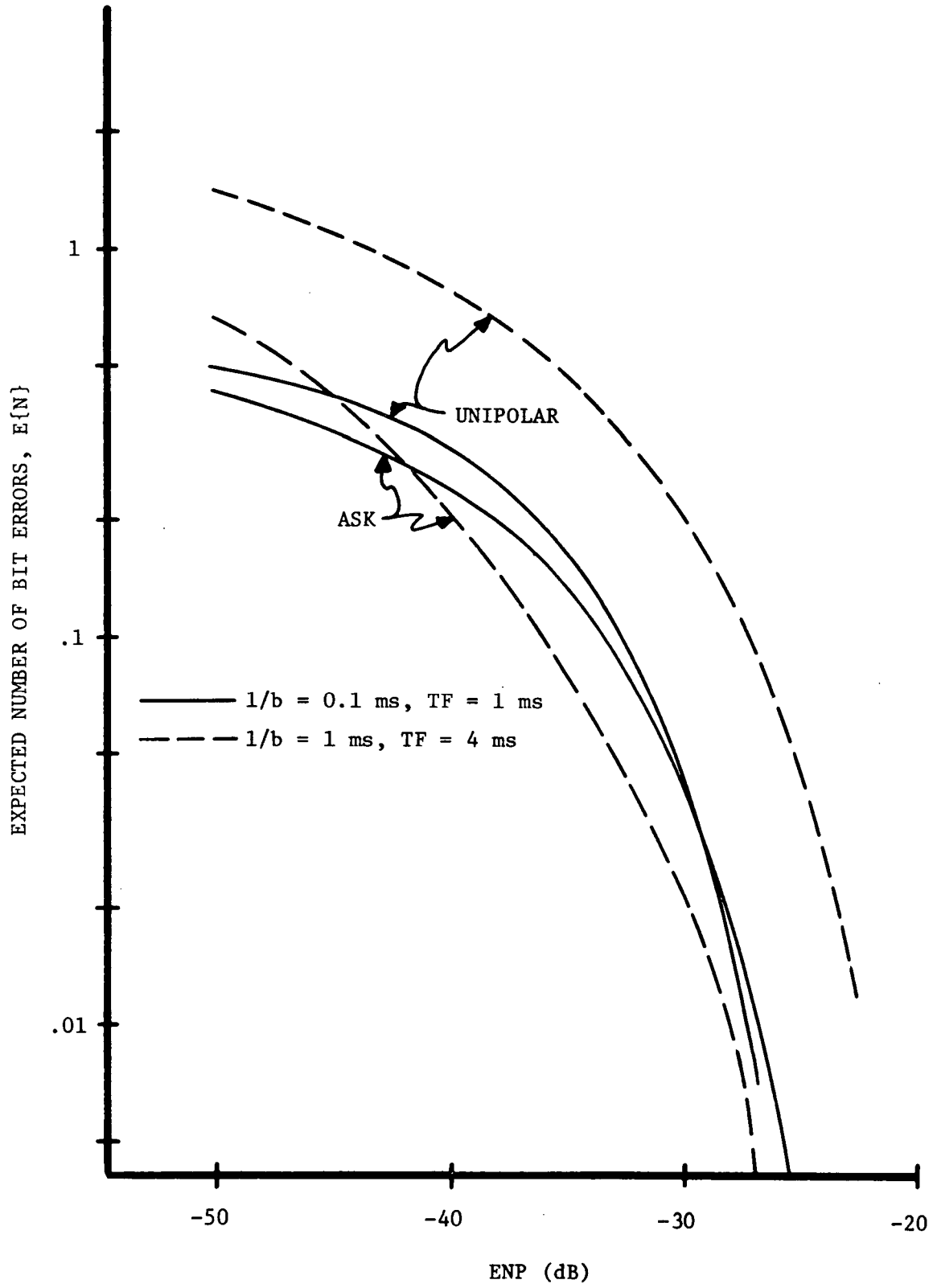

Fig. 4-6. Comparison of Unipolar and ASK Signal Sets for Decaying-Exponential Waveform

low ENP values. However, the ASK signal set has a larger peak value than the Unipolar set, which is reflected in the performance equations of (3.57) and (3.58), and accounts for the crossover of the curves for larger ENP values.

4.2.3 Signal Set

An error performance comparison for five signal sets is shown in Fig. 4-7 for a Gaussian p.d.f. description of I and the decaying-exponential noise waveform with a 0.2 ms time constant. Several conclusions can be made from a study of these results. The error performance of Polar (or PSK) signaling exhibits a 3 dB improvement in ENP value over that of Unipolar (or ASK). This result agrees with that observed for AWG noise. Conversely, it is apparent that a difference exists in the performances of Unipolar and ASK signals (or Polar and PSK) which is not present with AWG noise. Furthermore, the FSK signal set performance appears to approach that of ASK for large ENP values, which contradicts the AWG noise results for which the signal sets have equal performance. Furthermore, for ENP values below -33 dB the FSK error rate becomes less than that for PSK. Although the FSK-noise crosscorrelation is generally less than that obtained with the single sinusoid used for ASK and PSK, it does have slightly larger peak values. This explains the change in the relative performance of FSK as the ENP value increases.

The bound curves in Fig. 4-7 are upper bounds and it appears that the bound for $\rho = -1$, i.e., Polar or PSK signaling, could be used for all five signal sets. However, this conclusion is not valid, as it

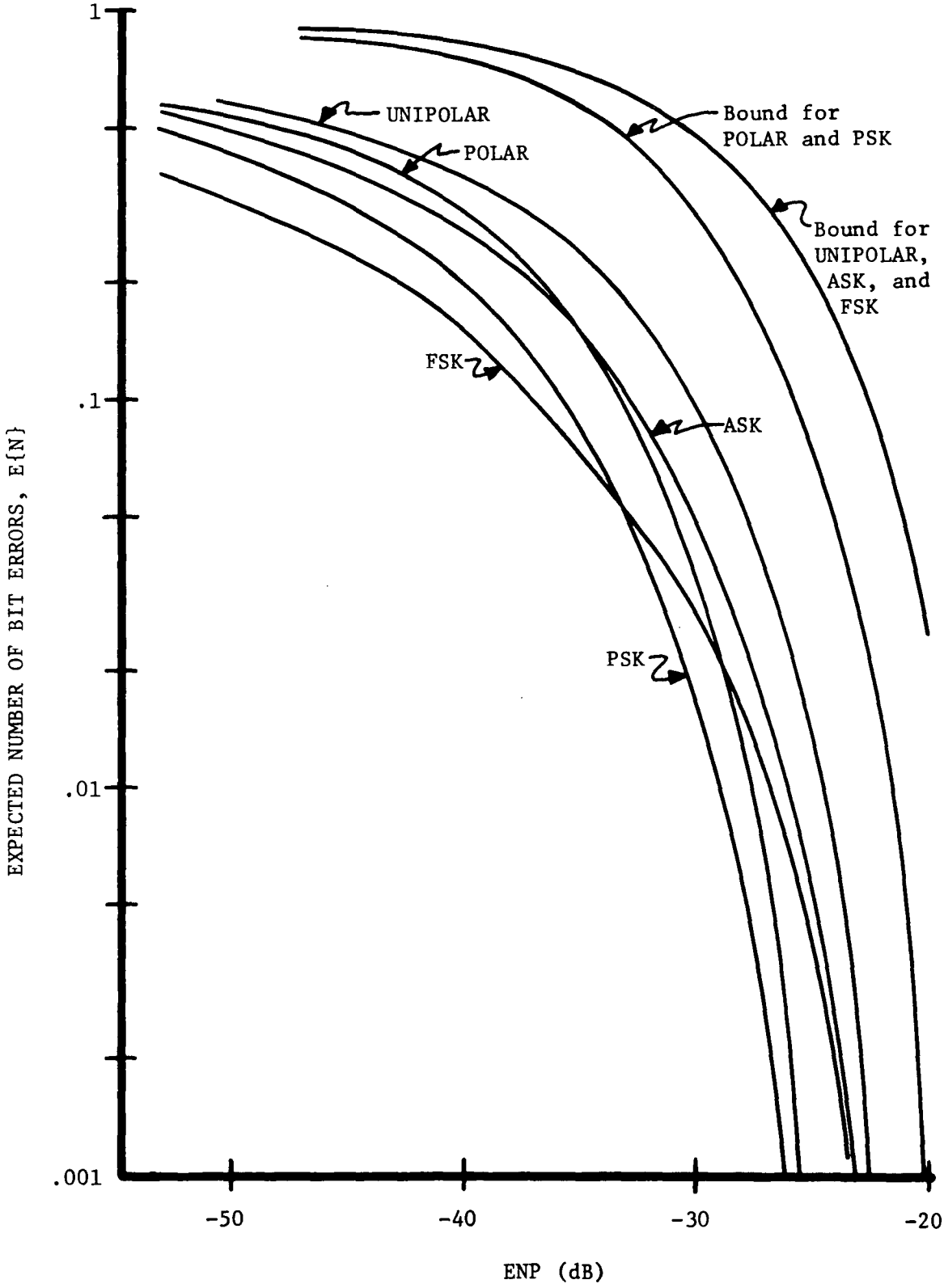

Fig. 4-7. Comparison of Five Signal Sets for Decaying-Exponential Waveform with 0.2 ms Time Constant

applies only for this particular set of assumptions regarding noise waveform, time constant, and weighting factor p.d.f.

4.3 PERFORMANCE RESULTS FOR EXPONENTIALLY-DECAYING SINUSOID

The effect of changing the noise waveform is demonstrated by considering the exponentially-decaying sinusoid of (4.3). Unipolar and ASK signal sets are compared in Fig. 4-8 for two values of the noise time constant and a Gaussian p.d.f. The higher error rate for ASK is explained by the larger correlation between the signal and noise waveforms. Similarly, the improvement experienced by Unipolar signaling as the time constant is increased is due to the decreased correlation between signal and noise. The relative performance of the two ASK curves reflects a generally larger crosscorrelation with the noise for the 2 ms time constant, but a larger peak cross-correlation for the 1 ms time constant.

A comparison of the five signal sets is presented in Fig. 4-9 for the exponentially-decaying sinusoidal noise waveform with a time constant of 1 ms. These results indicate the same 3 dB improvement of Polar over Unipolar and PSK over ASK as is obtained with an AWG noise assumption. The FSK performance is almost the same as the PSK over the range of ENP values shown, and thereby differs from the 3 dB differential for AWG noise results. The performance difference between Unipolar and ASK also contrasts with AWG results.

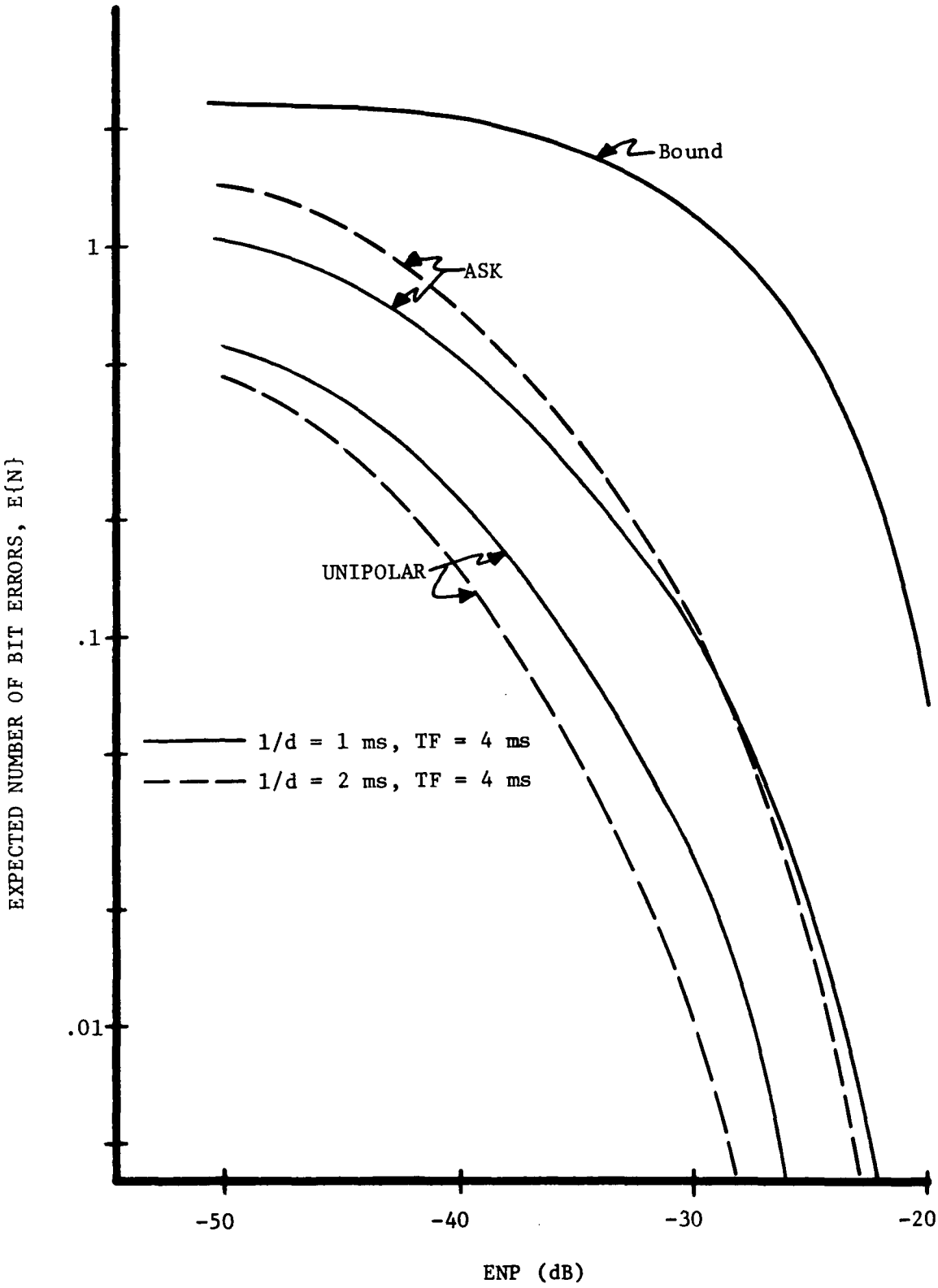

Fig. 4-8. Comparison of Unipolar and ASK Signal Sets for Exponentially-Decaying Sinusoid

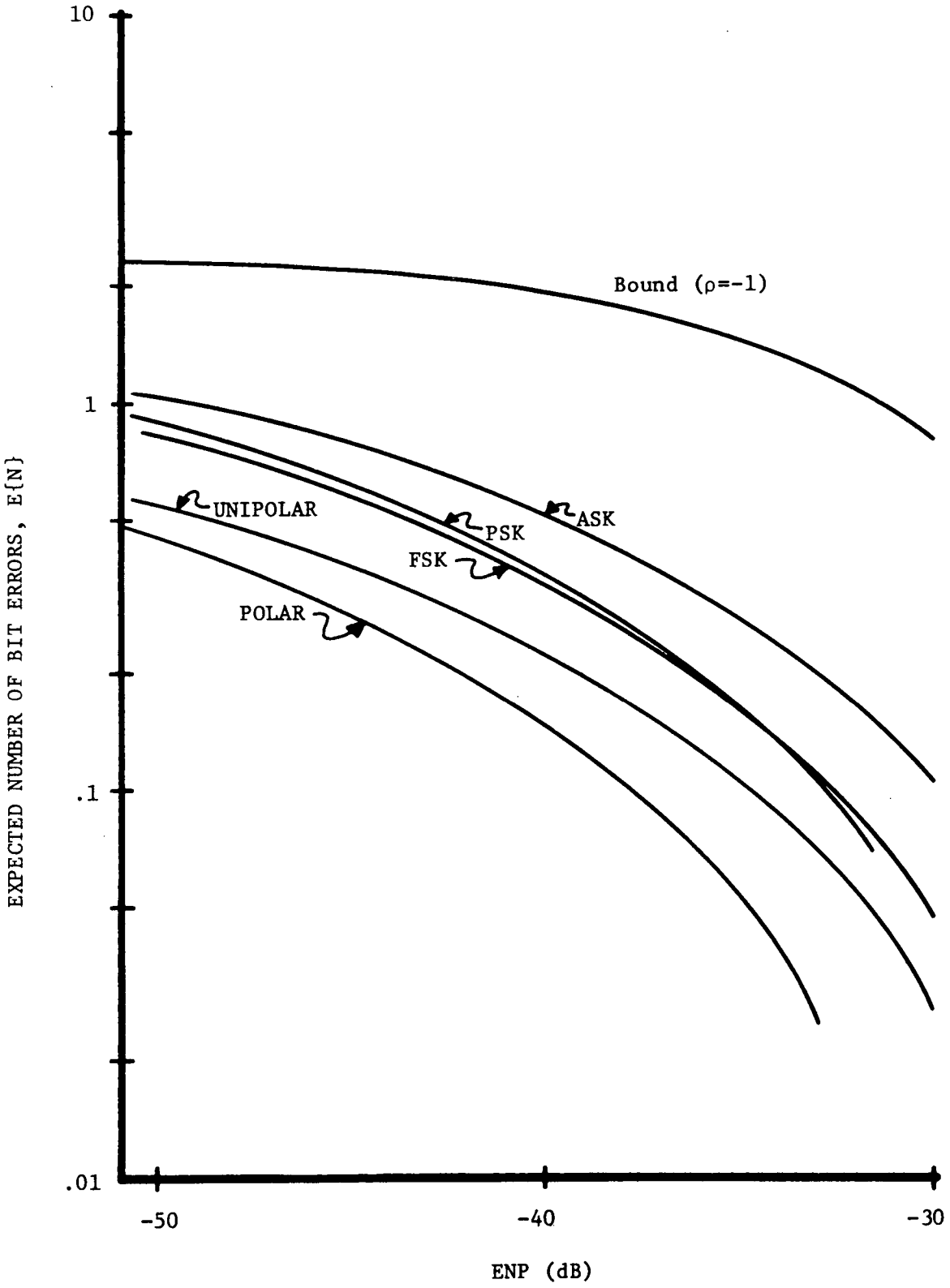

Fig. 4-9. Comparison of Five Signal Sets for Exponentially-Decaying Sinusoid with 1 ms Time Constant

4.4 EFFECT OF SIGNAL AND NOISE CORRELATION

The performances of Unipolar and ASK signals are compared in Fig. 4-10 using both the decaying-exponential and the exponentially-decaying-sinusoidal noise waveforms with the same time constant and a Gaussian p.d.f. for I. It is noted that the performance of ASK with the decaying-exponential noise is approximately equal to that of Unipolar with exponentially-decaying-sinusoidal noise. This is reasonable, since in both cases the signal and noise crosscorrelation are essentially equal. The larger peak value of the ASK signal set dictates the crossover in the relative performances as the ENP value increases. When the noise waveforms are interchanged, the ASK signal set has a small advantage over Unipolar, although both performances are inferior to the aforementioned combinations.

4.5 COMPARISON TO RESULTS FROM THE LITERATURE

The relative performance of various signal sets has received some attention in the literature. Usually, the comparisons are between signaling methods that utilize a carrier, e.g., ASK, PSK, or FSK. For idealized impulse noise and coherent demodulation, it has been shown by Ziemer [10] and Houts & Moore [11] that PSK exhibits a 3 dB improvement over ASK. Houts and Moore have also shown that the performance of FSK differs from ASK. Engels [24] and Bennett & Davey [38] have used more realistic noise models to show that PSK performs better than FSK. Experimental measurements reported by Bodonyi [23] have shown the presence of crossovers in

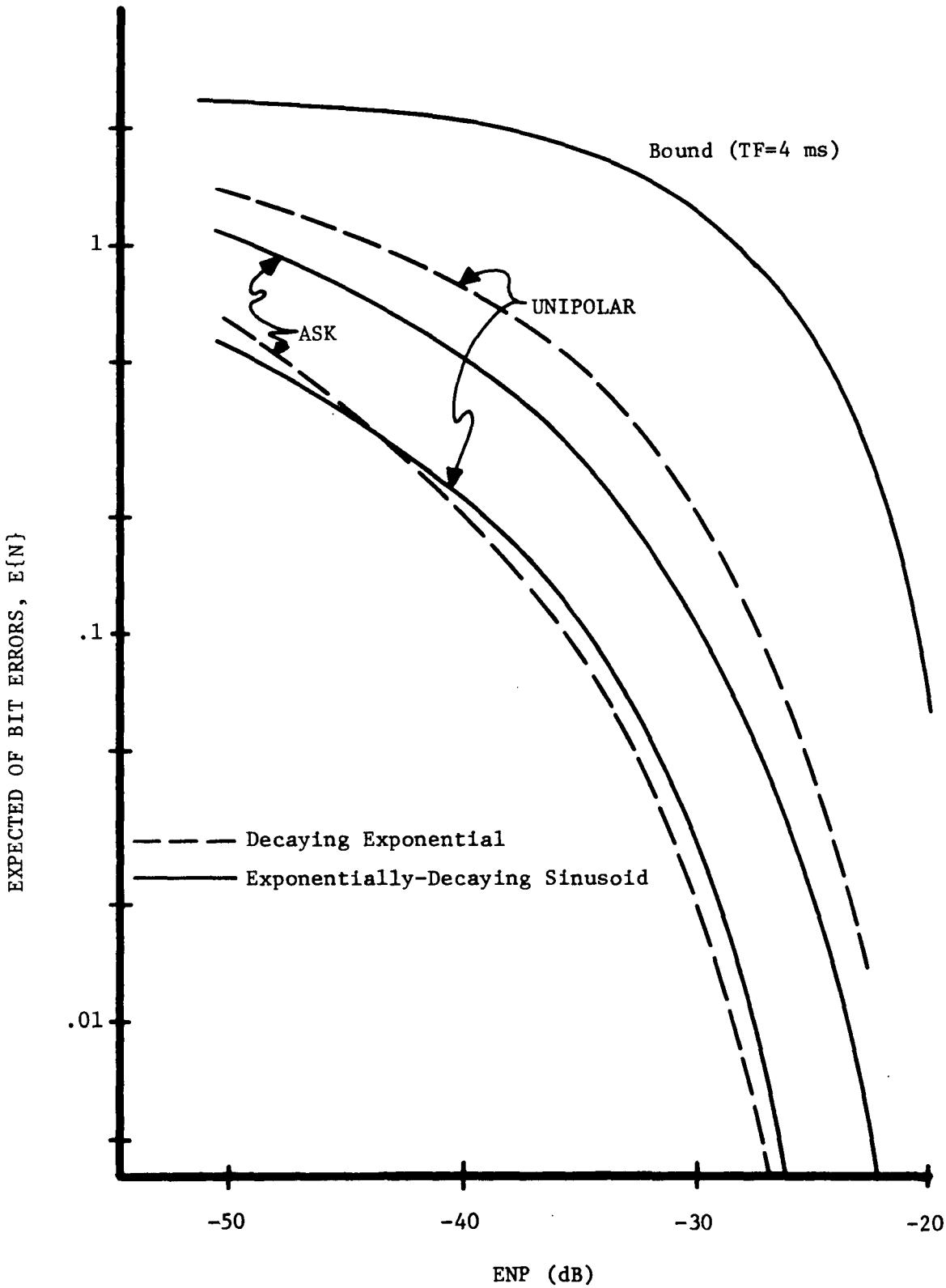

Fig. 4-10. Comparison of Unipolar and ASK Signal Sets for Waveforms with 1 ms Time Constants

the performance curves for noncoherent FSK and coherent PSK signaling techniques. However, for large SNR values it appears that PSK has an advantage. These results for carrier systems appear to support Bennett & Davey's hypothesis that the relative error rates of data transmission systems can be determined for nearly all noise environments by comparing performances in the presence of AWG noise.

Most of the above results are consistent with the results of Sections 4.2, 4.3 and 4.4. However, the performances of the On-Off, Binary Antipodal and Orthogonal signaling methods were shown to be dependent on the signal-set basis function, e.g., pulse or sinusoid. This represents a major exception to the AWG-relative-performance hypothesis proposed by Bennett & Davey. This discrepancy is caused by the error performance for impulse noise being dependent upon the signal-to-noise correlation, whereas AWG noise is uncorrelated with all signal sets. New conclusions have also been obtained. The 3 dB improvement of PSK over ASK has been established for the GIN (Unique Waveform) model, and for the conditions investigated, the FSK signal set can perform better than PSK for low ENP values. Similarly, a study of pulse signaling has revealed that the 3 dB advantage exist for Polar over Unipolar.

CHAPTER 5

METHODS FOR IMPROVING RECEIVER PERFORMANCE

The linear correlation receiver does not represent the optimum receiver for impulse noise corrupted signals. In fact, a variety of methods have been proposed for improving the receiver design. A survey of these recommendations is presented in Section 5.1, after which a specific improvement method is selected for analysis and the performance results are compared to the linear correlation receiver. Many factors other than the receiver design can affect the performance of a digital system, e.g., noise source proximity, system shielding, ground loops, etc. Such factors are not considered here.

5.1 SURVEY OF RECOMMENDATIONS FOR IMPROVED RECEIVER DESIGNS

The topic of designing receivers for impulse-noise corrupted signals has not received extensive treatment in the literature. However, several intuitively-motivated techniques have been reported which employ theoretical and/or experimental procedures. Generally, the proposed improvements attempt to counteract either the large amplitude or aperiodic nature of the impulse noise and will be classified as either amplitude- or time-based modifications to existing receivers.

The amplitude-based modifications act to suppress the large amplitude excursions of the impulse noise by including a nonlinear

device in the receiver. As discussed in Section 1.2, Snyder [31] and Rappaport & Kurz [32] have used the likelihood ratio to investigate optimum receivers for specific impulse noise models. Each design resulted in the use of a nonlinear device to suppress large amplitude excursions in conjunction with a linear receiver. The specification of the nonlinear device depends on the noise statistics and must be changed if the noise description changes. Sub-optimum receiver designs using nonlinear devices have been proposed with either intuitive or empirical justification. Specifically, several authors [13,26,27,39,40] have proposed clipping devices which limit the maximum magnitude of the received signal. Another suggestion [29] is to use a blanking device which has a zero output when the input signal exceeds specified positive and negative thresholds. It has been postulated that the reduction in noise power achieved through the use of clipping or blanking devices yields improved error performance; however, there is no such guarantee because of the possibility of improving the signal-to-noise crosscorrelation. Bello & Esposito [12] have reported the performance improvement obtained using a clipping device with PSK signaling and an atmospheric noise nodel. They assumed that the amplitude of the noise was much greater than that of the data signal.

The time-based modifications exploit the aperiodic and frequency spectrum properties of the impulse noise. Examples of this technique are the smearing-desmearing [30] and swept-frequency-modulation [41,42] systems. These systems use a special modulator or a filter to destroy the phase relationship of the components in the transmitted signal. At the receiver the inverse of this operation is performed which yields

the original phase relationship for the data signal, but destroys the phase relationship of the channel noise components. These techniques have not been employed extensively because of their poor performance [43]. One possible explanation for the poor performance is that the true characteristics of impulse noise are not represented by a model where amplitude peaks are caused by a phase relationship of noise components. Another time-based modification uses a pulse-width discriminator [28] to decide if the received signals are noise or data pulses. Those that qualify as data bits produce fixed-width pulses at the output of the discriminator. This system can only be effective if the time duration of the noise waveforms are short, compared to the data bit.

5.2 PERFORMANCE ANALYSIS FOR A NONLINEAR CORRELATION RECEIVER

The error performance of the system shown in Fig. 5-1 is determined using the general approach developed in Chapter 3. The first step is to find the conditional decision statistic, D^j, for the m^{th} bit, viz.,

$$D^j = \int_{(m-1)T_b}^{mT_b} \{s_j(t) + n(t)\}^o \, [s_1(t) - s_0(t)] \, dt - C \, , \tag{5.1}$$

where $\{\ \}^o$ represents the operation performed by the nonlinear device. Equation 5.1 can be changed into the form of (3.16). First, $s_j(t)$ is added and subtracted to the $\{\ \}^o$ term and the following notation is introduced.

$$\{n(t)\}^{oo} = \{s_j(t) + n(t)\}^o - s_j(t) \, . \tag{5.2}$$

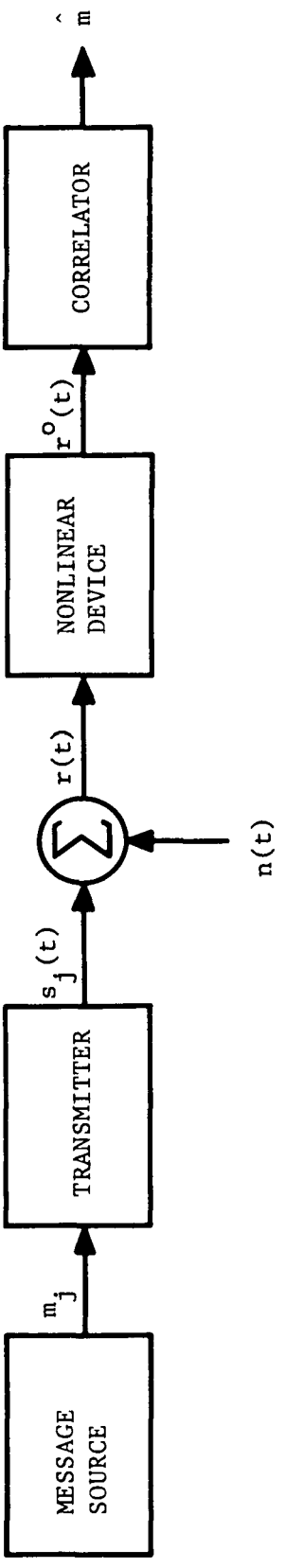

Fig. 5-1. Digital System with Nonlinear Correlation Receiver

Incorporating (5.2) into (5.1) and dropping the limits of integration gives

$$D^j = \int \{n(t)\}^{oo} [s_1(t) - s_0(t)] \, dt - C_j \, , \tag{5.3}$$

where C_j is defined by (3.17). Assuming noise which is represented by the GIN (Unique Waveform) model and ignoring the possibility of more than one burst in a bit interval yields

$$D^j|(NB=1) = \int \{I \, f(t-T)\}^{oo} [s_1(t) - s_0(t)] \, dt - C_j \, . \tag{5.4}$$

The normalized random variable $N=I/\sigma$ can be introduced by defining another nonlinear operation, namely,

$$\sigma \{N \, f(t-T)\}^{ooo} = \{\sigma(I/\sigma) \, f(t-T)\}^{oo} \, . \tag{5.5}$$

Thus

$$D^j|(NB=1) = \sigma \int \{N \, f(t-T)\}^{ooo} [s_1(t) - s_0(t)] \, dt - C_j \, . \tag{5.6}$$

Factoring the peak voltage V from the signal set and defining

$$V \, F_j(N,T) = \int \{N \, f(t-T)\}^{ooo} [s_1(t) - s_0(t)] \, dt \, , \tag{5.7}$$

yields

$$D^j|(NB=1) = \sigma \, V \, F_j(N,T) - C_j \, . \tag{5.8}$$

Following the procedure used in obtaining (3.32) the normalized probability of bit error can be written using (5.8) as

$$P_1[\varepsilon_m|m_j] = P[(-1)^j F_j(N,T) > (-1)^j C_j/(\sigma V)] . \tag{5.9}$$

Alternatively, (5.9) can be represented as

$$P_1[\varepsilon_m|m_j] = \int_n \int_\tau P[(-1)^j F_j(n,\tau) > (-1)^j C_j/(\sigma V) | N=n, T=\tau] \; p_N(n) p_T(\tau) \, d\tau dn , \tag{5.10}$$

or

$$P_1[\varepsilon_m|m_j] = \iint_{R_j} p_N(n) p_T(\tau) \, d\tau dn , \tag{5.11}$$

where R_j designates the region of N and T such that the inequality established on $F_j(n,\tau)$ in (5.10) holds. Assuming that T is uniformly distributed over the bit interval and integrating over τ yields

$$P_1[\varepsilon_m|m_j] = \frac{1}{T_b} \int_{-\infty}^{-N_n} T_R(n) p_N(n) \, dn + \frac{1}{T_b} \int_{N_p}^{\infty} T_R(n) p_N(n) \, dn , \tag{5.12}$$

where the time range $T_R(n)$ equals zero for $-N_n < n < N_p$.

The nonlinear device must be specified before numerical results can be obtained. The limiter model of Fig. 5-2 represents an extension of the clipping and blanking concepts discussed in Section 5.1 and is used by the computer program LIMITER, which is described in Appendix D, to determine the error performance given by (5.12). Values for α_p and α_n

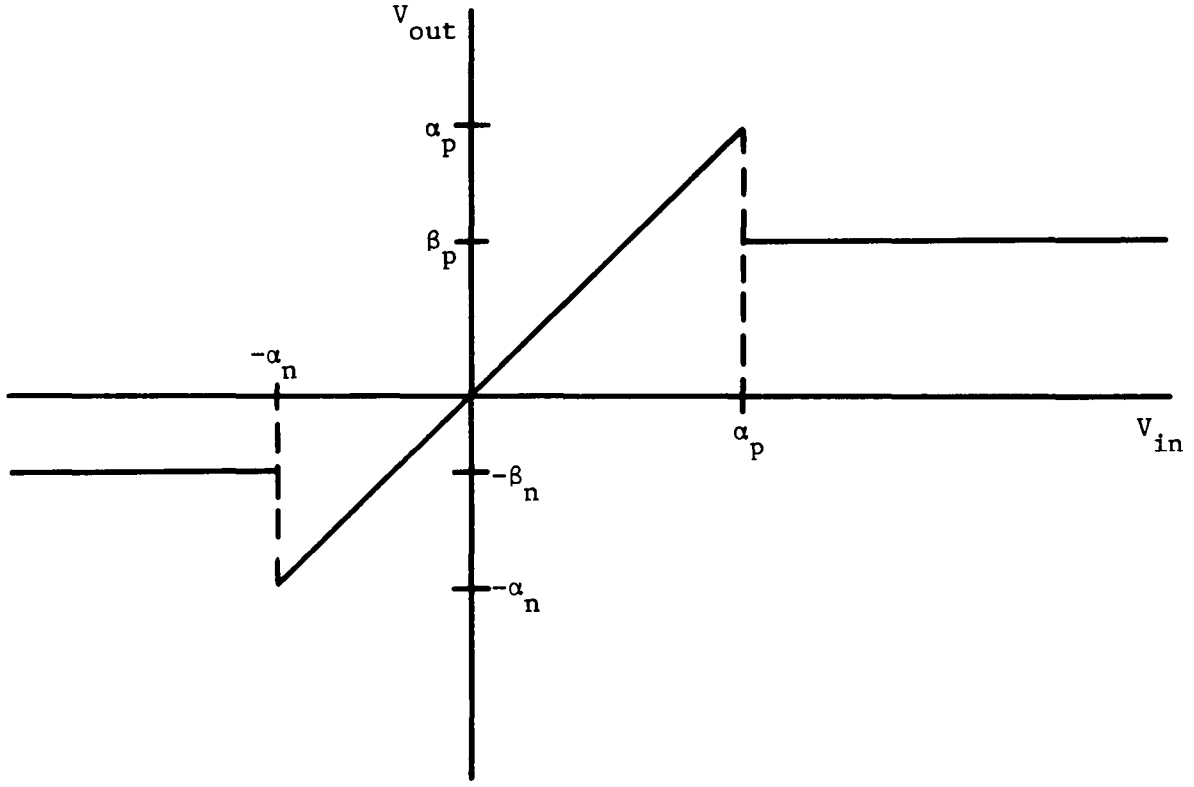

Fig. 5-2. Limiter Model

correspond to the magnitudes of the peak positive and negative signal set voltages, respectively. For ASK, PSK, FSK and Polar signal sets $\alpha_p = \alpha_n$, while for Unipolar and other one-polarity signal sets, $\alpha_n = 0$. The values of β_p and β_n are parameters specified by the user, thus either a specific limiter can be modeled or the values changed to determine their effect on the error performance.

5.3 COMPARISON OF LINEAR AND NONLINEAR CORRELATION RECEIVERS

Performance results for the linear and nonlinear correlation receivers are compared for several signal sets. The results for the nonlinear device were obtained by running the LIMITER program on the UNIVAC-1108 computer. Each value calculated required approximately 10 minutes of CPU time for each data bit analyzed, i.e., 40 minutes of computer time was required to obtain one point if the noise waveform overlapped four data bits. For this reason, a comprehensive study of signal sets, weighting factor p.d.f. and noise waveform parameters was not attempted. The results presented assumed a Gaussian p.d.f. for the weighting factor.

The error performance curves presented in Fig. 5-3 illustrate the effect of changing the clip levels β_n and β_p. When $\beta_p = \alpha_p$ and $\beta_n = 0$, a performance improvement of approximately 6 dB is obtained in comparison with the case where $\beta_p = \beta_n = \alpha_p$. This is intuitively satisfying, since setting $\beta_n = 0$ is a logical choice for Unipolar signaling. For both sets of clip-level values the performance improvement over the linear correlation receiver decreases as the ENP value increases. However, at a 10^{-3} error rate there is still an impressive 5 dB improvement over the

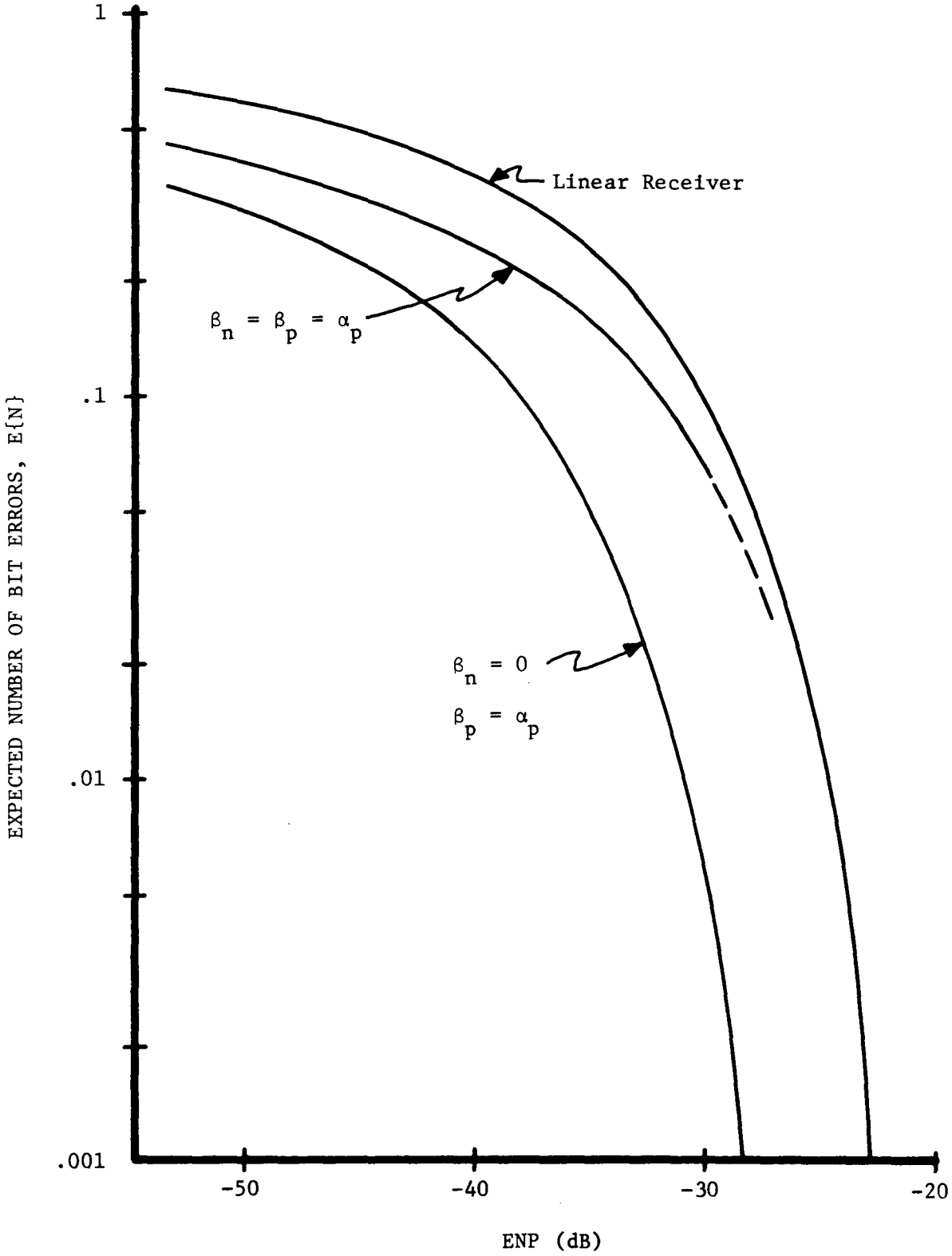

Fig. 5-3. Effect of Nonlinear Receiver on Unipolar Signal Performance in the Presence of Decaying-Exponential Noise with a 0.2 ms Time Constant

linear receiver for the case when $\beta_p=\alpha_p$ and $\beta_n=0$. It is reasonable to assume that the performance improvement decreases as ENP increases since the data signal begins to dominate the noise and the clipping device will have less overall effect. A similar conclusion is obtained from a study of Fig. 5-4 for ASK signaling and the decaying-exponential noise waveform. The clip levels correspond to the peak voltage of the signal set, i.e., $\beta_p=\beta_n=\alpha_p$. As before, the performance improvement decreases as the ENP value increases. It was shown in Chapter 4 that the Unipolar signaling performance was poorer than ASK when linear correlation detection was used in the presence of decaying-exponential noise. This disparity was attributed to the higher crosscorrelation between the Unipolar signal and the noise. However, a comparison of the error performances shown in Figs. 5-3 and 5-4 indicates that the Unipolar signal performs better than ASK when the limiter is inserted, at least for the chosen values of β_p and β_n.

The exponentially-decaying sinusoidal noise waveform with a 2 ms time constant was used to investigate the relative performance of ASK and PSK signaling. A comparison of ASK signaling performances for the linear and nonlinear receivers is shown in Fig. 5-5. The clip levels were not chosen to equal the peak signal value, instead they correspond to the rms value, i.e., $\beta_p=\beta_n=\alpha_p/\sqrt{2}$. Although for low ENP values a very small improvement is obtained, the curves have converged for an ENP greater than -30 dB. The PSK signaling performance is shown in Fig. 5-6 for two versions of the limiter. When $\beta_p=\beta_n=\alpha_p/\sqrt{2}$, the performance is actually poorer than it was for a linear correlation detector. It is evident that improved performance can be obtained through a

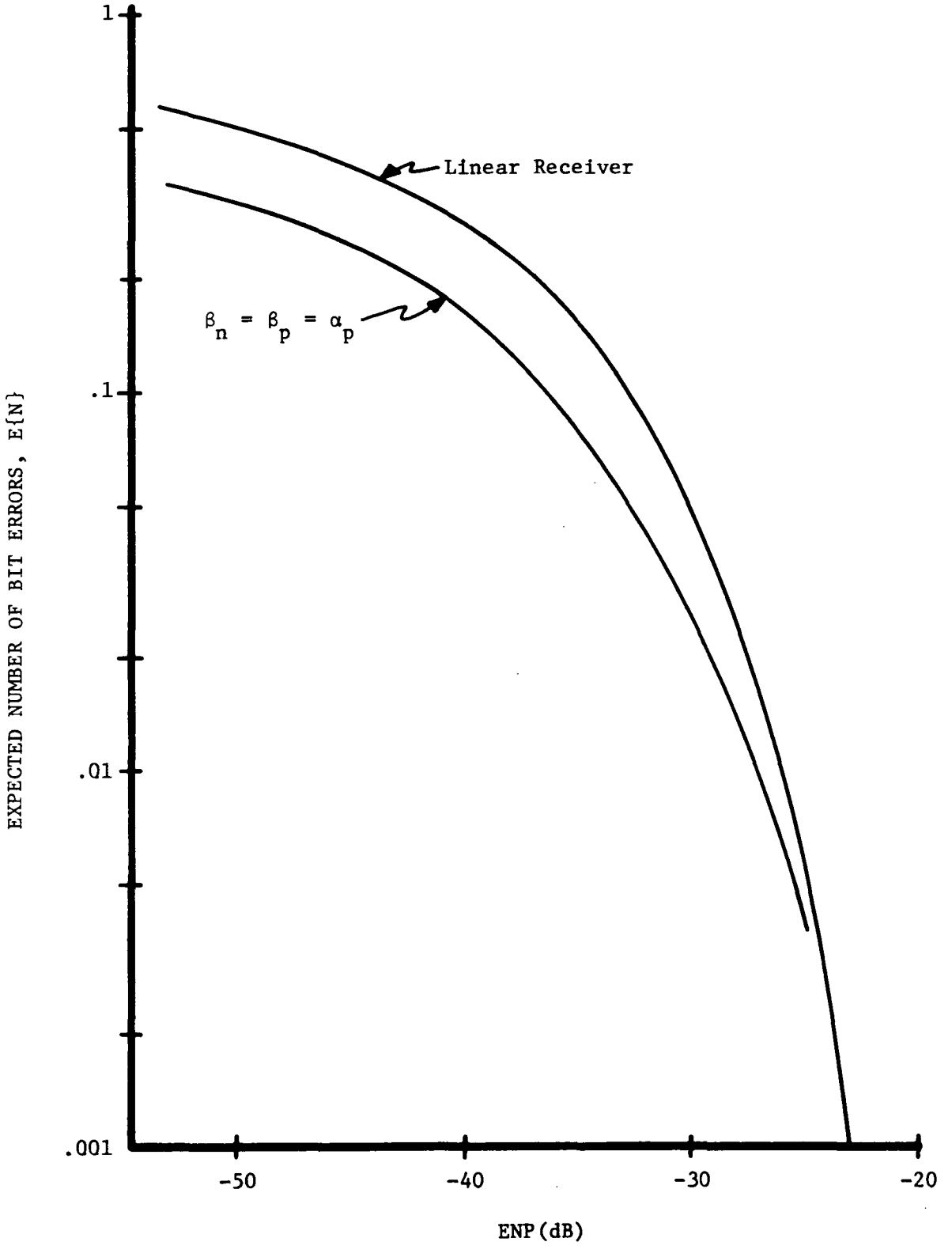

Fig. 5-4. Effect of Nonlinear Receiver on ASK Signal Performance in the Presence of Decaying-Exponential Noise with a 0.2 ms Time Constant

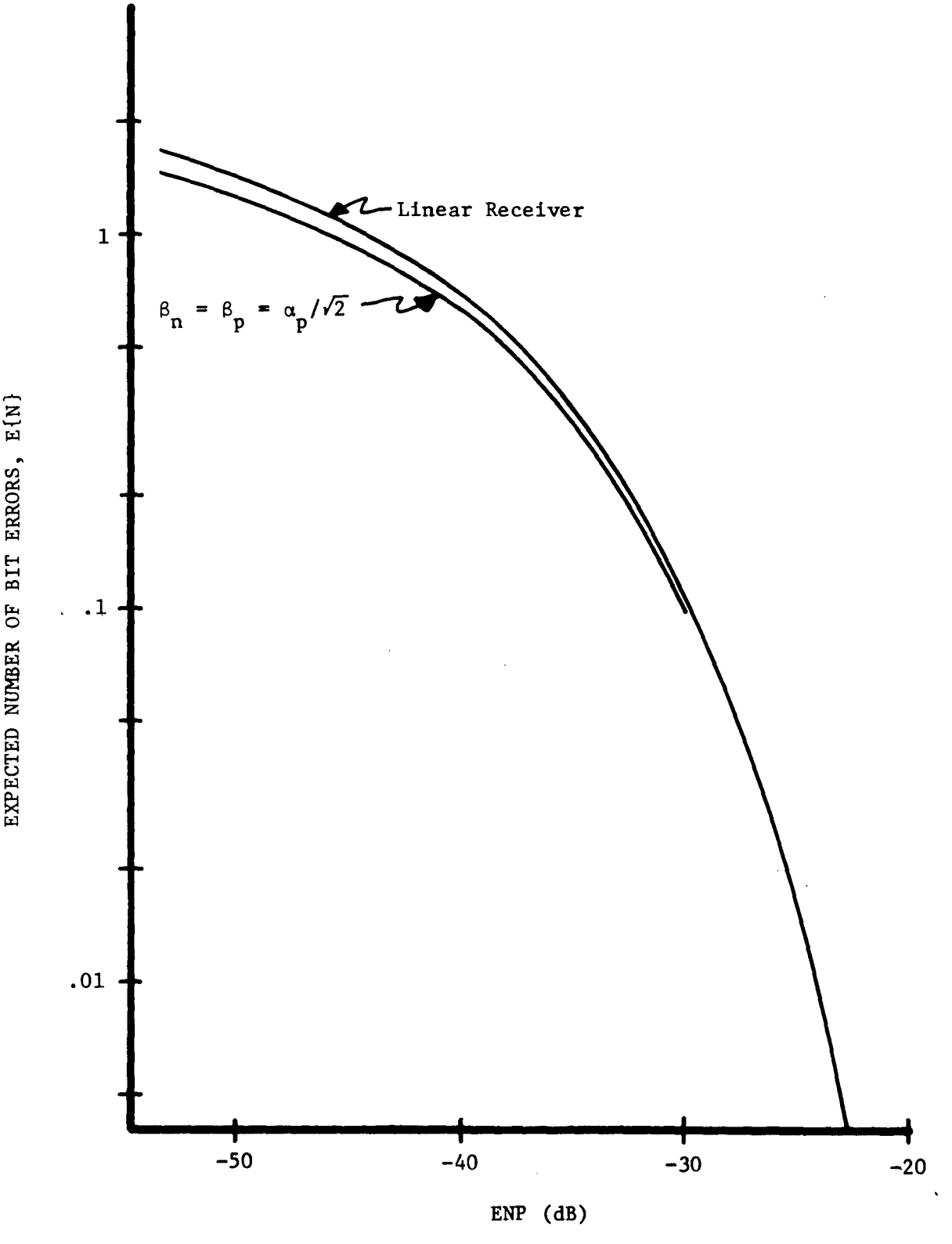

Fig. 5-5. Effect of Nonlinear Receiver on ASK Signal Performance in the Presence of Exponentially-Decaying-Sinusoidal Noise with a 2 ms Time Constant

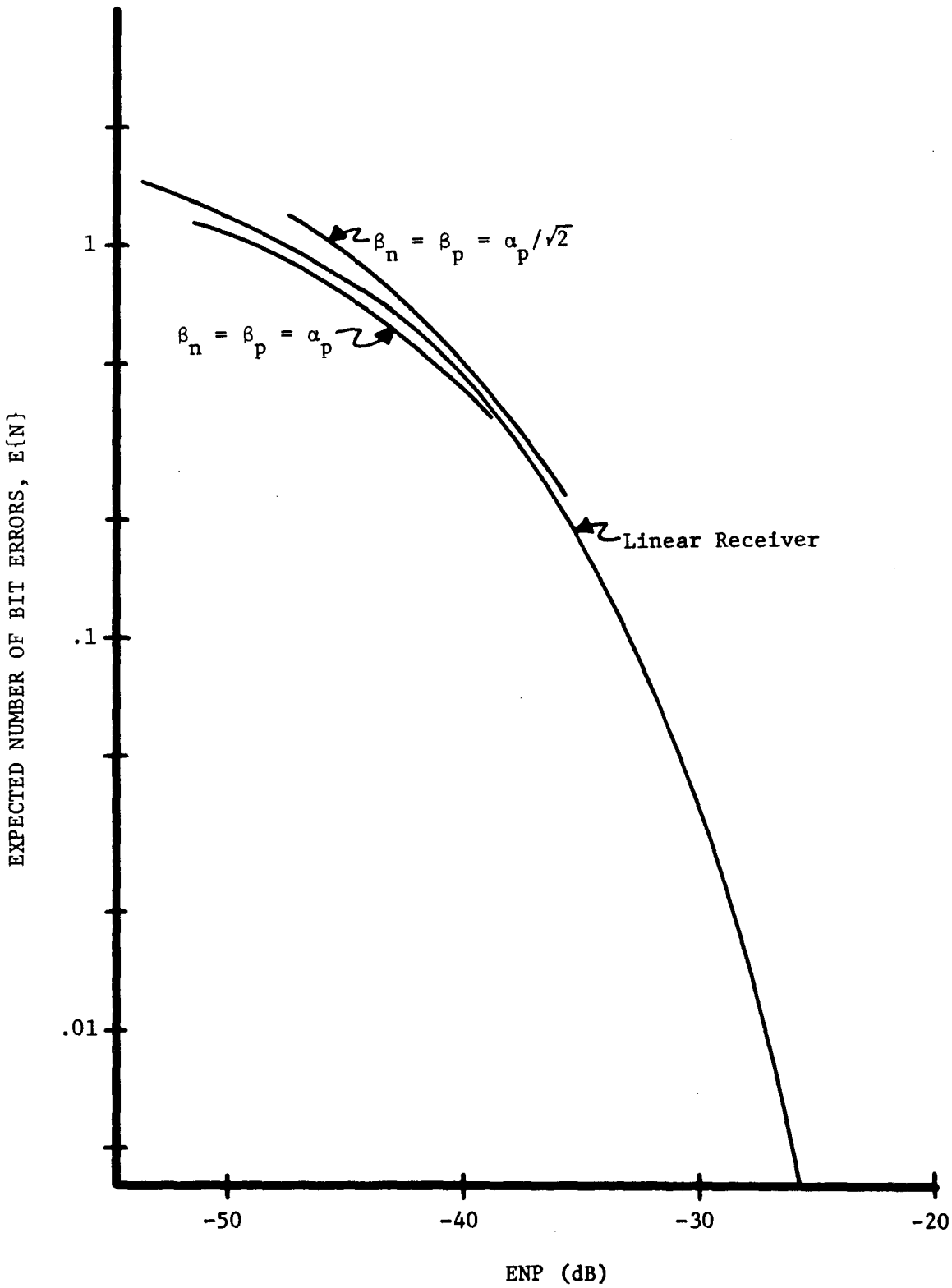

Fig. 5-6. Effect of Nonlinear Receiver on PSK Signal Performance in the Presence of Exponentially-Decaying-Sinusoidal Noise with a 2 ms Time Constant

more logical choice of clip levels, i.e., $\beta_p=\beta_n=\alpha_p$; however, the effect is minimal for either set of clip levels. Consequently, with a limiter, PSK does not possess the full 3 dB advantage over ASK which was present for linear correlation detection.

The results presented in this section indicate that error performance can be improved by the proper choice of clip levels in the nonlinear receiver. The improvement obtained by using the limiter would probably become more pronounced as the noise time constant decreases, since the peak noise voltage increases to meet the unit-energy assumption for the basic waveform f(t).

CHAPTER 6

CONCLUSIONS AND RECOMMENDATIONS

6.1 CONCLUSIONS

The generalized impulse noise (GIN) model can approximate the noise burst structure observed in many digital systems provided the average burst rate, expected number of waveforms per burst, sample function ensembles associated with the burst, and the weighting factor p.d.f. can be obtained. A specialized model, the GIN (Unique Waveform) model, is readily obtained by assuming that each noise burst contains a randomly weighted version of the same basic waveform. It has been shown that the power-density spectrum for this specialized model is not white because of the dependence on the noise waveform.

The GIN (Unique Waveform) model is used to determine the error performance equations for a correlation receiver. These results express the expected number of bit errors per noise burst as a function of the following parameters: (1) energy-to-noise parameter (ENP) of (2.12), (2) noise amplitude-weighting-factor p.d.f., (3) signal-set correlation coefficient, and (4) a time range function which depends on crosscorrelation between the signal-set basis functions and the noise waveform. The performance analysis for the GIN (Unique Waveform) model can be extended to the general model.

Comparison of the performance results for impulse and additive white Gaussian (AWG) noise reveals two major differences. For

impulse noise, Orthogonal signaling does not yield the same error performance as On-Off signaling with the same average energy. Also, the choice of the signal-set basis functions has an effect on the performance. These conclusions are supported by the dependence of impulse noise performance results on the correlation between the signal and noise waveforms. A conclusion which agrees with the AWG result is that Antipodal signaling has a 3 dB advantage over On-Off signaling.

The error performance can be upper bounded by equations which depend on the average signal energy, signal-set correlation coefficient, plus the noise weighting-factor variance and p.d.f. Specifically, the bounds do not depend on the signal-set basis functions or the noise waveform. Another upper bound, which is also independent of the weighting factor p.d.f., is formed by applying Chebyshev's inequality to the previous bound. It has been shown that for impulse noise the linear correlation receiver is not optimum, i.e., the probability of error is not minimized. This conclusion is supported by the dependence of the performance equations on the signal and noise cross-correlation. One method for improving the error performance is to insert an amplitude-dependent limiter, i.e., a nonlinear device, prior to the receiver input. It was shown that the error performance is dependent upon the choice of parameters used to specify the limiter.

6.2 RECOMMENDATIONS FOR FURTHER STUDY

Further work can be performed in several areas of this investigation. The relationship between signal-to-noise ratio (SNR) and

ENP has been established only for white Gaussian noise and idealized impulse noise. It would aid the comparison of results if the parameters were related for a bandlimited channel and the GIN model. This study has concentrated on the analysis of the correlation receiver, but an investigation of sampling receivers could be performed as suggested by the procedure of Chapter 2. The extension of the nonlinear receiver designs of Chapter 5 to an optimum receiver for impulse noise offers an opportunity for a significant contribution.

Although the bounds of Chapter 3 are useful, other techniques should be investigated in an attempt to improve the tightness of the bounds. It might be possible to approximate the error performance of the GIN (Single Ensemble) model by using an average waveform $\bar{G}(t)$ which is obtained by averaging over the sample functions in the ensemble. For example, the error expression of (3.7) might become,

$$E\{N\} = E\{NG\} \sum_{k=1}^{NE} E\{N_1 | G_k(t)\} \, P[G_k(t)] \simeq E\{NG\} \, E\{N_1 | \bar{G}(t)\} \qquad (6.1)$$

where

$$\bar{G}(t) = \sum_{k=1}^{NE} G_k(t) \, P[G_k(t)] \qquad (6.2)$$

Once $\bar{G}(t)$ is obtained, the evaluation of $E\{N_1 | \bar{G}(t)\}$ is equivalent to the techniques developed herein for the unique waveform model. Finally, the derivation of upper bounds for various nonlinear correlation receivers would reduce the computer time required to obtain specific results.

APPENDIX A

DERIVATION OF POWER-DENSITY SPECTRUM AND PROBABILITY DENSITY FUNCTIONS FOR THE GIN (UNIQUE WAVEFORM) MODEL

In order to characterize the GIN (Unique Waveform) model it is helpful to specify both the noise power-density spectrum and amplitude probability density function (p.d.f.). These expressions are derived in the following sections. In particular, two p.d.f. descriptions are obtained for the noise model. The first p.d.f. is based on the assumption that no more than one noise burst occurs in time T_n, and the second results from using a Poisson distribution to model the number of noise bursts.

A.1 POWER-DENSITY SPECTRUM

The power-density spectrum can be determined from the expression for the average power, P_{AVG}, by

$$P_{AVG} = E\left\{ \frac{1}{T_n} \int_0^{T_n} n^2(t)\, dt \right\} , \qquad (A.1)$$

where T_n is the duration time of the noise and the expected value $E\{\ \}$ is taken with respect to all of the random variables involved in describing the noise process. The first step is to apply Parseval's theorem, viz.,

$$\frac{1}{T_n}\int_0^{T_n} n^2(t)\,dt = \frac{1}{T_n}\int_{-\infty}^{\infty} |N(f)|^2\,df \quad , \tag{A.2}$$

where N(f) is the Fourier transform of a sample function from the noise process. For the GIN (Unique Waveform) model of (2.7),

$$N(f) = \sum_{k=1}^{NB} I_k\, F(f) e^{-j2\pi f T_k} \quad , \tag{A.3}$$

where F(f) is the Fourier transform of f(t). Thus

$$|N(f)|^2 = N(f)\cdot N^*(f) = \sum_{k=1}^{NB}\sum_{i=1}^{NB} I_k I_k |F(f)|^2\, e^{-j2\pi f(T_k - T_i)} \quad . \tag{A.4}$$

Substituting (A.2) into (A.1) and interchanging the order of integration and expectation gives

$$P_{AVG} = \frac{1}{T_n}\int_{-\infty}^{\infty} E\{|N(f)|^2\}\,df \quad . \tag{A.5}$$

The expected value of $|N(f)|^2$ with respect to I is given by

$$E_I\{|N(f)|^2\} = \sum_{k=1}^{NB}\sum_{i=1}^{NB} E_I\{I_k I_i\}\,|F(f)|^2\, e^{-j2\pi f(T_k - T_i)} \quad . \tag{A.6}$$

For the case where I_k and I_i are zero-mean independent random variables, it follows that $E_I\{I_k I_i\} = \sigma_k^2\,\delta_{ik}$, where $\delta_{ik} = 0$ if $i \neq k$ and σ_k^2 is the weighting factor variance. If σ_k^2 is a constant σ^2 for all bursts, then (A.6) becomes

$$E_I\{|N(F)|^2\} = NB\,\sigma^2\,|F(f)|^2 \quad . \tag{A.7}$$

Taking the expected value of (A.7) with respect to NB yields

$$E\{|N(f)|^2\} = E_{NB}\{E_I\{|N(f)|^2\}\} = \sigma^2 \, |F(f)|^2 \, E_{NB}\{NB\} \quad . \quad (A.8)$$

For a process where $E_{NB}\{NB\} = \nu_B T_n$ (e.g., a Poisson process with average rate ν_B) the average power expression of (A.5) becomes,

$$P_{AVG} = \int_{-\infty}^{\infty} \nu_B \sigma^2 \, |F(f)|^2 \, df \quad . \quad (A.9)$$

It follows from (A.9) that the one-sided power-density spectrum is

$$S_n(f) = 2 \, \nu_B \sigma^2 \, |F(f)|^2 \quad . \quad (A.10)$$

This result can be extended to the GIN (Single Function) model of (2.6) by replacing f(t) with the sample function $G_k(t)$ and taking the expected value with respect to the type of waveform. The result is

$$S_n(f) = 2 \, \nu_B \sigma^2 \sum_{k=1}^{NE} |\mathcal{F}\{G_k(t)\}|^2 \, P[G_k(t)] \quad , \quad (A.11)$$

where $\mathcal{F}\{G_k(t)\}$ is the Fourier transform of $G_k(t)$.

A.2 PROBABILITY DENSITY FUNCTIONS

The GIN (Unique Waveform) model is used in determining $p_n(\alpha)$, the amplitude p.d.f. for impulse noise. Two random variable models are examined for NB, the number of bursts that occur in time T_n.

The procedure used in the derivation is similar to that employed by Rice [35], Middleton [36], and Ziemer [10]. The characteristic function M(u) is determined first and the noise p.d.f. is obtained through an integral transform.

A.2.1 Basic Form of Characteristic Function

The characteristic function M(u) can be expressed in terms of the number of noise bursts that occur, viz.,

$$M(u) = \sum_{NB=0}^{\infty} M(u|NB)\ P[NB] \quad , \tag{A.12}$$

where

$$M(u|NB) = E\{e^{jun(t)}|NB\} = E\left\{\exp[ju \sum_{k=1}^{NB} I_k f(t-T_k)]\right\} \quad . \tag{A.13}$$

It is assumed that the random variables I_k and T_k are statistically independent and that I_k (or T_k) is independent of I_j (or T_j), $j \neq k$. It is further assumed that the p.d.f. descriptions for the weighting factor and occurrence time do not change between bursts. Hence, the subscripts are dropped and

$$M(u|NB) = [E\{e^{juIf(t-T)}\}]^{NB} \quad . \tag{A.14}$$

The expected value is given by

$$E\{e^{juIf(t-T)}\} = \int_i \int_\tau e^{juif(t-\tau)}\ p_I(i)\ p_T(\tau)\ d\tau di. \qquad (A.15)$$

Thus, the characteristic function can be expressed as

$$M(u) = \sum_{NB=0}^{\infty} \left[\int_i \int_\tau e^{juif(t-\tau)}\ p_I(i)\ p_T(\tau)\ d\tau di \right]^{NB} P[NB] \quad . \qquad (A.16)$$

Two models for P[NB] are examined, namely a single-burst assumption and multiple bursts with occurrence times described by a Poisson distribution.

A.2.2 Single-Burst Assumption

For some systems it is appropriate to assume that no more than one noise burst can occur in the time range of interest, i.e., $P[NB \geq 2] = 0$. With this assumption (A.16) becomes

$$M(u) = P[NB=0] + P[NB=1] \int_i \int_\tau e^{juif(t-\tau)}\ p_I(i)\ p_T(\tau)\ d\tau di \quad . \qquad (A.17)$$

The corresponding p.d.f. can be obtained from the integral transform

$$p_n(\alpha) = \frac{1}{2\pi} \int_{-\infty}^{\infty} M(u)\ e^{-ju\alpha}\ du \quad . \qquad (A.18)$$

Substituting (A.17) into (A.18) and interchanging the order of integration gives,

$$p_n(\alpha) = P[NB=0]\ \delta(\alpha) + P[NB=1] \int_i \int_\tau \delta(\alpha - if(t-\tau)) p_I(i) p_T(\tau)\ d\tau di. \qquad (A.19)$$

For given $p_I(i)$ and $p_T(\tau)$ this expression is difficult to evaluate because of the delta function $\delta(\alpha-if(t-\tau))$, but it can be used readily in determining functions that involve the integral pf $p_n(\alpha)$, e.g., the cumulative distribution function.

A.2.3 Poisson Distribution Assumption

The characteristic function of (A.12) can be expressed using a Poisson distribution to describe the number of noise bursts in time T_n, i.e.,

$$M(u) = \sum_{NB=0}^{\infty} M(u|NB) \frac{(\nu_B T_n)^{NB}}{NB!} e^{-\nu_B T_n} . \tag{A.20}$$

An expression for $M(u|NB)$ can be obtained by expanding the exponential term in (A.14) into a power series and taking the expectation of each term, namely,

$$M(u|NB) = \left[\sum_{m=0}^{\infty} \frac{(ju)^m}{m!} E\{I^m\} E\{f^m(t-T)\} \right]^{NB} , \tag{A.21}$$

where

$$E\{I^m\} = \int_{-\infty}^{\infty} i^m p_I(i) \, di \tag{A.22}$$

and

$$E\{f^m(t-T)\} = \int_{-\infty}^{\infty} f^m(t-\tau) p_T(\tau) \, d\tau . \tag{A.23}$$

If the burst occurrence times are uniformly distributed over T_n, then

$$E\{f^m(t-T)\} = \frac{1}{T_n} \int_0^{T_n} f^m(t-\tau)\, d\tau \quad . \tag{A.24}$$

Substituting (A.24) and (A.21) into (A.20), gives

$$M(u) = \sum_{NB=0}^{\infty} \frac{e^{-\nu_B T_n}}{NB!} \left[\nu_B \sum_{m=0}^{\infty} \frac{(ju)^m}{m!} E\{I^m\} \int_0^{T_n} f^m(t-\tau)\, d\tau \right]^{NB} \quad . \tag{A.25}$$

Letting

$$\lambda_m = \nu_B E\{I^m\} \int_0^{T_n} f^m(t-\tau)\, d\tau \quad , \tag{A.26}$$

then

$$\begin{aligned} M(u) &= e^{-\nu_B T_n} \sum_{NB=0}^{\infty} \frac{1}{NB!} \left[\sum_{m=0}^{\infty} \lambda_m \frac{(ju)^m}{m!} \right]^{NB} \\ &= e^{-\nu_B T_n} \exp\left[\sum_{m=0}^{\infty} \lambda_m \frac{(ju)^m}{m!} \right] \\ &= \exp\left[\sum_{m=1}^{\infty} \lambda_m \frac{(ju)^m}{m!} \right] \quad . \end{aligned} \tag{A.27}$$

When I is symmetrically distributed about a zero mean, it follows that $E\{I\} = 0$ and from (A.26) that $\lambda_1 = 0$. The p.d.f. for the noise can be determined from the transform relation of (A.18). It follows that

$$p_n(\alpha) = \frac{1}{2\pi} \int_{-\infty}^{\infty} \exp[-ju\alpha - u^2\lambda_2/2] \exp\left[\sum_{m=3}^{\infty} \lambda_m \frac{(ju)^m}{m!} \right] du \quad . \tag{A.28}$$

A series solution can be obtained by a two-step procedure, namely replace the second exponential by

$$\exp\left[\sum_{m=3}^{\infty} \lambda_m \frac{(ju)^m}{m!}\right] = 1 + \sum_{m=3}^{\infty} \lambda_m \frac{(ju)^m}{m!} + \frac{\lambda_3^2}{72}(ju)^6 + \ldots \quad , \qquad (A.29)$$

and perform a term-by-term integration using the integral relation

$$\int_{-\infty}^{\infty} (ju)^n \exp[-ju\alpha - u^2\lambda_2/2]\, du = (-1)^n \sqrt{\frac{2\pi}{\lambda_2}} \frac{d^n}{d\alpha^n} \exp[-\alpha^2/2\lambda_2] \quad . \qquad (A.30)$$

The derivation of (A.30) is presented in Section A.2.4. The p.d.f. becomes

$$p_n(\alpha) = \frac{1}{\sqrt{\lambda_2}} \psi^{(0)}(x) - \frac{\lambda_3 \lambda_2^{-2}}{3!} \psi^{(3)}(x) + \left[\frac{\lambda_4 \lambda_2^{-5/2}}{4!} \psi^{(4)}(x) + \frac{\lambda_3^2 \lambda_2^{-7/2}}{72} \psi^{(6)}(x)\right] + \ldots \quad , \qquad (A.31)$$

where $x = \alpha/\sqrt{\lambda_2}$ and

$$\psi^{(n)}(x) = \frac{1}{\sqrt{2\pi}} \frac{d^n}{dx^n}\left[e^{-x^2/2}\right] \qquad (A.32)$$

Note that terms have been collected according to the combined powers of the λ terms, or equivalently to the power of ν_B, cf., (A.26). Since the first term is of the Gaussian form, it is evident that the p.d.f. approaches Gaussian as ν_B becomes large.

A.2.4 Derivation of (A.30)

The integral relation of (A.30) is obtained from the definite integral

$$\int_{-\infty}^{\infty} e^{-y^2}\, dy = \sqrt{\pi} \quad . \tag{A.33}$$

Changing variables $y = t\sqrt{h/2}$ yields

$$\int_{-\infty}^{\infty} e^{-ht^2/2}\, dt = \sqrt{2\pi/h} \quad . \tag{A.34}$$

Differentiating n times with respect to h and multiplying by $(-1)^n\, 2^n$ gives

$$\int_{-\infty}^{\infty} t^{2n}\, e^{-ht^2/2}\, dt = \sqrt{2\pi}\, \frac{(2n)!}{2^n\, n!}\, h^{-n-1/2} \quad . \tag{A.35}$$

Next, consider the integral

$$\int_{-\infty}^{\infty} e^{-ju\alpha}\, e^{-u^2\lambda_2/2}\, du = \sum_{k=0}^{\infty} \frac{(-j\alpha)^k}{k!} \int_{-\infty}^{\infty} u^k\, e^{-u^2\,\lambda_2/2}\, du \quad . \tag{A.36}$$

The integral yields zero for odd values of k, thus the summation index can be changed and (A.35) used to obtain

$$\sum_{m=0}^{\infty} \frac{(-j\alpha)^{2m}}{(2m)!} \int_{-\infty}^{\infty} u^{2m}\, e^{-u^2\,\lambda_2/2}\, du = \sum_{m=0}^{\infty} \frac{1}{m!} \sqrt{\frac{2\pi}{\lambda_2}} \left[\frac{-\alpha^2}{2\lambda_2}\right]^m \quad . \tag{A.37}$$

and

$$\int_{-\infty}^{\infty} e^{-ju\alpha} \exp[-u^2\lambda_2/2]\, du = \sqrt{\frac{2\pi}{\lambda_2}}\ \exp[-\alpha^2/2\lambda_2] \quad . \qquad (A.38)$$

Differentiating n times with respect to α, and multiplying by $(-1)^n$ gives the integral relation of (A.30).

APPENDIX B

ALTERNATIVE METHOD FOR FINDING THE CONDITIONAL BIT ERROR PROBABILITY

An alternative method exists for finding the conditional probability of bit error for the correlation receiver using the GIN (Unique Waveform) model with the additional restriction of a single noise burst per bit time. The approach is to find the p.d.f. description for the decision statistic, D^k, given that one burst has occurred. From (3.31),

$$D^k|(NB=1) = I\ V\ F(T) - C_k \quad . \qquad k = 0,1 \quad . \tag{B.1}$$

The p.d.f. for $D^k|(NB=1)$, i.e., $p_D(\alpha)$, is obtained by finding the corresponding characteristic function, $M_D(u)$ and then taking the integral transform, viz.,

$$p_D(\alpha) = \frac{1}{2\pi} \int_{-\infty}^{\infty} M_D(u)\ e^{-ju\alpha}\ du \quad , \tag{B.2}$$

where

$$M_D(u) = E\{e^{juD^k}\} = E\{e^{ju[IVF(T)-C_k]}\} \quad . \tag{B.3}$$

Assuming that the random variables I and T are statistically independent, (B.3) becomes

$$M_D(u) = \int_i \int_\tau e^{ju[iVF(\tau)-C_k]}\, p_I(i)\, p_T(\tau)\, d\tau di \quad . \tag{B.4}$$

Substituting (B.4) into (B.2) and interchanging the order of integration gives

$$p_D(\alpha) = \int_i \int_\tau p_I(i)\, p_T(\tau) \int_{-\infty}^{\infty} e^{-ju[\alpha-iVF(\tau)+C_k]}\, du d\tau di$$

$$= \int_i \int_\tau p_I(i)\, p_T(\tau)\, \delta(\alpha - iVF(\tau) + C_k)\, d\tau di \quad . \tag{B.5}$$

Using the receiver decision rule for message symbol m_0 yields

$$P_1[\varepsilon_m|m_0] = P[D^0 > 0|NB=1] = \int_0^{\infty} p_D(\alpha)\, d\alpha$$

$$= \int_i \int_\tau p_I(i)\, p_T(\tau) \int_0^{\infty} \delta(\alpha - iVF(\tau) + C_0)\, d\alpha d\tau di. \tag{B.6}$$

The integral of the delta function will equal one if

$$iVF(\tau) - C_0 > 0 \quad , \tag{B.7}$$

otherwise the integral equals zero. It follows that

$$P_1[\varepsilon_m|m_0] = \int_{R_0} \int p_I(i)\, p_T(\tau)\, d\tau di \quad , \tag{B.8}$$

where R_0 is the region such that $iVF(\tau) > C_0$. An analogous development for message symbol m_1 results in

$$P_1[\varepsilon_m|m_1] = P[D^1 < 0|NB=1] = \iint_{R_1} p_I(i)\ p_T(\tau)\ d\tau di \quad , \qquad (B.9)$$

where R_1 is the region such that $iVF(\tau) < C_1$. Since (B.8) and (B.9) are equivalent to (3.35), the remainder of the error analysis is unchanged.

APPENDIX C

COMPUTER PROGRAM: GINIMP

This appendix contains the flow chart, Fortran-IV program listing and description for an IBM System/360 computer program which implements the GIN model performance analysis derived in Chapter 3. The program name, GINIMP, is an acronym for Generalized-Impulse-Noise Implementation of Model Performance.

C.1 GENERAL INFORMATION

The performance analysis for $P_1[\varepsilon_m]$, is implemented for a specified data bit, signal set, ENP value, noise waveform, and weighting-factor probability density function (p.d.f.). The user can specify the data bit, ENP value, and one of five weighting factor density functions through input data cards. The signal set and noise waveform are specified by means of input data and a function subprogram, GRANF(x). Five typical signal sets (Unipolar, Polar, ASK, PSK, FSK) have been incorporated into the program. Others can be added at the user's discretion by modifying the subprogram. The input data format and GRANF construction are explained in Section C.2.

The normalized probability of error, from (3.42), is given by

$$P_1[\varepsilon_m] = \frac{1}{T_b} \int_{I_{min}/\sigma}^{\infty} T_{R1}(n) p_N(n)\, dn \quad . \tag{C.1}$$

Numerical techniques are used to approximate the integral solution. Specifically, values for the p.d.f. $p_N(n)$ and the time-range function $T_{R1}(n)$ are calculated for values of n between a minimum value CXN, i.e., I_{min}/σ and a maximum value XNM. An estimate to the integral is obtained by using the trapazoidal rule with upper and lower bound calculations. An explanation of how these steps are performed is given in Section C.2.

C.2 FLOW CHART, PROGRAM LISTING AND EXPLANATION

The flow chart of the GINIMP computer program is shown in Fig. C-1. A program listing is presented in Fig. C-2 which is found at the end of this Appendix. The numbers positioned beside the flow-chart symbols indicate the level of statement numbers used in the main program.

In the first step, two data cards are read and interpreted according to the format and data identification given in Tables C.1 and C.2. The input ENP and SIGSET values are used to calculate the FENP values, where

$$\text{FENP} = \frac{C_0}{(1-\rho)V\sigma} \quad . \tag{C.2}$$

It has been shown in Section 3.3 that for selected signal sets this is a function of the ENP value. The signal-set parameter SIGSET determines the function to be used, cf., (3.55) and (3.56) for specific examples. In addition, parameters used in other parts of the program are calculated and initialized.

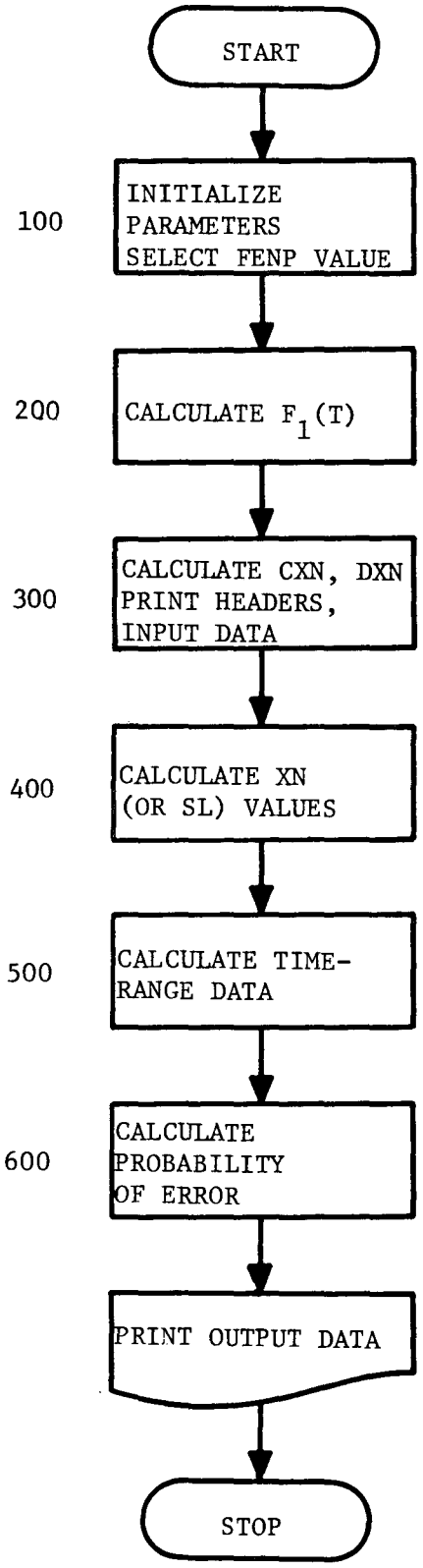

Fig. C-1. GINIMP Flow Chart

TABLE C.1

DATA CARD 1 FORMAT AND IDENTIFICATION

SYMBOL	COLUMN LOCATION	FORMAT	EXPLANATION
KBIT	1-2	I2	KBIT*TB = Starting time of data bit being analyzed
TB	3-14	F12.6	Bit duration (in ms)
TF	15-26	F12.6	Noise Waveform duration (in ms)
ENP	27-38	F12.6	Energy-to-Noise Parameter = $E_{AVG}T_b/\sigma^2$
M	39-40	I2	Specifies p.d.f., Gaussian M=1, Rayleigh M=2, Lognormal M=3, Uniform M=4, Hyperbolic M=5
PA	41-52	F12.6	Parameter value associated with p.d.f.
D	53-64	F12.6	Parameter associated with noise waveform
FREQ	65-76	F12.6	Parameter associated with noise waveform
NENP	77-80	I4	Number of ENP values used

TABLE C.2

DATA CARD 2 FORMAT AND IDENTIFICATION

SYMBOL	COLUMN LOCATION	FORMAT	EXPLANATION
DF	1-5	F5.2	Specifies even step increments for Slice Level (DF < 0), or weighting factor (DF $\geq$ 0)
KKK	6-9	I4	Number of interpolated $F_1(T)$ values
KK	10-13	I4	Number of calculated $F_1(T)$ values
II	14-17	I4	Number of Weighting-Factor values (and Slice Levels) used
ISLM	18-21	I4	Specifies calculation of CXN (ISLM $\leq$ 0)
SLM	22-33	F12.6	Maximum Slice-Level value to be used
XNM	34-45	F12.6	Maximum Weighting-Factor value to be used
SIGSET	46-48	F3.1	Signal Set to be analyzed, Unipolar = 1, Polar = 2, ASK = 3, PSK = 4, FSK = 5

The calculation of the $F_1(T)$ data is accomplished in the second step using (3.48), i.e.,

$$F_1(T) = \frac{F(T)}{1-\rho} = \frac{1}{(1-\rho)V} \int_{(KBIT)TB}^{(KBIT+1)TB} f(t-T)[s_1(t)-s_0(t)]\, dt \quad . \qquad (C.3)$$

The program calculates KK+1 values for the F1 array corresponding to $F_1(T_J)$ for the values of $T_J=(J-1)TB/KK$, where J=1,2,..., (KK+1). Since f(t-T)=0 for t<T, it follows for the first bit that KBIT=0 and the integral in (C.3) becomes

$$F_1(T) = \int_0^{TB} GRANF(t)dt = \int_T^{TB} GRANF(t)dt \quad , \qquad (C.4)$$

where

$$GRANF(t) = \frac{f(t-T)[s_1(t)-s_0(t)]}{(1-\rho)V} \quad . \qquad (C.5)$$

A similar result holds for (t-T)>TF. The proper limits of integration (A to B) are determined by subroutine LIMINT which is called using the statement CALL LIMINT(KBIT,TB,T,TF,A,B,). GRANF is provided as a function subprogram, and for the example shown in Fig. C-2 contains the exponentially-decaying-sinusoid noise waveform, i.e.,

$$f(t-T) = C \sin[2\pi f_o(t-T)] \exp[-d(t-T)] \qquad (C.6)$$

Input data is used to specify f_o, d, and the time duration by the use of the mnemonics FREQ, D and TF as defined in Table C.1. The subprogram

calculates C such that f(t) has unit energy. The SIGSET parameter, defined in Table C.2, is used to determine the signal set difference $[s_1(t)-s_0(t)]/[(1-\rho)V]$. The user must modify the f(t) and signal set descriptions if additional forms are to be used in GRANF(t). The integration of GRANF for each T_J is accomplished by the IBM subroutine QATR [44]. The accuracy of each integration is specified by FPS, and the subroutine returns an error message (IER) to indicate if the accuracy was obtained. A printout of the header I and IER is produced. All values of IER that indicate the accuracy FPS was not obtained are also printed. If all integrations are within the required accuracy the statement "ALL INTEGRATIONS WITHIN SPECIFIED ACCURACY" is printed. The maximum value stored in the F1 array, FMAX, is determined and at the user's option ($ISLM \leq 0$) used to calculate the maximum slice level SLM.

The third step of the program, i.e., the 300 block, calculates the beginning n-value CXN, the step size DXN for equal steps of n values, and CC for equal slice-level step values. Printout includes headers, input data and calculated parameters.

Values for n and the slice levels are calculated and stored in the XN (or SL) array in the fourth step. The user specifies by the value of DF whether the program uses equal step-size values for XN ($DF<0$) or equal step-size values for SL ($DF \geq 0$).

During the fifth step the time-range function $T_{R1}(n)$ is approximated by calculating values for the TR array. This is accomplished by comparing each value in the F1 array to each value in the SL array and increasing the number in the TR array by one if F1(I)>SL(J). A

linear interpolation is performed between the calculated F1 values and each point is classified as above. The elements of the TR array can be divided by the number of F1 points considered to yield an approximation to $T_{R1}(n)/T_b$.

The probability of error is calculated in the last operation. First, the TR array is modified to obtain $T_{R1}(n)/T_b$, and the result multiplied by the corresponding p.d.f. value obtained from the function subprogram PDF(X,M,PA). The user selects one of five p.d.f. descriptions by selecting the proper m-parameter value as listed in Table C.1. The PA value is a parameter used by either the lognormal (PA>0) or the hyperbolic 3<PA<6 distributions. The numerical-integration subroutine QTFGB is then used to calculate the approximation of $P_1[\varepsilon_m]$. The subroutine is similar to the IBM subroutine QTFG [44], but has been modified to include upper and lower bounds for the integral.

A printout is made from the various arrays, the most significant of which are the cumulative probability of errors obtained from the integration subroutine, namely POEL the lower bound, POE the probability of error, and POEU the upper bound. The last value in the POE array represents $P_1[\varepsilon_m]$, and two checks for accuracy can be performed. First, the values of POE should converge to the last value. If this does not happen, the user should increase the maximum value of n, XNM, and repeat the computation until convergence is obtained. Second, the lower and upper bounds can be compared to the POE value to determine if a sufficient number of XN values (II) were used.

```
      DIMENSION TR(500),SL(500),ANP(500),AUX(500),F1(500)
      DOUBLE PRECISION CXN,DXN,XN(500),POE(500),POEL(500)
      DOUBLE PRECISION POEU(500)
      EXTERNAL GRANF
      COMMON T,TF,FREQ,D,ISIG
      READ(5,101)KBIT,TB,TF,ENP,M,PA,D,FREQ,NENP
101   FORMAT(I2,3F12.6,I2,3F12.6,I4)
      READ(5,102)DF,KKK,KK,II,ISLM,SLM,XNM,SIGSET
102   FORMAT(F5.2,4I4,2F12.6,F3.1)
      IRE=0
      III=500
      ISIG=SIGSET
      DO 605 IENP=1,NENP
      IF(IENP.EQ.1) GO TO 107
      ENP=10.*ENP
107   CONTINUE
      GO TO(103,104,105,103,103),ISIG
103   FENP=SQRT(ENP/2.)
      GO TO 106
104   FENP=SQRT(ENP)
      GO TO 106
105   FENP=SQRT(ENP/4.)
106   CONTINUE
      IF(IENP.GE.2) GO TO 301
C*************************************************************
C     SETS UP CONDITIONS, DETERMINES LIMITS, CALCULATES F(T)
C     FOR EACH VALUE OF T SPECIFIED, AND STORES RESULTS IN
C     THE F1 ARRAY
C
      FMAX=0.
      DTT=TB/(1000.*KK*KKK)
      KK1=KK+1
      KKK1=KKK+1
      WRITE(6,200)
200   FORMAT('0',4X,'I',4X,'IER',/,'**********************',
     1'**********************************')
      DO 204 I=1,KK1
      T=(I-1)*TB/KK
      CALL LIMINT(KBIT,TB,T,TF,A,B)
      FPS=1.0E-7
      A=A*.001
      B=B*.001
      CALL QATR(A,B,FPS,III,GRANF,Y,IER,AUX)
      F1(I)=Y
      IF(IER) 201,203,201
201   CONTINUE
      IRE=IRE+1
      WRITE(6,202)I,IER
```

Fig. C-2. GINIMP Program Listing

```
202   FORMAT(2X,2I4)
203   CONTINUE
      YABS=ABS(Y)
      IF(YABS.LT.FMAX)GO TO 204
      FMAX=YABS
204   CONTINUE
      IF(IRE) 508,506,508
506   WRITE(6,507)
507   FORMAT(2X,'ALL INTEGRATIONS WITHIN SPECIFIED ACCURACY')
508   CONTINUE
      IF(ISLM)205,205,301
205   SLM=FMAX+.000001
C*****************************************************
C     CALCULATES PARAMETERS BASED ON INPUT DATA,
C     HEADER AND DATA OUTPUT
C
301   CXN=FENP/SLM
      DXN=(XNM-CXN)/(II-1)
      TR(1)=0.
      SL(1)=0.
      XN(II)=10**4
      XN(1)=CXN
      SL(II)=FENP/CXN
      CC=SLM/(II-1)
      WRITE(6,302) SIGSET
302   FORMAT('1',20X,'PERFORMANCE ANALYSIS FOR GIN MODEL ',
     1'AND SIGSET=',F3.1,/,2X,'**************************',
     1'**************************************',
     1'*****',/,2X,'THE INPUT PARAMETERS ARE',/)
      WRITE(6,304)
304   FORMAT(6X,'KBIT',8X,'TB',10X,'TF',9X,'ENP',9X,'M',9X,
     1'PA',10X,'D',10X,'FREQ')
      WRITE(6,305) KBIT,TB,TF,ENP,M,PA,D,FREQ
305   FORMAT(7X,I2,5X,3F12.8,2X,I2,1X,3F12.4,/)
      WRITE(6,306)
306   FORMAT(9X,'DF',8X,'KKK',1X,'KK',2X,'II',4X,'CXN',9X,
     1'DXN',9X,'SLM')
      WRITE(6,307)DF,KKK,KK,II,CXN,DXN,SLM
307   FORMAT(6X,F12.8,3I4,3F12.8)
      WRITE(6,309)
309   FORMAT(2X,12(/),2X,'NOISE WAVEFORM USED****',
     1'EXPONENTIALLY DECAYING SINUSOID')
C*****************************************************
C     CALCULATES EVEN SL OR EVEN XN
C
      IF(DF)403,401,401
401   DO 402 J=2,II
      TR(J)=0.
```

Fig. C-2 (Continued). GINIMP Program Listing

```
      SL(J)=(J-1)*CC
402   XN(II+1-J)=FENP/SL(J)
      GO TO 405
403   DO 404 I=2,II
      TR(I)=0.
      XN(I)=XN(I-1)+DXN
404   SL(II+1-I)=FENP/XN(I)
405   CONTINUE
C*****************************************************************
C     INTERPOLATES AND CLASSIFIES THE F(T) VALUES
C
      DO 505 I=2,KK1
      IF(I.LT.KK1) GO TO 501
      JJK=KKK1
      GO TO 502
501   JJK=KKK
502   DO 504 J=1,JJK
      TT=(J-1)*DTT
      F2=ABS((F1(I)-F1(I-1))*((J-1)/KKK)+F1(I-1))
      DO 504 L=1,II
      IF(F2.GE.SL(L)) GO TO 503
      GO TO 504
503   TR(L)=TR(L)+1
504   CONTINUE
505   CONTINUE
C*****************************************************************
C     CALCULATES THE PROBABILITY OF ERROR
C
      WRITE(6,601)
601   FORMAT('1',80X,'CUMULATIVE PROBABILITY OF ERROR',/,5X,
     1'I',10X,'XN',14X,'SL',14X,'TR',13X,'ANP',12X,'LOWER',
     111X,'AVERAGE',9X,'UPPER',/,2X,'**********************',
     1'**************************************************',
     1'**************************************************')
      DO 604 I=1,II
      TR(I)=TR(I)/(KK*KKK+1)
      INEW=II+1-I
      YPDF=PDF(XN(INEW),M,PA)
      ANP(INEW)=TR(I)*YPDF
604   CONTINUE
      CALL QTFGB(XN,ANP,POE,POEL,POEU,II)
      WRITE(6,603)(I,XN(I),SL(II+1-I),TR(II+1-I),ANP(I),
     1POEL(I),POE(I),POEU(I),I=1,II)
603   FORMAT(2X,I4,7F16.9)
605   CONTINUE
      STOP
      END
```

Fig. C-2 (Continued). GINIMP Program Listing

```
      SUBROUTINE QTFGB(X,Y,Z,ZL,ZU,NDIM)
      DIMENSION Y(500)
      DOUBLE PRECISION X(500),Z(500),ZL(500),ZU(500)
      DOUBLE PRECISION SUM2,SUML2,SUMU2
      SUM2=0.
      SUML2=0.
      SUMU2=0.
      IF(NDIM-1)4,3,1
1     DO 2 I=2,NDIM
      SUM1=SUM2
      SUML1=SUML2
      SUMU1=SUMU2
      DELTAX=X(I)-X(I-1)
      SUMP=.5*DELTAX*(Y(I)+Y(I-1))
      SUM2=SUM2+SUMP
      DELTAY=Y(I)-Y(I-1)
      DELY2=Y(I+1)-Y(I)
      DELY0=Y(I-1)-Y(I-2)
      DELYY2=DELY2-DELTAY
      DELYY1=DELTAY-DELY0
      S1=DELY0/(X(I-1)-X(I-2))
      S2=DELY2/(X(I+1)-X(I))
      IF(S1.EQ.S2) GO TO 10
      IF(I.EQ.2.OR.I.EQ.NDIM) GO TO 8
      D=(DELTAY-S2*DELTAX)/(S1-S2)
      DI=DELTAX-D
      A=(Y(I-1)+D*S1/2.)*D+(Y(I)-DI*S2/2.)*DI
      IF(DELYY2.GE.0..AND.DELYY1.GE.0.) GO TO 5
      IF(DELYY2.LT.0..AND.DELYY1.LT.0.) GO TO 6
      SUML2=SUML2+SUMP
      SUMU2=SUMU2+SUMP
      GO TO 7
5     SUML2=SUML2+A
      SUMU2=SUMU2+SUMP
      GO TO 7
6     SUML2=SUML2+SUMP
      SUMU2=SUMU2+A
      GO TO 7
8     A1=(I-2)*(Y(NDIM-1)+S1*DELTAX/2.)/(NDIM-2)+
     1(I-NDIM)*(Y(2)-S2*DELTAX/2.)/(2-NDIM)
      A=A1*DELTAX
      IF(DELYY2.GE.0..AND.I.EQ.2) GO TO 9
      IF(DELYY1.GE.0..AND.I.EQ.NDIM) GO TO 9
      SUML2=SUML2+SUMP
      SUMU2=SUMU2+A
      GO TO 7
9     SUML2=SUML2+A
      SUMU2=SUMU2+SUMP
```

Fig. C-2 (Continued). GINIMP Program Listing

```
      GO TO 7
 10   SUML2=SUML2+SUMP
      SUMU2=SUMU2+SUMP
    7 ZL(I-1)=SUML1
      ZU(I-1)=SUMU1
2     Z(I-1)=SUM1
3     Z(NDIM)=SUM2
      ZL(NDIM)=SUML2
      ZU(NDIM)=SUMU2
4     RETURN
      END
C*************************************************************
C
      SUBROUTINE LIMINT(KBIT,TB,T,TF,A,B)
      J=TF/TB
      IF(KBIT.GT.0..AND.KBIT.LT.J) GO TO 50
      IF(KBIT.EQ.0..AND.J.EQ.0.) GO TO 53
      IF(KBIT.GT.0..AND.J.EQ.KBIT) GO TO 55
      IF(KBIT.EQ.(J+1.)) GO TO 51
      IF(KBIT.EQ.0..AND.J.GT.0.) GO TO 57
      GO TO 58
 50   A=KBIT*TB
      B=(KBIT+1.)*TB
      GO TO 58
 51   IF((T+TF).LE.KBIT*TB) GO TO 52
 56   A=KBIT*TB
      B=T+TF
      GO TO 58
 52   A=0.
      B=0.
      GO TO 58
 53   IF((T+TF).LE.TB) GO TO 54
 57   A=T
      B=TB
      GO TO 58
 54   A=T
      B=T+TF
      GO TO 58
 55   IF((T+TF).LE.((KBIT+1.)*TB)) GO TO 56
      GO TO 50
 58   RETURN
      END
```

Fig. C-2 (Continued). GINIMP Program Listing

```
      FUNCTION GRANF(X)
      COMMON T,TF,FREQ,D,ISIG
      F=FREQ
      TFF=TF*.001
      PI=3.14159265358979
      A=1./(PI*F)*SQRT((D*(D**2+4.*(PI*F)**2))/(1-EXP(-
     12.*D*TFF)))
      GRANF=A*SIN(2.*PI*F*(X-T*.001))*EXP(-D*(X-T*.001))
      GO TO(1,1,2,2,3),ISIG
    1 RETURN
    2 GRANF=GRANF*SIN(2000.*PI*X)
      RETURN
    3 GRANF=GRANF*(SIN(2000.*PI*X)-SIN(4000.*PI*X))
      RETURN
      END
C*************************************************************
C
      FUNCTION PDF(X,M,PA)
      PI=3.14159265358979
      GO TO(1,2,3,4,5),M
    1 PDF=(1/SQRT(2.*PI))*EXP(-X**2/2.)
      RETURN
    2 PDF=ABS(X)*EXP(-X**2)
      RETURN
    3 PD1=1/(SQRT(8.*PI)*PA*ABS(X))
      PD2=EXP(-(ALOG(ABS(X))+PA**2)**2/(2.*PA**2))
      PDF=PD1*PD2
      RETURN
    4 Z=ABS(X)
      IF(Z-SQRT(3.))41,41,42
   41 PDF=1/SQRT(12.)
      RETURN
   42 PDF=0
      RETURN
    5 PD3=(PA-1)*((PA-2.)*(PA-3.))**((PA-1)/2.)
      PD4=(SQRT((PA-2.)*(PA-3.))+SQRT(2.)*ABS(X))**PA
      PDF=1/SQRT(2.)*PD3/PD4
      RETURN
      END
```

Fig. C-2 (Continued). GINIMP Program Listing

APPENDIX D

COMPUTER PROGRAM: LIMITER

The Fortran-IV computer program LIMITER implements the performance results of Section 5.2. The program name is a mnemonic to emphasize the association with the generalized limiter of Fig. 5.2. A succinct explanation of this program is presented by the use of a flow chart and program listing.

D.1 GENERAL INFORMATION

The program implements (5.12) to calculate $P_1[\varepsilon_m|m_j]$ for a given data bit, signal set, ENP value, noise waveform, limiter parameters, and weighting factor p.d.f. The use of either positive or negative values for the weighting factor must also be controlled. These parameters are specified by input data and function subprograms. Four typical signal sets (Unipolar, Polar, ASK and PSK) and the five weighting-factor p.d.f.s of Table 3.1 have been incorporated into the program. Numerical techniques are used to approximate the integral solutions. The minimum weighting-factor value can be specified or calculated in the program by an iteration process. An explanation of the program operation is given in Section D.2.

D.2 FLOW CHART, PROGRAM LISTING AND EXPLANATION

The LIMITER program flow chart is shown in Fig. D-1. A program listing is presented in Fig. D-2, which is located at the end of this Appendix. The first symbol represents the operations performed by statement numbers 0 through 299. Five data cards are read by the format and data identification given in Tables D.1 through D.5. Two arrays are calculated based on the function subprogram specification of the signal set and noise waveform. The ENP value is selected from the ENPA array and the program is initialized for positive or negative weighting-factor calculations. The calculation of $C_0/(\sigma V)$ is made according to the signal set selected. Headers and data are printed and parameters are initialized for the weighting factor iteration process.

TABLE D.1

DATA CARD 1 FORMAT AND IDENTIFICATION

SYMBOL	COLUMN LOCATION	FORMAT	EXPLANATION
ENPA(1) ENPA(2) ENPA(3)	2-13 14-25 26-37	F12.10 F12.10 F12.10	ENPA is a one-dimensional array with three elements containing the ENP Values

The second step in the flow chart corresponds to operations performed by statements with numbers 300 through 899. Normally, the iteration process for the minimum positive (or maximum negative) weighting factor will be utilized (by specifying ISCH = 1). The

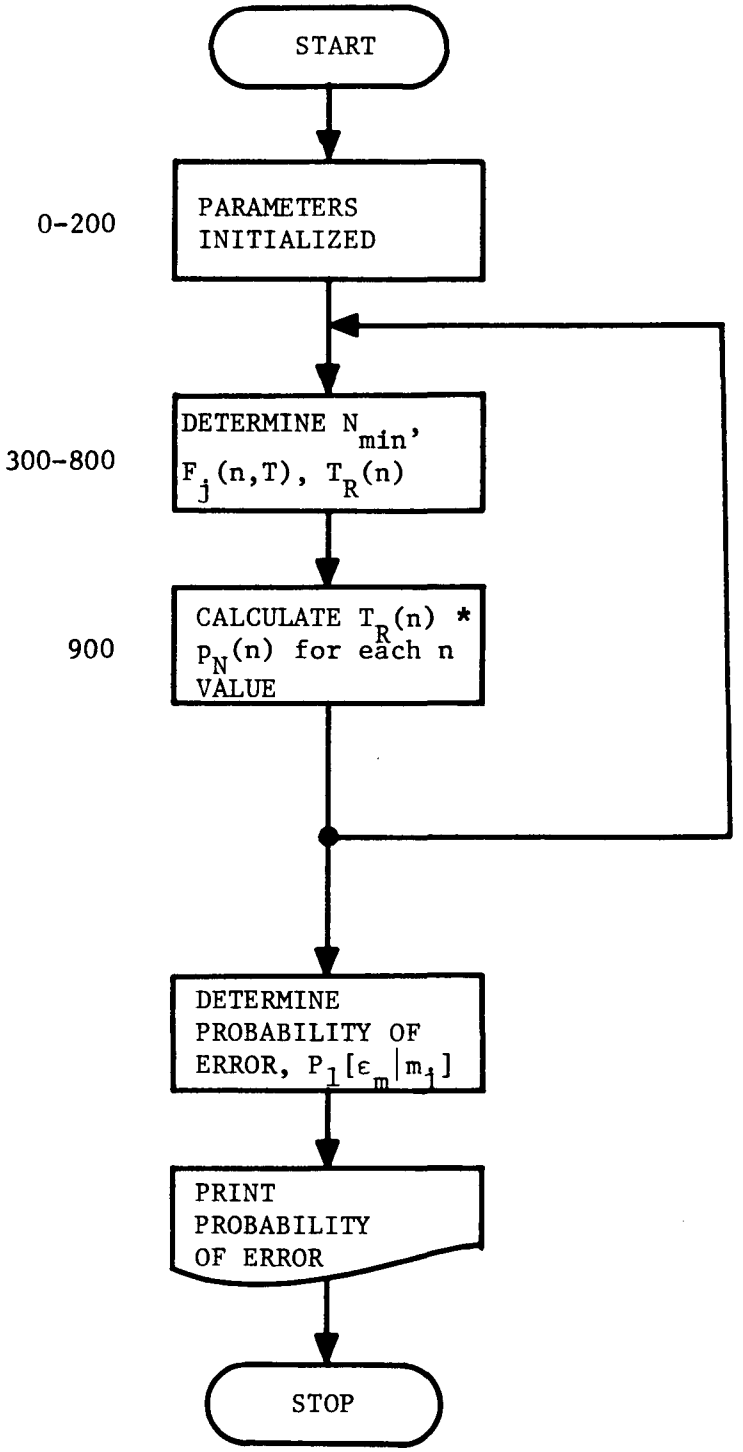

Fig. D-1. LIMITER Flow Chart

time-range function is calculated for a weighting-factor value of CXO/2. Successive approximation steps in the weighting-factor value are made in the iteration attempt to locate the largest value that gives a zero value for the time range. After this operation is complete, the array of weighting-factor values is finalized. The nonlinear operation $\{Nf(t-T)\}^{ooo}$ is performed in the series of steps through the 500-level statement numbers. These results are multiplied by the signal-set array data and integrated in the 600-level statements. An approximation to the time-range function is made in the 700-level statements by classifying and interpolating the integral results that exceed $C_0/(\sigma V)$.

TABLE D.2

DATA CARD 2 FORMAT AND IDENTIFICATION

SYMBOL	COLUMN LOCATION	FORMAT	EXPLANATION
SIGSET	3-13	F10.4	Signal Set to be analyzed, Unipolar = 1, Polar = 2, ASK = 3, PSK = 4
F1	14-23	F10.4	Frequency of $s_1(t)$ for ASK and PSK
F0	24-33	F10.4	Not used, intended for frequency of $s_0(t)$ for FSK.
KBIT	34-37	I4	KBIT*TB = Starting time of data bit being analyzed
MPDF	38-41	I4	Specifies p.d.f., Gaussian = 1, Rayleigh = 2, Lognormal = 3, Uniform = 4, and Hyperbolic = 5
PA	42-51	F10.8	Parameter value associated with p.d.f.
TB	52-61	F10.8	Bit duration (in sec)

Multiplication of the time-range data by the corresponding p.d.f. values is accomplished by the 900-level program statements. Headers

and output data are printed. An estimate of the error probability is calculated in the last step. The results are presented graphically with the final value in the graph representing the estimate. Checks for convergence of the integral and correct weighting-factor step size should be made.

TABLE D.3

DATA CARD 3 FORMAT AND IDENTIFICATION

SYMBOL	COLUMN LOCATION	FORMAT	EXPLANATION
NIPF	3-6	I4	Number of interpolated points between each time-shift point
NTL	7-10	I4	Number of sample points used in bit time T_b
NTLT	11-14	I4	Number of NTL samples per time shift
NXN	15-18	I4	Number of Weighting-Factor values used between minimum and maximum values
CONN	19-28	F10.3	Defines LIMITER operation, $\beta_n = \sqrt{CONN}\ \alpha_n$
CONP	29-38	F10.3	Defines LIMITER operation, $\beta_p = \sqrt{CONP}\ \alpha_p$
XNMP	39-48	F10.4	Maximum positive Weighting-Factor value
XNMN	49-58	F10.4	Minimum negative Weighting-Factor value

TABLE D.4

DATA CARD 4 FORMAT AND IDENTIFICATION

SYMBOL	COLUMN LOCATION	FORMAT	EXPLANATION
CXNP(1)	1-10	F10.7	CXNP is a one-dimensional area with three elements containing the minimum positive Weighting-Factor values for each of the three ENP values. CXNN is a similar array for the maximum negative Weighting-Factor values.
CXNN(1)	11-20	F10.7	
CXNP(2)	21-30	F10.7	
CXNN(2)	31-40	F10.7	
CXNP(3)	41-50	F10.7	
CXNN(3)	51-60	F10.7	

TABLE D.5

DATA CARD 5 FORMAT AND IDENTIFICATION

SYMBOL	COLUMN LOCATION	FORMAT	EXPLANATION
MJ	3-6	I4	Message symbol to be analyzed m_0=0,m_1=1
ICXN	7-10	I4	Specifies sign of Weighting-Factor values Positive = 1, Negative = 2
ISCH	11-14	I4	Specifies use CXNP or CXNN (ISCH=0) or iteration routine to calculate value (ISCH=1)
CXO	15-26	F12.6	Maximum value of iteration step

```
      DIMENSION XN(600),TIME(600),XNF(1200),SXNF(600),
     1SA(600),YY(101),Z(600),ZZ(100),ANS(100),ENPA(3),CXNN(3),
     1FA(1200),CXNP(3)
      COMMON F1,F0
      PI=3.14159265358979
      READ(5,6)(ENPA(I),I=1,3)
    6 FORMAT(1X,3F12.10)
      READ(5,1)SIGSET,F1,F0,KBIT,MPDF,PA,TB
    1 FORMAT(2X,3F10.4,2I4,2F10.8)
      READ(5,2)NIPF,NTL,NTLT,NXN,CONN,CONP,XNMP,XNMN
    2 FORMAT(2X,4I4,4F10.3)
      READ(5,5)(CXNP(I),CXNN(I),I=1,3)
    5 FORMAT(6F10.7)
      READ(5,4)MJ,ICXN,ISCH,CXO
    4 FORMAT(2X,3I4,F12.6)
      WRITE(6,3)SIGSET,F1,F0,KBIT,MPDF,PA,TB,NIPF,NTL,NTLT,
     1NXN,CONN,CONP,XNMP,XNMN
    3 FORMAT('1',2X,'**********************************************',
     1'**********************************',/,10X,
     1'PERFORMANCE ANALYSIS USING LIMITER',/,3X,'SIGSET',
     14X,'F1',8X,'F0',8X,'KBIT',1X,'MPDF',1X,'PA',9X,'TB',
     1/,2X,3F10.4,2I4,2X,F10.8,1X,F10.8,//,2X,'NIPF',1X,
     1'NTL',1X,'NTLT',1X,'NXN',4X,'CONN',6X,'CONP',6X,
     1'XNMP',6X,'XNMN',/,2X,4I4,4F10.3)
      ISIG=SIGSET
      DTL=TB/(NTL-1)
C     CALCUATE SA AND FA ARRAYS
      DO 101 I=1,NTL
      TL=(I-1)*DTL
      TIME(I)=TL
      SA(I)=S(TL,ISIG)
      TTL=(KBIT-1)*TB+TL
      TTTL=TTL+TB
      FA(I)=F(TTL)
  101 FA(NTL+I)=F(TTTL)
C     SELECT ENP, CXN, XNM AND FENP
C     PRINT HEADER AND INPUT DATA
C     INITIALIZE FOR CXN ITERATION
      DO 910 IENP=1,3
      IF(ICXN-1)202,202,203
  202 CXN=CXNP(IENP)
      XNM=XNMP
      GO TO 204
  203 CXN=CXNN(IENP)
      XNM=XNMN
  204 CONTINUE
      ENP=ENPA(IENP)
      GO TO (210,211,212,213,214),ISIG
```

Fig. D-2. LIMITER Program Listing

```
210    FENP=SQRT(ENP/2.)
       GO TO 215
211    FENP=SQRT(ENP)
       GO TO 215
212    FENP=SQRT(ENP/4.)
       GO TO 215
213    FENP=SQRT(ENP/2.)
       GO TO 215
214    FENP=SQRT(ENP/2.)
215    CONTINUE
       WRITE(6,292) ENP,MJ,ICXN,CXN
292    FORMAT('1','THE FOLLOWING ANALYSIS IS FOR ENP=',F12.8,
      15X,'MJ=',I2,5X,'ICXN=',I2,5X,'CXN=',F12.6,/)
       CXS=CXO
       ICYXN=0
       ISTEP=0
       IXFX=ISCH
C      ITERATION FOR CXN (PART 1)
868    CXS=CXS/2.
       ISTEP=ISTEP+1
       WRITE(6,872)ISTEP,ICYXN,CXN
872    FORMAT(2X,'THE',I3,2X,'STEP YIELDS ICYXN=',I5,2X,'AND',
      1' CXN=',F12.6)
       IF(ISTEP.EQ.50) GO TO 910
       IF(ISTEP.EQ.2.AND.ICYXN.EQ.0) GO TO 910
       IF(ICYXN)866,866,867
866    CXN=CXN+CXS
       GO TO 860
867    CXN=CXN-CXS
860    DXN=(XNM-CXN)/(NXN-9)
C      CALCUATE XN VALUES
       DO 201 IXN=1,NXN
       ICYXN=0
       IF(IXN.GE.1.AND.IXN.LT.11) GO TO 250
       XXN=(IXN-9)*DXN+CXN
       GO TO 251
250    XXN=(IXN-1)*(DXN/9.)+CXN
251    XN(IXN)=XXN
C      MULTIPLY EACH FA BY XN
       DO 301 I=1,NTL
       XNF(I)=XXN*FA(I)
       INTL=NTL+I
301    XNF(INTL)=XXN*FA(INTL)
C      TIME SHIFT XN*FA
       NT=(NTL/NTLT)+1
       DO 401 J=1,NT
       IT=(J-1)*NTLT
C      THE INDEX IT CORRESPONDS TO THE TIME SHIFT T
```

Fig. D-2 (Continued). LIMITER Program Listing

```
      DO 405 L=1,NTL
405   SXNF(L)=XNF(NTL-IT+L)
C     CLIP SHIFTED XN*FA
      DO 509 L=1,NTL
      TL=(KBIT-1)*TB+(L-1)*DTL
      IF(MJ-1)507,508,508
507   GO TO (5071,5072,5073,5074,5075),ISIG
5071  DUML=0.
      DUMU=SQRT(2.*ENP/(TB**2))
      GO TO 510
5072  DUML=0.
      DUMU=SQRT(4.*ENP/(TB**2))
      GO TO 510
5073  DUML=-SQRT(4.*ENP/(TB**2))
      DUMU=SQRT(4.*ENP/(TB**2))
      GO TO 510
5074  DUML=-SQRT(2.*ENP/(TB**2))*(1.-SIN(2.*PI*F1*TL))
      DUMU=SQRT(2.*ENP/(TB**2))*(1.+SIN(2.*PI*F1*TL))
      GO TO 510
5075  DUML=0.
      DUMU=0.
      GO TO 510
508   GO TO (5081,5082,5083,5084,5085),ISIG
5081  DUML=-SQRT(2.*ENP/(TB**2))
      DUMU=0.
      GO TO 510
5082  DUML=-SQRT(4.*ENP/(TB**2))
      DUMU=0.
      GO TO 510
5083  DUML=-SQRT(4.*ENP/(TB**2))*(1.+SIN(2.*PI*F1*TL))
      DUMU=SQRT(4.*ENP/(TB**2))*(1.-SIN(2.*PI*F1*TL))
      GO TO 510
5084  DUML=-SQRT(2.*ENP/(TB**2))*(1.+SIN(2.*PI*F1*TL))
      DUMU=SQRT(2.*ENP/(TB**2))*(1.-SIN(2.*PI*F1*TL))
      GO TO 510
5085  DUML=0.
      DUMU=0.
510   CONTINUE
      IF(SXNF(L).GE.DUML.AND.SXNF(L).LE.DUMU) GO TO 517
      IF(SXNF(L).GT.DUMU.AND.MJ.EQ.0) GO TO 513
      IF(SXNF(L).GT.DUMU.AND.MJ.EQ.1) GO TO 514
      IF(SXNF(L).LT.DUML.AND.MJ.EQ.0) GO TO 515
      IF(SXNF(L).LT.DUML.AND.MJ.EQ.1) GO TO 516
513   GO TO (5131,5132,5133,5134,5135),ISIG
5131  SXNF(L)=SQRT(2.*CONP*ENP/(TB**2))
      GO TO 517
5132  SXNF(L)=SQRT(ENP/(TB**2))*(SQRT(CONP)+1.)
      GO TO 517
```

Fig. D-2 (Continued). LIMITER Program Listing

```
5133   SXNF(L)=SQRT(4.*CONP*ENP/(TB**2))
       GO TO 517
5134   SXNF(L)=SQRT(2.*ENP/(TB**2))*(SQRT(CONP)+
      1SIN(2.*PI*F1*TL))
       GO TO 517
5135   SXNF(L)=0.
       GO TO 517
514    GO TO (5141,5142,5143,5144,5145),ISIG
5141   SXNF(L)=SQRT(2.*ENP/(TB**2))*(SQRT(CONP)-1.)
       GO TO 517
5142   SXNF(L)=SQRT(ENP/(TB**2))*(SQRT(CONP)-1.)
       GO TO 517
5143   SXNF(L)=SQRT(4.*ENP/(TB**2))*(SQRT(CONP)-
      1SIN(2.*PI*F1*TL))
       GO TO 517
5144   SXNF(L)=SQRT(2.*ENP/(TB**2))*(SQRT(CONP)-
      1SIN(2.*PI*F1*TL))
       GO TO 517
5145   SXNF(L)=0.
       GO TO 517
515    GO TO (5151,5152,5153,5154,5155),ISIG
5151   SXNF(L)=-SQRT(2.*CONN*ENP/(TB**2))
       GO TO 517
5152   SXNF(L)=SQRT(ENP/(TB**2))*(-SQRT(CONN)+1.)
       GO TO 517
5153   SXNF(L)=-SQRT(4.*CONN*ENP/(TB**2))
       GO TO 517
5154   SXNF(L)=SQRT(2.*ENP/(TB**2))*(-SQRT(CONN)+
      1SIN(2.*PI*F1*TL))
       GO TO 517
5155   SXNF(L)=0.
       GO TO 517
516    GO TO (5161,5162,5163,5164,5165),ISIG
5161   SXNF(L)=SQRT(2.*ENP/(TB**2))*(-SQRT(CONN)-1.)
       GO TO 517
5162   SXNF(L)=SQRT(ENP/(TB**2))*(-SQRT(CONN)-1.)
       GO TO 517
5163   SXNF(L)=SQRT(4.*ENP/(TB**2))*(-SQRT(CONN)-
      1SIN(2.*PI*F1*TL))
       GO TO 517
5164   SXNF(L)=SQRT(2.*ENP/(TB**2))*(-SQRT(CONN)-
      1SIN(2.*PI*F1*TL))
       GO TO 517
5165   SXNF(L)=0.
517    CONTINUE
509    CONTINUE
C      SXNF NOW REPRESENTS SHIFTED AND CLIPPED XNF
C
```

Fig. D-2 (Continued). LIMITER Program Listing

```
C       MULTIPLY CLIPPED XN*FA BY SA
C       INTEGRATE TO OBTAIN FJ(N,T) AND STORE IN YY ARRAY
        DO 601 M=1,NTL
601     SXNF(M)=SXNF(M)*SA(M)
        CALL QTFG(TIME,SXNF,Z,NTL)
        IF(MJ)602,602,603
602     YY(J)=Z(NTL)
        GO TO 401
603     YY(J)=-Z(NTL)
401     CONTINUE
C       INTERPOLATE AND CLASSIFY FJ(N,T) VALUES TO OBTAIN
C       TIME RANGE DATA
        DO 701 IC=2,NT
        IF(YY(IC-1).LT.FENP.AND.YY(IC).LT.FENP) GO TO 701
        IF(IC-NT)704,705,705
705     NIP=NIPF
C       NIPF IS THE NUMBER OF INTERPOLATED POINTS FIXED
        GO TO 706
704     NIP=NIPF-1
706     DO 703 ICC=1,NIP
C       NIP IS NUMBER INTERPOLATED POINTS
        YDUM=((YY(IC)-YY(IC-1))*(ICC-1))/(NIPF-1)+YY(IC-1)
        IF(YDUM-FENP)703,707,707
707     ICYXN=ICYXN+1
703     CONTINUE
701     CONTINUE
C       ITERATION FOR CXN (PART 2)
        YK=ICYXN
        IF(IXFX.EQ.0)GO TO 970
        IF(ICYXN.GT.0.AND.ICYXN.LE.4)GO TO 871
        GO TO 868
871     IXFX=0
C       MULTIPLY TIME RANGE DATA BY PDF VALUES
C       PRINT HEADER AND OUTPUT DATA
970     ANS(IXN)=(YK/((NIPF-1)*(NT-1)+1))*PDF(XN(IXN),MPDF,PA)
        IF(IXN-1)973,973,974
973     WRITE(6,975)
975     FORMAT(3X,'IXN',15X,'YK',18X,'ANS')
974     WRITE(6,991) IXN,YK,ANS(IXN)
991     FORMAT(2X,I4,10X,F12.6,10X,F12.6)
201     CONTINUE
C       CALCUATE PROBABILITY OF ERROR
900     CALL QTFG(XN,ANS,ZZ,NXN)
        CALL GRAPH1(XN,ZZ,NXN,2)
        WRITE(6,499) (YY(J),J=1,NT)
499     FORMAT(2X,10F11.6)
910     CONTINUE
        STOP
        END
```

Fig. D-2 (Continued). LIMITER Program Listing

```
      FUNCTION S(TL,ISIG)
      COMMON F1,F0
      PI=3.14159265358979
      GO TO(1,2,3,4,5),ISIG
   1  S=1.
      RETURN
   2  S=1.
      RETURN
   3  S=SIN(2.*PI*F1*TL)
      RETURN
   4  S=SIN(2.*PI*F1*TL)
      RETURN
   5  S=SIN(2.*PI*F1*TL)-SIN(2.*PI*F0*TL)
      RETURN
      END
C*************************************************************
C
      FUNCTION F(X)
      IF(X)9,8,8
 8    CONTINUE
      TFF=.004
      IF(X-TFF)11,11,9
 11   D=500.
C      FREQ=G
      G=1000.
      PI=3.14159265358979
      A=1./(PI*G)*SQRT((D*(D**2+4.*(PI*G)**2))/(1-EXP(-2*D*TFF)))
      F=A*SIN(2.*PI*G*X)*EXP(-D*X)
      GO TO 10
 9    F=0.
 10   RETURN
      END
```

Fig. D-2 (Continued). LIMITER Program Listing

LIST OF REFERENCES

1. J. H. Fennick, "Amplitude Distributions of Telephone Channel Noise and a Model for Impulse Noise," Bell System Technical Journal, vol. 48, pp. 3243-3263, December 1969.

2. M. Kurland and D. A. Molony, "Observations on the Effects of Pulse Noise in Digital Data Transmission Systems," IEEE Transactions on Communication Technology, vol. COM-15, pp. 552-555, August 1967.

3. P. Mertz, "Model of Impulsive Noise for Data Transmission," IRE Convention Record, Part 5 - Communication Systems, pp. 247-259, March 1960.

4. P. Mertz, "Model of Error Burst Structure in Data Transmission," Proceedings of the National Electronics Conference, vol. 16, pp. 232-240, October 1960.

5. P. Mertz, "Appraisal of Error Performance in Data Transmission," DDC Report No. AD 606 658, July 1962.

6. B. Shepelavey, "Non-Gaussian Atmospheric Noise in Binary-Data, Phase-Coherent Communication Systems," IEEE Transactions on Communication Systems, vol. CS-11, pp. 280-284, September 1963.

7. A. J. Rainal, "Statistical Properties of Noise Pulses," The John Hopkins University Carlyle Barton Laboratory, Technical Report No. AF-109, June 1964.

8. K. F. Tuncer, "Non-Gaussian Noise," NASA Research Grant 19-003-003, Progress Report, May 1970.

9. J. C. Lindenlaub and K. A. Chen, "Performance of Matched Filter Receivers in Non-Gaussian Noise Environments," IEEE Transactions on Communication Technology, vol. COM-13, pp. 545-547, December 1965.

10. R. E. Ziemer, "Character Error Probabilities for M-ary Signaling in Impulsive Noise Environments," IEEE Transactions on Communication Technology, vol. COM-15, pp. 32-44, February 1967.

11. R. C. Houts and J. D. Moore, "Study of Correlation Receiver Performances in the Presence of Impulse Noise," Technical Report No. 129-102, Communication Systems Group, Bureau of Engineering Research, University of Alabama, February 1971.

12. P. A. Bello and R. Esposito, "A New Method for Calculating Probabilities of Errors Due to Impulsive Noise," IEEE Transaction on Communication Technology, vol. COM-17, pp. 368-379, June 1969.

13. P. A. Bello and R. Esposito, "Error Probabilities Due to Impulsive Noise in Linear and Hard-Limited DPSK Systems," IEEE Transactions on Communication Technology, vol. COM-19, pp. 14-20, February 1971.

14. L. R. Halsted, "On Binary Data Transmission Error Rates Due to Combinations of Gaussian and Impulse Noise," IEEE Transactions on Communication Systems, vol. CS-11, pp. 428-435, December 1963.

15. J. H. Halton and A. D. Spaulding, "Error Rates in Differentially Coherent Phase Systems in Non-Gaussian Noise," IEEE Transactions on Communication Technology, vol. COM-14, pp. 594-601, October 1966.

16. G. D. Arndt and F. J. Loch, "Correlation Detection of Impulse Noise for FM Threshold Extension," Proceedings of IEEE, vol. 58, pp. 1141-1143, July 1970.

17. R. W. Chang, "A New Digital Frequency Detection Scheme," IEEE Transactions on Communication Technology, vol. COM-18, pp. 305-312, August 1970.

18. A. M. Conda, "The Effect of Atmospheric Noise on the Probability of Error for an NCFSK System," IEEE Transactions on Communication Technology, vol. COM-13, pp. 280-284, September 1965.

19. R. Esposito and J. F. Roche, "Characterization of Man-Made Noise and Prediction of Error Rate in VHF Digital Systems," 1970 International Conference on Communications, vol. 1, pp. 10-(1-5), June 1970.

20. J. H. Fennick, "A New Method for the Evaluation of Data Systems Subject to Large Noise Pulses," IEEE International Convention Record, Part I, Communications 1, Wire and Data Communications, pp. 106-110, March 1965.

21. R. E. Ziemer, "Error Probabilities Due to Additive Combinations of Gaussian and Impulsive Noise," IEEE Transactions on Communication Technology, vol. COM-15, pp. 471-474, June 1967.

22. P. A. Bello, "Error Probabilities Due to Atmospheric Noise and Flat Fading in HF Ionospheric Communication Systems," IEEE Transactions on Communication Technology, vol. COM-13, pp. 266-279, September 1965.

23. A. B. Bodonyi, "Effects of Impulse Noise on Digital Data Transmission," IRE Transactions on Communication Systems, vol. CS-9, pp. 355-361, December 1961.

24. J. S. Engel, "Digital Transmission in the Presence of Impulsive Noise," Bell System Technical Journal, vol. 44, pp. 1699-1743, October 1965.

25. J. B. Millard and L. Kurz, "Adaptive Threshold Detection of M-ary Signals in Statistically Undefined Noise," IEEE Transactions on Communication Technology, vol. COM-14, pp. 601-610, October 1966.

26. W. L. Black, "An Impulse Noise Canceller," IEEE Transactions on Communication Systems, vol. CS-11, p. 506, December 1963.

27. M. Brilliant, "An Impulse Noise Canceller," IEEE Transactions on Communication Technology, vol. COM-12, pp. 104-105, September 1964.

28. C. A. Herbst, "Single Hex Inverter Picks Data Signal from Noise," Electronics, vol. 43, no. 18, p. 69, August 31, 1970.

29. A. F. Nicholson and M. J. Kay, "Reduction of Impulse Interference in Voice Channels," IEEE Transactions on Communication Technology, vol. COM-12, pp. 218-220, December 1964.

30. R. A. Wainwright, "On the Potential Advantage of A Smearing-Desmearing Filter Technique in Overcoming Impulse Noise Problems in Data Systems," IRE Transactions on Communication Technology, vol. 9, pp. 362-366, December 1961.

31. D. L. Snyder, "Optimal Binary Detection of Known Signals in a Non-Gaussian Noise Resembling VLF Atmospheric Noise," Wescon Technical Papers, pp. 1-8, 1968.

32. S. S. Rappaport and L. Kurz, "An Optimal Nonlinear Detector for Digital Data Transmission Through Non-Gaussian Channels," IEEE Transactions on Communication Technology, vol. COM-14, pp. 266-274, June 1966.

33. J. R. Stansberry, "Impulsive Electro-Magnetic Interference Characterization; Test Results," Technical Note TN# S-5.0-013, SCI Electronics Inc., March 1971.

34. A. F. d'Aquin, "The Susceptibility of Candidate Data Bus Cables to Electromagnetic Interference," Test Report, The Boeing Company Aerospace Division, 1970.

35. S. O. Rice, "Mathematical Analysis of Random Noise," Bell System Technical Journal, vol. 23, pp. 282-332, July 1944.

36. D. Middleton, An Introduction to Statistical Communication Theory. New York: McGraw-Hill, 1960, pp. 490, 834.

37. J. M. Wozencraft and I. M. Jacobs, Principles of Communication Engineering. New York: John Wiley and Sons, 1967, pp. 211-222, 486.

38. W. R. Bennett and J. R. Davey, Data Transmission. New York: McGraw-Hill, 1965, pp. 190-195.

39. E. Toth, "Noise and Output Limiters, Part II," Electronics, vol. 19, no. 12, pp. 120-125, December 1946.

40. N. Bishop, "Noise Limiter for Mobile VHF," Electronics, vol. 26, no. 6, pp. 164-165, June 1953.

41. J. C. Dute and C. A. Hines, "Swept Frequency Modulation A Means of Reducing the Effects of Impulse Noise," Technical Documentary Report No. ASD-TDR-62-836, University of Michigan, December 1962.

42. D. R. Brundage, E. K. Holland-Moritz, and J. C. Dute, "The SFM Data Generator," Technical Report AFAL-TR-65-158, University of Michigan, July 1965.

43. R. W. Lucky, J. Salz, E. J. Weldon, Jr., Principles of Data Communication. New York: McGraw-Hill, 1968, p. 10.

44. IBM, "System/360 Scientific Subroutine Package (360A-CM-03X) Version II, Programmer's Manual H20-0205-1," 1967, pp. 6, 95.

UNCITED REFERENCES

1. E. Arthurs and H. Dym, "On the Optimum Detection of Digital Signals in the Presence of White Gaussian Noise--A Geometric Interpretation and a Study of Three Basic Data Transmission Systems," IRE Transactions on Communication Systems, vol. CS-10, pp. 336-372, December 1962.

2. W. R. Bennett, Electrical Noise. New York: McGraw-Hill, 1966, pp. 250-269.

3. L. B. Browne and L. L. Lay, "A Comprehensive Amplitude Probability Distribution for Atmospheric Radio Noise," 1970 International Conference on Communications, vol. 2, pp. 29-(8-14), June 1970.

4. R. G. Enticknap, "Errors in Data Transmission Systems," IRE Transactions on Communication Systems, vol. CS-9, pp. 15-20, March 1961.

5. J. H. Fennick, "A Report on Some Characteristics of Impulse Noise in Telephone Communication Systems," IEEE Transactions on Communications and Electronics, vol. 83, pp. 700-705, November 1964.

6. D. R. Klose and L. Kurz, "A New Representation Theory and Detection Procedures for a Class of Non-Gaussian Channels," IEEE Transactions on Communication Technology, vol. COM-17, pp. 225-234, April 1969.

7. J. G. Kneuer, "A Simplified Physical Model for Amplitude Distribution of Impulsive Noise," IEEE Transactions on Communication Technology, vol. COM-12, pp. 220-222, December 1964.

8. P. Mertz, "Model of Impulsive Noise for Data Transmission," IRE Transactions on Communication Systems, vol. CS-9, pp. 130-137, June 1961.

9. P. Mertz, "Statistics of Hyperbolic Error Distribution in Data Transmission," IRE Transactions on Communication Systems, vol. CS-9, pp. 377-382, December 1961.

10. D. Middleton, "Acoustic Signal Detection by Simple Correlators in the Presence of Non-Gaussian Noise. I. Signal-to-Noise Ratios and Canonical Forms," Journal of the Acoustical Society of America, vol. 34, pp. 1598-1609, October 1962.

11. J. N. Petrie and E. L. Murphy, "Influence of Component Configuration on Noise," Automatic Electric Technical Journal, vol. 11, no. 3, pp. 102-108, July 1968.

12. D. B. Smith and W. E. Bradley, "The Theory of Impulse Noise in Ideal Frequency-Modulation Receivers," Proceedings of the IRE, vol. 34, pp. 743-751, October 1946.

COMMUNICATION SYSTEMS GROUP

RECENT REPORTS

AM-Baseband Telemetry Systems, Vol. 1: Factors Affecting a Common Pilot System, R. S. Simpson and W. H. Tranter, February, 1968.

Waveform Distortion in an FM/FM Telemetry System, R. S. Simpson, R. C. Houts and F. D. Parsons, June, 1968.

A Digital Technique to Compensate for Time-Base Error in Magnetic Tape Recording, R. S. Simpson, R. C. Houts and D. W. Burlage, August, 1968.

A Study of Major Coding Techniques for Digital Communication, R. S. Simpson and J. B. Cain, January, 1969.

AM-Baseband Telemetry Systems, Vol. 2: Carrier Synthesis from AM Modulated Carriers, R. S. Simpson and W. H. Tranter, June, 1969.

AM-Baseband Telemetry Systems, Vol. 3: Considerations in the Use of AGC, R. S. Simpson and W. H. Tranter, July, 1969.

AM-Baseband Telemetry Systems, Vol. 4: Problems Relating to AM-Baseband Systems, R. S. Simpson and W. H. Tranter, August, 1969.

AM-Baseband Telemetry Systems, Vol. 5: Summary, R. S. Simpson and W. H. Tranter, August, 1969.

Study of Correlation Receiver Performances in the Presence of Impulse Noise, R. C. Houts and J. D. Moore, February, 1971.

Computer-Aided Design of Digital Filters, R. C. Houts and D. W. Burlage, March, 1971.